UNIVERSITI SAINS MALAYSIA

Pejabat Pengurusan dan Kreativiti Penyelidikan
Research Creativity and Management Office

Memorandum

Universiti Sains Malaysia
Aras 6, Bangunan Canselori
11800, USM Pulau Pinang, Malaysia
T : (6)04-653 3108/3178/3988/5019
F : (6)04-656 6466/8470
: (6)04-653 2350
L : www.research.usm.my
www.usm.my

Ruj. Kami : P3268
Tarikh 21 Jun 2013

Profesor Dr. Othman Bin Sulaiman
Pusat Pengajian Teknologi Industri
Universiti Sains Malaysia
Kampus Induk
11800 Pulau Pinang

PERINGATAN PENGHANTARAN LAPORAN AKHIR GERAN PENYELIDIKAN JANGKA PENDEK YANG TELAH TAMAT TEMPOH

TAJUK PROJEK	:	Adsorption Behaviour of Water Pollutants onto Surfactant Modified Oil Palm Biomass
NO. AKAUN	:	304/PTEKIND/639062
TEMPOH PROJEK	:	15 November 2009 - 14 November 2011
JUMLAH PERUNTUKAN	:	RM40,000.00

Dengan hormatnya perkara di atas dirujuk.

2. Untuk makluman Tuan/Puan, semakan dan rekod Pejabat ini menunjukkan Tuan/Puan masih belum mengemukakan laporan akhir bagi projek penyelidikan seperti di atas. Memandangkan geran tersebut telah tamat tempoh, kerjasama Tuan/Puan untuk mengemukakan laporan akhir kepada Pejabat ini dengan kadar segera amatlah dihargai.

3. Sekiranya Pejabat ini tidak menerima laporan akhir daripada Tuan/Puan dalam masa **30 hari** daripada tarikh surat ini, projek penyelidikan ini akan dibekukan. Pihak Universiti memandang penting projek-projek yang berstatus beku dan pada masa hadapan, penyelidik yang mempunyai projek penyelidikan beku akan ditangguhkan penilaian untuk permohonan projek baru bagi Geran Dalaman Universiti.

4. Untuk melancarkan urusan ini, Tuan/Puan boleh memuat turun Borang Laporan Akhir Geran Penyelidikan Jangka Pendek melalui laman web Bahagian Penyelidikan & Inovasi. Untuk makluman bersama, borang laporan akhir ini perlu dinilai di Jawatankuasa Penyelidikan di Peringkat PTJ terlebih dahulu sebelum dikemukakan ke Pejabat ini untuk tindakan selanjutnya. Sekiranya Tuan/Puan mempunyai sebarang pertanyaan berkaitan perkara ini, sila hubungi Pegawai berikut:

- *Ahmad Imran Bin Kamis, 04 - 653 4365, aimran@usm.my*

5. Sila maklumkan kepada Pejabat RCMO sekiranya Tuan/Puan telah mengemukakan laporan akhir tersebut di Jawatankuasa Penyelidikan di Peringkat PTJ untuk perhatian dan tindakan lanjut Pejabat ini.

Di atas perhatian dan kerjasama Tuan/Puan berkaitan perkara ini saya dahului dengan ucapan terima kasih.

Sekian.

"BERKHIDMAT UNTUK NEGARA"
'Memastikan Kelestarian Hari Esok'

(PROF. MADYA LEE KEAT TEONG)
Pengarah
Pejabat Pengurusan & Kreativiti Penyelidikan

P.M. Lee

Pengarah

20/9/13

Professor Dr. Othman Sulaiman
PhD, DIC (Imperial College London)
Bioresource, Paper &Coatings Technology
School of Industrial Technology
11800 Universiti Sains Malaysia, Penang, Malaysia
Tel : +604 653 2241 / 2933 Fax : +604 657 3678
Email: othman@usm.my, osulaiman@gmail.com

s.k. Dekan
Pusat Pengajian Teknologi Industri

Timbalan Bendahari
Bahagian Perancangan & Pengurusan Kewangan
Bangunan C04
Jabatan Bendahari

UNIVERSITI SAINS MALAYSIA

LAPORAN AKHIR PROJEK PENYELIDIKAN JANGKA *PENDEK*

FINAL REPORT OF SHORT TERM RESEARCH PROJECT

Sila kemukakan laporan akhir ini melalui Jawatankuasa Penyelidikan di Pusat Pengajian dan Dekan/Pengarah/Ketua Jabatan kepada Pejabat Pelantar Penyelidikan

1. Nama Ketua Penyelidik: Assoc. Prof. Dr. Othman Sulaiman

[/] Profesor Madya/ *Assoc. Prof.* [ ] Dr./ *Dr.* [ ] Encik/Puan/Cik *Mr/Mrs/Ms*

2. Pusat Tanggungjawab (PTJ): School of Industrial Technology
School/Department

RECEIVED 26 SEP 2013 Pej. Pengarah RCMO

3. Nama Penyelidik Bersama:
Name of Co-Researcher

Dr. Mohd Rafatullah (Who was at that time the Postdoctoral Fellow), Dr. Rokiah Hashim, Dr. Anees Ahmad

4. Tajuk Projek:
Title of Project

Adsorption behaviour of water pollutants onto surfactant modified oil palm biomass
Account No: 304/PTEKIND/639062 (1/9/2009 – 31/8/2011)

5. Ringkasan Penilaian/*Summary of Assessment*:	Tidak Mencukupi *Inadequate* 1	2	Boleh Diterima *Acceptable* 3	Sangat Baik *Very Good* 4	5
i) Pencapaian objektif projek: *Achievement of project objectives*	[ ]	[ ]	[ ]	[/]	[ ]
ii) Kualiti output: *Quality of outputs*	[ ]	[ ]	[ ]	[/]	[ ]
iii) Kualiti impak: *Quality of impacts*	[ ]	[ ]	[ ]	[/]	[ ]
iv) Pemindahan teknologi/potensi pengkomersialan: *Technology transfer/commercialization potential*	[ ]	[ ]	[/]	[ ]	[ ]
v) Kualiti dan usahasama : *Quality and intensity of collaboration*	[ ]	[ ]	[ ]	[/]	[ ]
vi) Penilaian kepentingan secara keseluruhan: *Overall assessment of benefits*	[ ]	[ ]	[ ]	[/]	[ ]

6. Abstrak Penyelidikan

(Perlu disediakan di antara 100 - 200 perkataan di dalam **Bahasa Malaysia dan juga Bahasa Inggeris**. Abstrak ini akan dimuatkan dalam Laporan Tahunan Bahagian Penyelidikan & Inovasi sebagai satu cara untuk menyampaikan dapatan projek tuan/puan kepada pihak Universiti & masyarakat luar).

Penjerap yang novel, biomas kelapa sawit seperti daun telah digunakan untuk mengeluarkan (II) ion kuprum daripada larutan akues. Daun kelapa sawit telah kering, dihaluskan, dibasuh menggunakan air suling dan disaring ke dalam saiz yang berbeza. Kesan pembolehubah yang berbeza sistem, iaitu, masa sentuhan, pH, dos bahan penjerap, saiz zarah bahan penjerap dan logam awal kepekatan ion biosorption kuprum (II) ion telah dikaji. Hasil kajian menunjukkan bahawa nilai pH optimum untuk maksimum biosorption ditentukan adalah 6.0 untuk (II) ion kuprum. Langmuir, Freundlich dan Temkin penjerapan isoterma pemalar dikira untuk mencari kesesuaian mereka untuk sistem dan keputusan telah dibincangkan. Parameter termodinamik seperti tenaga bebas, entalpi dan perubahan entropi bagi biosorption daripada (II) ion kuprum dikira untuk meramalkan sifat proses biosorption. Kesimpulannya, daun sawit zarah mungkin sesuai untuk digunakan sebagai kos rendah penjerap untuk penyingkiran kuprum (II) ion dari larutan akueus.

Abstract of Research

(An abstract of between 100 and 200 words must be prepared in Bahasa Malaysia and in English).
This abstract will be included in the Annual Report of the Research and Innovation Section at a later date as a means of presenting the project findings of the researcher/s to the University and the community at large)

A novel adsorbent, oil palm biomass such as leaves were used to remove copper (II) ions from aqueous solutions. Oil palm leaves were dried, grounded, washed using distilled water and sieved into different sizes. The effects of different system variables, viz, contact time, pH, dosage of adsorbent, size of adsorbent particles and initial metal ion concentration on biosorption of copper (II) ions were studied. The results showed that the optimum pH value for maximum biosorption determined was 6.0 for copper (II) ions. The Langmuir, Freundlich and Temkin adsorption isotherm constants were calculated to find their applicability for the system and the results were being discussed. The thermodynamic parameters such as free energy, enthalpy and entropy changes for the biosorption of copper (II) ions were computed to predict the nature of biosorption process. In conclusion, the oil palm leaves particles were found possible to be used as a low cost adsorbent for removal of copper (II) ions from aqueous solution.

7. Sila sediakan laporan teknikal lengkap yang menerangkan keseluruhan projek ini.
[Sila gunakan kertas berasingan]

Applicant are required to prepare a Comprehensive Technical Report explaning the project.
(This report must be appended separately)
The report provided is meant only for internal use and not for distribution. This is because it is being used for journal submission.

Senaraikan kata kunci yang mencerminkan penyelidikan anda:
List the key words that reflects your research:

Bahasa Malaysia	*Bahasa Inggeris*
Daun Kelapa sawit, Penjerapan bio,kuprum,isoterma, termodinamik	Oil palm leaf; Biosorption; Copper (II); Isotherm; Thermodynamic

8. Output dan Faedah Projek

Output and Benefits of Project

(a) * **Penerbitan Jurnal**
Publication of Journals
(Sila nyatakan jenis, tajuk, pengarang/editor, tahun terbitan dan di mana telah diterbit/diserahkan)
(State type, title, author/editor, publication year and where it has been published/submitted)

Sulaiman, O., Mohamad Amini, M.H., Rafatullah, M., Hashim, R., Ahmad, A. (2010). Adsorption Equilibrium and Thermodynamic Studies of Copper (II) Ions from Aqueous Solutions by Oil Palm Leaves. International Journal of Chemical Reactor Engineering. Vol. 8: A108.

Rafatullah, M., Sulaiman, O., Hashim, R., Ahmad, A. (2010). Adsorption of methylene blue on low cost adsorbents: A review. Journal of Hazardous Materials. 177(1-3):70-80.

Sulaiman, O., Rafatullah, M., Hashim, R., Ahmad, A. (2010). Kinetic modelling to remove methyl orange from aqueous solutions using oil palm trunk fiber. National Symposium on Recent Trends in Chemical Sciences [NSRTCS-2010], India, 24 and 25 February, 2010.

Amini, M.H.M. Rafatullah, M., Sulaiman, O. Hashim, R., Ahmad, A. (2010). Biosorption of copper (II) ions from aqueous solution by oil palm leaves International Conference on Environmental Research and Technology (ICERT 2010). Penang. p506-513. ISBN 978-967-5417-79-5.

Ahmad, T., Rafatullah, M., Ghazali, A., Sulaiman, O., Hashim, R. 2011. Oil palm biomass-based adsorbents for the removal of water pollutants a review. Journal of Environmental Science and Health - Part C Environmental Carcinogenesis and Ecotoxicology Reviews 29(3):177-222.

(b) **Faedah-faedah lain seperti perkembangan produk, pengkomersialan produk/pendaftaran paten atau impak kepada dasar dan masyarakat.**
State other benefits such as product development, product commercialisation/patent registration or impact on source and society.

Technical information on different parts of oil palm biomass is known along with its potential use in Bioresource Technology. Data and methods of the study can provide as a basis for the industrial development of the country in an eco-friendly manner.

* Sila berikan salinan/*Kindly provide copies*

(c) **Latihan Sumber Manusia**
Training in Human Resources

i) Pelajar Sarjana:
Graduates Students
(Perincikan nama, ijazah dan status)
(Provide names, degrees and status)

ii) Lain-lain: This project is part of the project for Postdoctoral candidate Dr. M. Rafatullah and Final Year Projects
Others

9. Peralatan yang Telah Dibeli:

20 Sep 2013

Tandatangan Penyelidik
Signature of Researcher

Tarikh
Date

Komen Jawatankuasa Penyelidikan Pusat Pengajian/Pusat
Comments by the Research Committees of Schools/Centres

Penyelidikan telah berjalan dengan jayanya. Sebanyak 5 penerbitan telah dihasilkan.

Tutup Geran

25/9/13

TANDATANGAN PENGERUSI
JAWATANKUASA PENYELIDIKAN
PUSAT PENGAJIAN/PUSAT
Signature of Chairman
[Research Committee of School/Centre]

24/9/13

Tarikh
Date

Adsorption of Copper (II) Ions onto Surfactant-Modified Oil Palm Leaf Powder

M. Rafatullah*, O. Sulaiman, R. Hashim, M. H. M. Amini and M. Danish

Division of Bioresource, Paper and Coatings Technology, School of Industrial Technology, Universiti Sains Malaysia, 11800 Penang, Malaysia

ABSTRACT

Oil palm leaf powder (OPLP), an agricultural solid waste was used as adsorbent for the removal of copper (II) ions after modification with an anionic surfactant, sodium dodecyl benzene sulfonate (SDBS), $CH_3(CH_2)_{11}C_6H_4SO_3Na$. The copper (II) ions adsorption is highly dependent on pH and maximum removal was observed at pH 6, above which copper (II) started to precipitate. The equilibrium adsorption data were fitted into the Langmuir and Freundlich isotherms. The Freundlich isotherm model fitted well to data with 0.989 regression coefficient (R^2). The kinetics of the adsorption of copper (II) ions onto the surfactant-modified OPLP was best described by a pseudo-second-order model. Comparison of this SDBS-modified-OPLP to previously investigated adsorbents showed comparably good result, offering this material as a promising adsorbent for the treatment of waste waters containing lower concentrations of copper (II) ions.

Keywords: Oil palm leaf, Surfactant, Adsorption, Copper (II), Kinetic.

---

*Corresponding author:

E-mail address: mohd_rafatullah@yahoo.co.in; mrafatullah@usm.my (M. Rafatullah)

Tel: +604 653 4302/5217; fax: +604 657 3678

INTRODUCTION

Heavy metals are polluting water around the world, creating a world-wide environmental problem. Metals such as copper, nickel, lead, mercury, chromium, cadmium and zinc, which have been considered as hazardous heavy metals are commonly found in waste. These heavy metals are toxic and their presence in steams leads to accumulation in living organisms, causing health problems in human beings, plants, and animals.[1] It has been reported that excessive intake of copper by humans may lead to severe mucosal irritation, hepatic and renal damage, capillary damage, gastrointestinal irritation and central nervous system irritation.[2] So the removal of these metals from waste water is necessary. Several processes have been suggested to remove heavy metals from waste water. These processes include chemical precipitation, ion exchange, cementation,[3] coagulation and flocculation,[4] complexation, adosorption,[5, 6]and membrane processes.[7]

At present, there is growing interest in using low-cost, commercially available materials for the adsorption of heavy metals. The use of agricultural wastes for the treatment of polluted water is also an attractive and promising option for the environment[2]. A wide variety of agricultural waste materials are being used as low-cost alternatives to expensive adsorbents. Attention was given to utilization of oil palm leaf as an adsorbent, Malaysia was the largest producer and exporter of palm oil in the world in 2006, comprising of 52 % or 26.3 million tonnes of the total world oil and fat production and the demand is forecasted to be increasing each year, which means more and more waste will be produced.[8]

To enhance the capacity of adsorbent to adsorb heavy metal ions, many chemical or physical treatment and surface modification methods have been introduced. Among these methods, surface modification method using surfactants can significantly enhance the capacities

of adsorbent to absorb heavy metal ions.[9-13] Surfactants are chemicals that have molecules with a hydrophobic tail and a hydrophilic head, and have been applied to modify the surface properties of a solid surface.

In this study, we attempted to improve the capacity of oil palm leaf powder (OPLP) to adsorb copper (II) ions. We modified the surface of the OPLP by impregnating it with the anionic surfactants sodium dodecyl benzene sulfonate (SDBS). Capacities of the SDBS-modified-OPLP to adsorb copper (II) ions were examined under various conditions. The adsorption isotherms, kinetics and its mechanism at different concentrations are discussed.

MATERIALS AND METHODS

Adsorbent Preparation

Oil palm leaves (*Elaeis guineensis*) were obtained from an oil palm plantation in Kedah, Malaysia. Oil palm leaves were washed with distilled water to remove dust and soluble substances. The leaves were dried, ground and washed thoroughly with distilled water for several times and dried in an oven at 60 ± 5°C for 48 hours. For modification of adsorbent, Sodium dodecyl benzene sulfonate (SDBS), ($CH_3(CH_2)_{11}C_6H_4SO_3Na$) analytical grade from Sigma-Aldrich were used. Method from Namasivayam and Sureshkumar (2006) [14] was adopted with modification of treatment period. Each ten grams of OPLP were mixed with 100 ml of 2 % SDBS and stirred using magnetic stirrer for 24 hours. SDBS-modified-OPLP were filtered and washed with distilled water for several times to remove excessive surfactant. SDBS-modified-OPLP particles were dried inside an oven at 50 ± 2°C, sieved to get particle size between 250-500 µm and stored for further studies.

Adsorbate Solutions

Stock solution of metal ions were prepared using copper (II) nitrate hemipentahydrate ($Cu(NO_3)_2 \cdot 2.5H_2O$) analytical grade from Sigma-Aldrich, dissolved into distilled water to a concentration of 1000 mg/L. Stock solution was further diluted to different desired concentrations.

Batch Adsorption Studies

Batch adsorption studies were carried out by shaking 0.5 g of the SDBS-modified-OPLP with 50 ml of the aqueous solutions of copper (II) in different conical flasks using a temperature-controlled shaker. The solution-adsorbents mixtures were stirred at 125 rpm and at the end of pre-determined time interval the reaction mixtures were filtered out and analyzed for its metal ion concentrations using Atomic Absorption Spectrometer, AAS (Analyst 100 Perkin Elmer). The adsorption experiments were also conducted to determine the equilibrium time (20, 40, 60, 80, 100, 120, 140, 160, 180 and 300 min.), pH of the solution (2, 3, 4, 5, 6, 7, 8 and 9), initial concentrations (1, 10, 25, 50, 100 and 200 mg/L) and dosage of the adsorbent (0.5, 1.0, 1.5, 2.0, 2.5, 3.0, 3.5, 4.0, 4.5 and 5.0 g) for maximum adsorption. All the investigations were carried out in triplicate to avoid any discrepancy in experimental results. Metal solution controls were kept throughout the experiment to maintain quality control. The percentage of metal adsorption by the adsorbents was computed using the equation:

$$\% \text{ adsorption} = \{(Ci - Ce) / Ci\}\ 100 \qquad (1)$$

where, Ci and Ce are the initial and equilibrium concentration of metal ion (mg/L) in the solution.

RESULTS AND DISCUSSION

Scanning Electron Microscopy of SDBS-modified-OPLP

Scanning electron microscopy (Carl-Ziess SMT, Oberkochen, Germany) analysis was carried out on SDBS-modified-OPLP to study its surface morphology before and after adsorption of copper (II) ions. Figure 1 (a) and 1 (b) shows the SEM micrographs of SDBS-modified-OPLP adsorbents before and after copper (II) adsorption. Figure 1 (a) shows that the SDBS- modified-OPLP consist a rough surface morphology with pores of different sizes. These pores are very useful for copper (II) adsorption. Figure 1 (b) shows that the surface of copper (II) loaded SDBS-modified-OPLP is covered with copper (II) ions.

Effect of Contact Time and Initial Concentration

The effect of contact time and initial concentration of copper (II) ions on the percentage removal by SDBS-modified-OPLP is shown in Figure 2. The adsorption of copper (II) ions onto SDBS-modified-OPLP increases with time and then attains equilibrium value at a time of about 120 min. The removal of copper (II) ions was found to be dependent on the initial concentration; the percent adsorption increasing with increase in initial concentration. Further, the time curve shows that the percent removal of copper (II) ions is rapid but it gradually slows down until it reaches the equilibrium. At low concentrations the ratio of available surface to the initial copper (II) concentration is larger, so the removal becomes independent of initial concentrations. However, in the case of higher concentrations this ratio is low; the percentage removal then depends upon the initial concentration and had only a small influence on the time of contact necessary to reach equilibrium. On changing the initial concentration from 1 to 200 mg/L, the percent removal increased from 93.82 to 98.75 % for a time period of 120 min. The plots are

smooth and continuous, suggesting the possible adsorption of copper (II) ions on the surface of SDBS-modified-OPLP. Consequently, the concentration of copper (II) will greatly affect the extent and rate of copper (II) uptake onto SDBS-modified-OPLP.

Point of Zero Charge (pH_{ZPC}) Determination and Effect of pH

The effect of pH on the adsorption of copper (II) ions by SDBS-modified-OPLP was studied by varying pH of the solution over the range of 2-9 using different concentration. The determination of pH_{ZPC} of SDBS-modified-OPLP was performed according to the solid addition method.[15] 50mL of 0.01M KNO_3 solution was placed in conical flasks. The initial pH of the solutions was adjusted to a value between 2 and 9 by adding 0.1M HCl or NaOH solutions. Then, 1 g of SDBS-modified-OPLP was added to each flask, strirred and the final pH of the solutions was measured after 24 h. The value of pH_{ZPC} can be determined from the curve that cuts the pH_0 line of the plot ΔpH versus pH_0. The pH_{ZPC} of an adsorbent is a very important characteristic that determines the pH at which the adsorbent surface has net electrical neutrality. At this value, the acidic or basic functional groups no longer contribute to the pH of the solution. The value of pH_{ZPC} is close to the value of pH of aqueous slurry which is 5.9. The effect of pH on the adsorption of copper (II) ions on SDBS-modified-OPLP is presented in Figure 3. It shows that the adsorption of copper (II) in the pH range of 2 to 5 varies between 52 % and 80 %. The percentage removal of copper (II) ions was minimum at the pH 2 and increased with further increase in pH. At pH value lower than 5, the adsorption capacities were found to be low due to the competitive adsorption of HO_3^+ ions and metal ions for the same active adsorption site. As the pH increased, the adsorption surface become less positive and therefore electrostatic attraction between the metal ions and SDBS-modified-OPLP surface is likely to be increased. However, at higher pH values of 6 to 9 the metal adsorption decreased. A decrease in adsorption

at high pH is due to the formation of soluble hydroxyl complexes. The maximum sorption efficiency is around pH 6.

Effect of Adsorbent Dosage

Effect of adsorbent dosage on the percent adsorption was conducted to evaluate the efficiency of adsorption at different amount of adsorbent. Figure 4 shows the removal of copper (II) ions by SDBS-modified-OPLP at different dosage of adsorbent (0.5–5.0 g) at initial concentration of 100 mg/L of copper (II) solution and 30 °C. From figure 4 it was observed that, the percentage of copper (II) removal increased from 68.92 to 97.27 % with an increase in adsorbent dosage from 0.5 to 5.0 g. The percentage removal increased with the SDBS-modified-OPLP dosage, the increase in adsorption of copper (II) with adsorbent dosage can be attributed to increased surface area and the availability of more adsorption sites.

Adsorption Isotherm Studies

To quantify the adsorption capacity of SDBS-modified-OPLP for the removal of copper (II) from aqueous solution, the Freundlich and Langmuir isotherm models were used.

Freundlich Adsorption Isotherm Model

The Freundlich model can be applied for non-ideal adsorption on heterogeneous surfaces and multilayer adsorption.[16] According to this model:

$$q_e = (K_F)\,(C_e^{1/n}) \qquad (2)$$

$$\ln q_e = \ln K_F + 1/n \ln C_e \qquad (3)$$

where, C_e is the equilibrium concentration (mg/L) and q_e is the amount adsorbed per specified amount of adsorbent (mg/g)., K_F is Freundlich equilibrium constant, n is an empirical constant. Thus, a plot of $\ln q_e$ vs $\ln C_e$ should be a straight line with a slope 1/n and an intercept of $\ln K_F$ as shown in Figure 5. The correlation coefficient (R^2) value of 0.989 indicated that the adsorption

data of copper (II) ions onto SDBS-modified-OPLP was well fitted to the Freundlich isotherm. The related parameters were calculated and reported in Table 1. The Freundlich type adsorption isotherm is an indication of surface heterogeneity of the adsorbent and thus is responsible for multilayer adsorption due to the presence of energetically heterogeneous adsorption sites. This leads to the conclusion that the surface of SDBD-modified-OPLP is made up of small heterogeneous adsorption patches which are very much similar to each other in respect of adsorption phenomenon.

Langmuir Adsorption Isotherm Model

This model assumes that the adsorptions occur at specific homogeneous sites on the adsorbent and is used successfully in many monolayer adsorption processes.[17] The data of the equilibrium studies for adsorption of copper (II) onto SDBS-modified-OPLP may follow the following form of Langmuir model:

$$C_e/q_e = (1/b)\,(1/K_L) + (1/b)\,(C_e) \qquad (4)$$

Where, K_L is the Langmuir equilibrium constant and b is the amount of adsorbate required to form a monolayer. Hence, a plot of C_e/q_e vs C_e should be a straight line with a slope (1/b) and an intercept as $(1/b.K_L)$ as shown in Figure 6. The Langmuir type adsorption isotherm indicates surface homogeneity of the adsorbent and hint towards the conclusion that the surface of adsorbent is made up of small adsorption patches which are energetically equivalent to each other in respect to adsorption phenomenon. The values of constants K_L and b were calculated and reported in Table 1.

It appears that Freundlich isotherm model best fits the experimental results than Langmuir isotherm model over the experimental range with good correlation coefficient

(R^2=0.989). Model constants of both Freundlich and Langmuir along with correlation co-efficient values are listed in Table 1.

Kinetic Studies

This study describes the solute uptake rate and evidently this rate controls the residence time of adsorbate uptake at the solid-liquid interface. The mechanism of adsorption depends on the physical and chemical characteristics of the SDBS-modified-OPLP. In order to determine the adsorption kinetics of copper (II), the First-order reversible reaction, pseudo-first order and pseudo-second order models were checked. The conformity between experimental data and the model predicted values was expressed by correlation coefficient (R^2).

First-Order-Reversible Model

A simple first-order reversible reaction model can be expressed as

$$A + SDBS - OPLP \underset{k_{-1}}{\overset{k_1}{\rightleftharpoons}} B \qquad (5)$$

The rate equation for the reaction is expressed as

$$\frac{d[B]}{dt} = -\frac{d[A]}{dt} = k_1[A] - k_{-1}[B] = [A]\frac{dX_A}{dt}$$

$$= k_1([A_0] - [A_0]X_A) - k_{-1}([B_0] + [A_0]X_A) \qquad (6)$$

Here, [B] (mg/g) is the concentration of adsorbate on the adsorbent and [A] (mg/L) is the concentration of adsorbate in solution at any time. $[B_0]$ and $[A_0]$ are the initial concentrations of the adsorbate on adsorbent and solution, respectively.

X_A= Fraction of adsorbate

k_1 & k_{-1}= Forward and backward rate constants of first order reaction

Under equilibrium conditions, the rates of forward and backward reactions are equal, therefore:

$$K_C = \frac{[B_e]}{[A_e]} = \frac{[B_0]+[A_0]X_{Ae}}{[A_0]-[A_0]X_{Ae}} = \frac{k_1}{k_{-1}}$$

$$k_C[A_0](1-X_{Ae}) = [B_0]+[A_0]X_{Ae}$$

$$K_C[A_0]-[B_0] = X_{Ae}(K_C[A_0]+[A_0])$$

$$X_{Ae} = \frac{K_C[A_0]-[B_0]}{K_C[A_0]+[A_0]}$$

$$X_{Ae} = \frac{K_C - ([B_0]/[A_0])}{K_C+1} \qquad (7)$$

In the above reaction A_e represents the equilibrium concentration of solute A and K_C is the equilibrium constant. The rate equation in terms of equilibrium conversion can be obtained from eq. (6) and (7):

$$\frac{dX_A}{dt} = (k_1 + k_{-1})(X_{Ae} - X_A) \qquad (8)$$

By rearranging and integrating eq. (8) and substituting $k_{-1} = k_1/K_C$, we get

$$-\ln(1-\frac{X_A}{X_{Ae}}) = k_1(1+\frac{1}{K_C}) \qquad (9)$$

We define here new term fractional attainment of equilibrium, U, and net rate constant k_n,

$$U = \frac{[A_0]-[A_t]}{[A_0]-[A_e]} = \frac{X_A}{X_{Ae}} \qquad (10)$$

$$k_n = k_1(1+\frac{1}{K_C}) = k_1 + k_{-1} \qquad (11)$$

Eq. (9) can be rewritten with the help of eq. (10) and (11):

$$\ln(1-U) = -k_n t \qquad (12)$$

Plot of Eq. (12) was made for SDBS-modified-OPLP at different concentrations. The representation of plot is shown in Figure 7. Approximate linear fits were generally observed for different concentrations indicating that adsorption reaction can be approximated to be of the first-order reversible kinetics. Correlation coefficients were found to be from 0.937 to 0.981 which implies there is no good correlation for the first order kinetic model. Constants k_n, k_1, k_{-1} and K_C were calculated and are summarised in Table 2.

Pseudo-First-order Model

The pseudo-first order rate model equation given by Lagergren (1898) is:[18]

$$\frac{dq_t}{dt} = k_1'(q_e - q_t) \qquad (13)$$

Where,

q_t = adsorption capacity at time t, in mg/g, q_e = adsorption capacity at equilibrium, in mg/g and k_1' = rate constant for pseudo first order adsorption, in min.$^{-1}$

Eq. (13) on integration under boundary conditions, t = 0 to t = t and $q_t = 0$ to $q_t = q_t$ gives

$$\int_0^{q_t} \frac{1}{(q_e - q_t)} dq_t = \int_0^t k_1' dt$$

$$\ln\left(\frac{q_e}{q_e - q_t}\right) = k_1' t$$

$$q_t = q_e(1 - e^{-k_1' t})$$

Above equation can be rearranged to give the following equation:

$$\ln(q_e) - \ln(q_e - q_t) = k_1' t$$

$$\log(q_e - q_t) = \log(q_e) - \frac{k_1'}{2.303} t \qquad (14)$$

This is the most popular form of pseudo-first-order kinetic model equation. Plot of eq. (14) was done for SDBS-modified-OPLP at different concentrations (Figure 8). Approximately linear fits were observed for different concentrations. The smallest correlation coefficients were to be found from 0.938 to 0.974. Therefore, it can be concluded that although this model does not satisfy, but is better than the earlier model. Constants k_1' and correlation coefficients for all possible changes have been calculated and are summarised in Table 2.

Pseudo-Second-Order Model

The kinetic data were analyzed using the pseudo-second-order model[19] which, can be expressed as:

$$\frac{dq_t}{dt} = k_2(q_e - q_t)^2 \qquad (15)$$

Where, q_e and q_t (in mg/g) are the adsorption capacities at equilibrium and at time t, respectively, and k_2 is the rate constant of the pseudo- second order reactions, with unit g/mg/min.

On integrating eq. (15) with boundary conditions t = 0 to t = t and $q_t = 0$ to $q_t = q_t$ we get

$$\int_0^{q_t} \frac{1}{(q_e - q_t)^2} dq_t = \int_0^t k_2 dt$$

$$\frac{1}{(q_e - q_t)} = \frac{1}{q_e} + k_2 t \qquad (16)$$

Eq. (16) is the integrated rate law for pseudo second order adsorption. It can be rearrange to the linear form given below:

$$\frac{t}{q_t} = \frac{1}{k_2 q_e^2} + \frac{t}{q_e} \qquad (17)$$

The above equation can be rewritten as follows:

$$\frac{t}{q_t} = \frac{1}{h} + \frac{1}{q_e} t \qquad (18)$$

Where, h is initial sorption rate as $q_t/t \rightarrow 0$, hence $h = k_2 q_e^2$

Eq. (17) does not have the disadvantage of assigning an effective q_e if pseudo-second order kinetics is applicable, the plot of t/q_t against t of eq. (17) should give a linear relationship, from which q_e, k_2 and h can be calculated from the slope and intercept of the plot and there is no need to know any parameter beforehand. The sample plot for SDBS-modified-OPLP at different concentrations is given in Figure 9 and values for q_e, k_2 and h were calculated and are reported in Table 2. The correlation coefficient (R^2) values for this model are 0.990 to 0.996 which is very much close to the ideal correlation coefficient value. Hence it can be established that the adsorption of copper (II) ions onto SDBS-modified-OPLP perfectly follows the pseudo second order kinetic model.

Comparison With Other Adsorbents

Table 3 showed comparison of SDBS-modified-OPLP with various adsorbents in removal of copper (II) ions from aqueous solution. Adsorption capacity of SDBS-modified-OPLP is comparably high to some other available adsorbents, showing its advantage over the others as water or wastewater cleaning material.

CONCLUSIONS

The present study showed that SDBS-modified-OPLP, an agricultural waste material, can be used as an adsorbent for the removal of copper (II) ions from aqueous solutions. Equilibrium data fitted very well in the Freundlich isotherm equation, confirming the multilayer adsorption capacity of copper (II) ions onto SDBS-modified-OPLP with adsorption capacity of 75.98 mg/g. The rate of adsorption was found to conform to pseudo-second-order kinetics with a good correlation. Taking into consideration of the above results, it can be concluded that the SDBS-

modified-OPLP can be an alternative material for more costly adsorbents used for copper (II) ions removal in wastewater treatment processes.

ACKNOWLEDGEMENTS

The study was funded through USM short term grant number 304/ PTEKIND/ 639062. One of the authors (M. Rafatullah) is grateful to the University Sains Malaysia, for providing assistance under the post doctoral scheme and research facilities.

REFERENCES

[1] Jiang, Y., Pang, H., and Liao, B. (2009) *Journal of Hazardous Materials*, 164: 1-9.

[2] Larous, S., Meniai, A. H., and Lehocine, M. B. (2005) *Desalination*, 185: 483-490.

[3] Dean, J. G., Bosqui, F. L., and Lanouette, K. H. (1972) *Environmental Science Technology*, 6(6): 518-522.

[4] Amuda, O .S., Amoo, I. A., and Ajayi, O. O. (2006) *Journal of Hazardous Materials*, B129: 69-72.

[5] Ahmad A., Rafatullah M., Sulaiman O., Ibrahim M. H., Chii Y. Y., and Siddique B. M. (2009) *Desalination*, 247: 636-646.

[6] Rafatullah, M., Sulaiman, O., Hashim, R., and Ahmad, A. (2009) *Journal of Hazardous Materials*,170: 969-977.

[7] Aydiner, C., Bayramoglu, M., Kara, S., Keskinler, B., and Ince, O. (2006) *Industrial Engineering Chemistry Research*, 45: 3926-3933.

[8] Sumathi, S., Chai, S. P., and Mohamed, A.R. (2008) *Renewable and Sustainable Energy Reviews,* (12): 2404-2421.

[9] Ahmad, A., Rafatullah, M., and Danish, M. (2007) *Holz als Roh und Werkstoff,* 65: 429-436.

[10] Danish, M., Sulaiman, O., Rafatullah, M., Hashim, R., and Ahmad, A. (2010) *Journal of Dispersion Science & Technology*, 31: 248-259.

[11] Amuda, O. S., Giwa, A. A., and Bello, I. A. (2007) *Biochemical Engineering Journal*, 36: 174-181.

[12] Afkhami, A., Madrakian, T., Amini, A., and Karimi, Z. (2008) *Journal of Hazardous Materials,* 150: 408-412.

[13] Choi, H. D., Cho, J. M., Baek, K., Yang, J. S., and Lee, J. Y. (2009) *Journal of Hazardous Materials*, 161: 1565-1568.

[14] Namasivayam, C., and Sureshkumar, M. V. (2006) *Journal of Applied Polymer Science*, 100: 1538-1546.

[15] Wan Ngah, W. S., and Hanafiah, M. A. K. M., (2008) *Biochemical Engineering Journal*, 39: 521-530.

[16] Freundlich, H., (1907) *Zeitschrift für Physikalische Chemie,* 57: 385-470.

[17] Langmuir, I., (1981) *Journal of the American Chemical Society*, 40: 1361-1403.

[18] Lagergren, S. (1898) *kungliga Svenska Vetenskapsakademiens, Handlingar, Band,* 24: 1-39.

[19] Ho, Y. S., Ng, J. C. Y., and Mckay, G. (2000) *Separation Purification Methods*, 29: 189-232.

[20] Eren, E. (2008) *Journal of Hazardous Materials,* 159: 235-244.

[21] Demirbas, E., Dizge, N., Sulak, M. T., and Kobya, M. (2009) *Chemical Engineering Journal*, 148: 480-487.

[22] Feng, N., Guo, X., and Liang, S. (2009) *Journal of Hazardous Materials*, 164: 1286-1292.

[23] Popuri, S. R., Vijaya, Y., Boddu, V. M., and Abburi, K. (2009) *Bioresource Technology*, 100: 194-199.

[24] Sulaiman, O., Amini, M. H. M., Rafatullah, M., Hashim, R., and Ahmad, A. (2010) *International Journal of Chemical Reactor Engineering*, 8: A108.

Figure Captions

FIG. 1. SEM micrographs of SDBS-modified-OPLP (magnification 500): (a) before adsorption and (b) after adsorption.

FIG. 2. Effect of contact time and initial concentration for the adsorption of copper (II) ions: pH = 6, Temperature = 30 °C, Volume of solution = 50 ml, Adsorbent dosage = 10 g/L.

FIG. 3. Effect of solution pH for the adsorption of coper (II) ions: Contact time = 120 min., Initial concentration = 100 mg/L, Temperature = 30 °C, Volume of solution = 50 ml, Adsorbent dosage = 10 g/L.

FIG. 4. Effect of adsorbent dosage for the adsorption of copper (II) ions: Contact time = 120 min., pH = 6, Initial concentration = 100 mg/L, Temperature = 30 °C, Volume of solution = 50 ml.

FIG. 5. Freundlich adsorption isotherm plots for the adsorption of copper (II) ions at 30°C.

FIG. 6. Langmuir adsorption isotherm plots for the adsorption of copper (II) ions at 30°C.

FIG. 7. First-order-reversible kinetic plots for copper (II) adsorption onto SDBS-modified-OPLP.

FIG. 8. Pseudo-first-order kinetic plots for copper (II) adsorption onto SDBS-modified-OPLP.

FIG. 9. Pseudo-second-order kinetic plots for copper (II) adsorption onto SDBS-modified-OPLP.

TABLE 1

Adsorption isotherm constants and correlation coefficients for the adsorption of copper (II) ions onto SDBS-modified-OPLP at 30 °C

Freundlich isotherm constants	**Langmuir isotherm constants**
K_F (mg/g) = 75.98	b (mg/g) = 86.95
n = 1.146	K_L (L/mg) = 1.353
R^2 = 0.989	R^2 = 0.785

TABLE 2

First-order-reversible-reaction, Pseudo-first-order and pseudo-second-order models for the adsorption of copper (II) onto SDBS-modified-OPLP at different concentrations

Kinetic Models and its Parameters	**Initial concentrations (mg/L)**				
	10	20	50	100	200
$q_{e,\,exp.}$ (mg/g)	1.023	1.524	1.820	2.534	3.286
First-order-reversible-reaction kinetic model					
k_n (min^{-1})	0.426	0.033	0.031	0.028	0.018
k_1 (min^{-1})	0.032	0.024	0.023	0.019	0.010
k_{-1} (min^{-1})	0.010	0.009	0.008	0.009	0.008
K_c	3.210	3.015	2.654	2.201	1.532
R^2	0.964	0.937	0.981	0.954	0.955
Pseudo-first-order kinetic model					
$q_{e,\,cal.}$ (mg/g)	0.014	0.016	0.025	0.036	0.139
k_1' (min^{-1})	0.043	0.035	0.030	0.027	0.018
R^2	0.971	0.953	0.974	0.931	0.956
Pseudo-second-order kinetic model					
$q_{e,\,cal.}$ (mg/g)	0.280	0.517	1.077	2.012	3.656
k_2 (g $mg^{-1}min^{-1}$)	0.223	0.328	0.342	0.268	0.372
h (mg $g^{-1}min^{-1}$)	0.017	0.087	0.396	1.084	4.972
R^2	0.990	0.995	0.996	0.992	0.997

TABLE 3

Comparison of adsorption capacities of various adsorbents for copper (II) ions

Adsorbents	Adsorption capacity (mg/g)	Refferences
SDBS-modified-OPLP	75.98	This study
Modified bagasse	101.01	(Jiang et al., 2009)[1]
Raw bentonite	42.41	(Eren, 2008)[20]
Hazelnut shell activated carbon	51.52	(Demirbas et al., 2009)[21]
Orange peel	44.28	(Feng et al., 2009)[22]
Chitosan coated PVC beads	87.92	(Popuri et al., 2009)[23]
Unmodified OPLP	11.22	(Othman et al., 2010)[24]

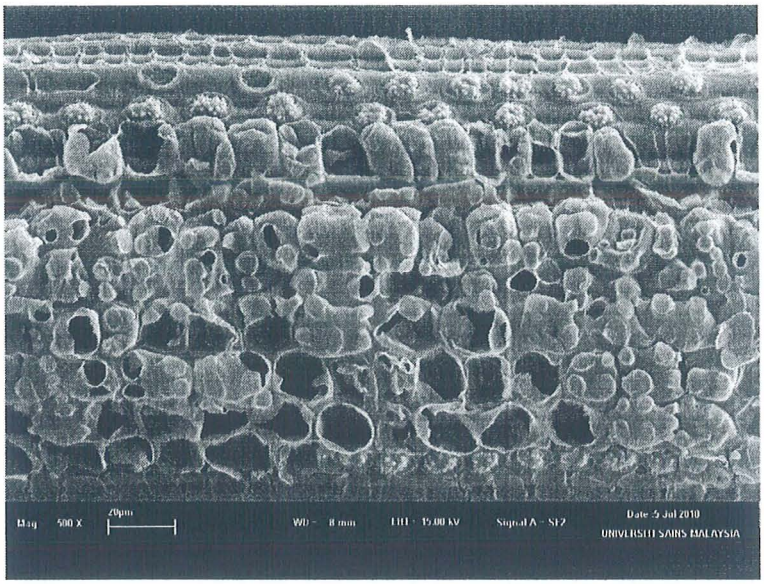

(a)

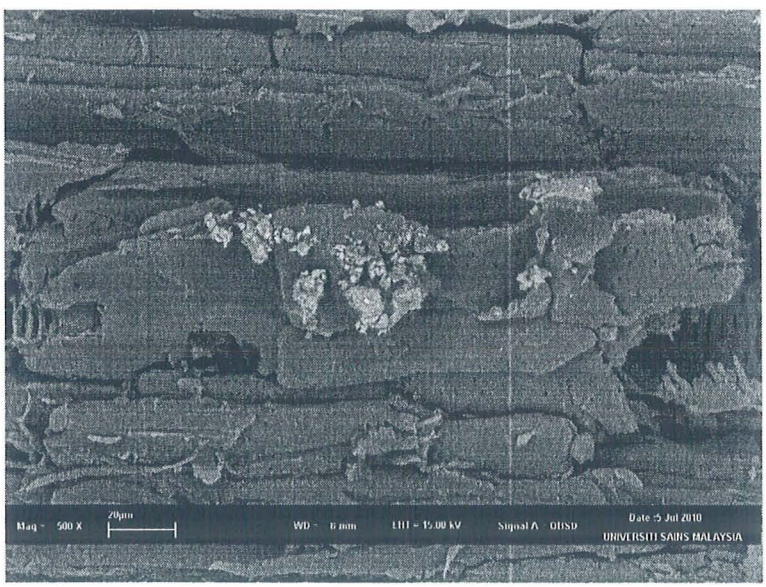

(b)

FIG. 1. SEM micrographs of SDBS-modified-OPLP (magnification 500): (a) before adsorption and (b) after adsorption.

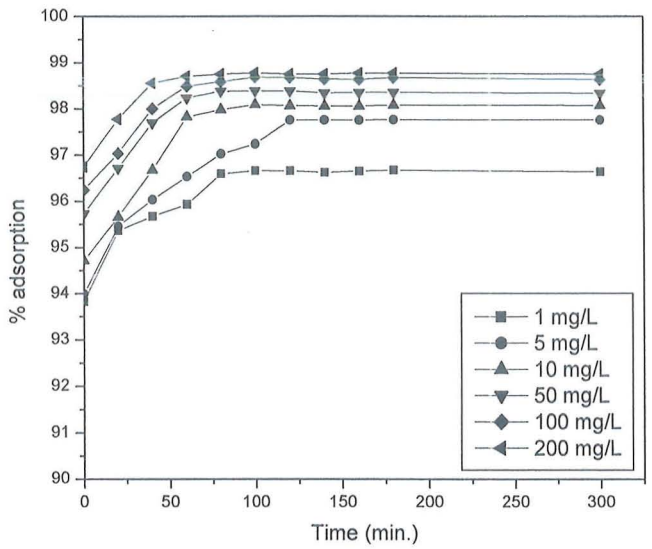

FIG. 2. Effect of contact time and initial concentration for the adsorption of copper (II) ions: pH = 6, Temperature = 30 °C, Volume of solution = 50 ml, Adsorbent dosage = 10 g/L.

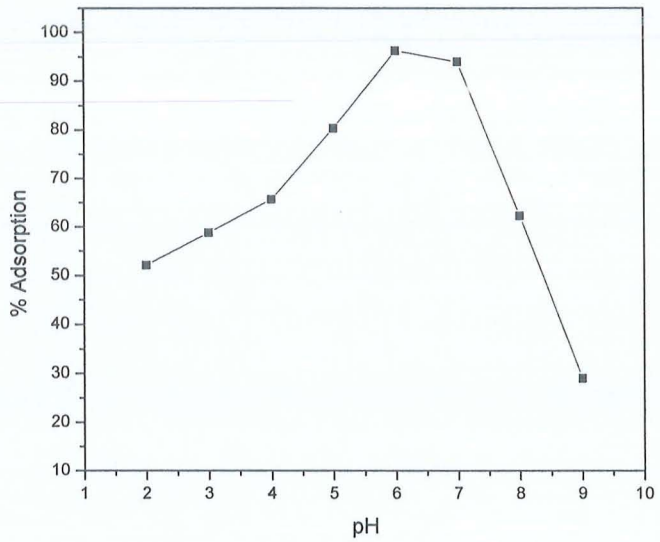

FIG. 3. Effect of solution pH for the adsorption of coper (II) ions: Contact time = 120 min., Initial concentration = 100 mg/L, Temperature = 30 °C, Volume of solution = 50 ml, Adsorbent dosage = 10 g/L.

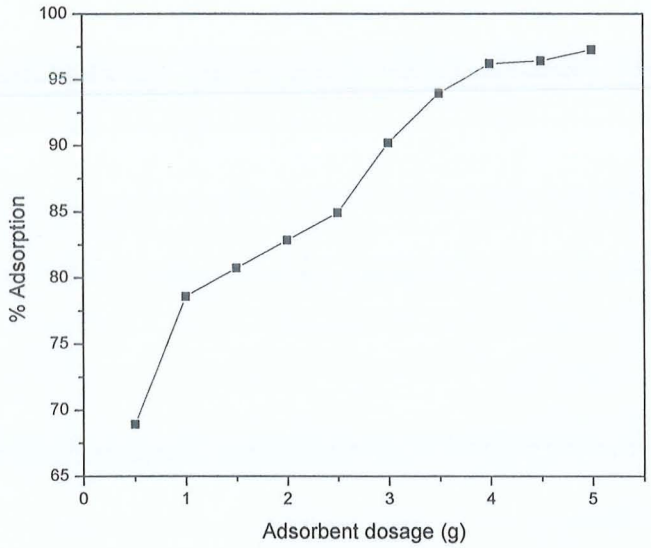

FIG. 4. Effect of adsorbent dosage for the adsorption of copper (II) ions: Contact time = 120 min., pH = 6, Initial concentration = 100 mg/L, Temperature = 30 °C, Volume of solution = 50 ml.

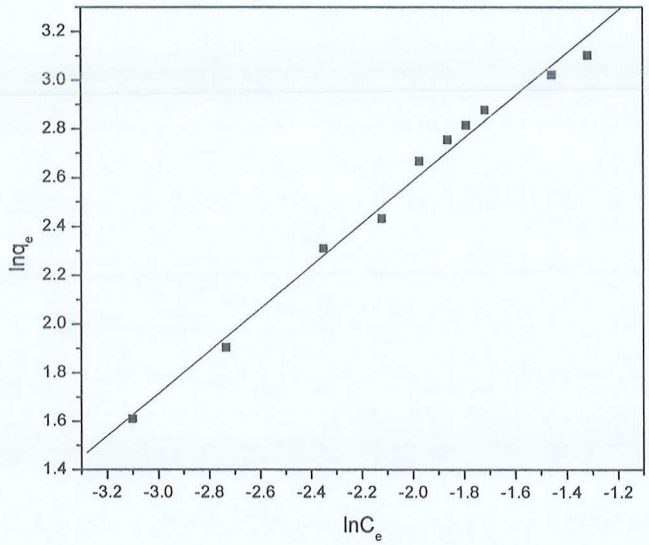

FIG. 5. Freundlich adsorption isotherm plots for the adsorption of copper (II) ions at 30°C.

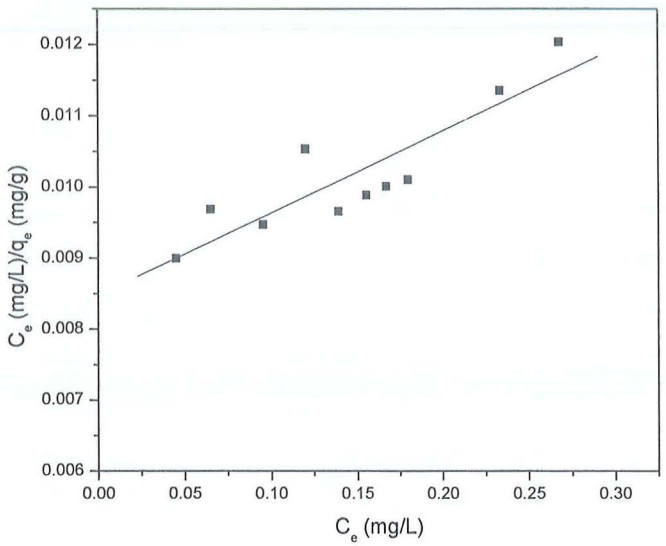

FIG. 6. Langmuir adsorption isotherm plots for the adsorption of copper (II) ions at 30°C.

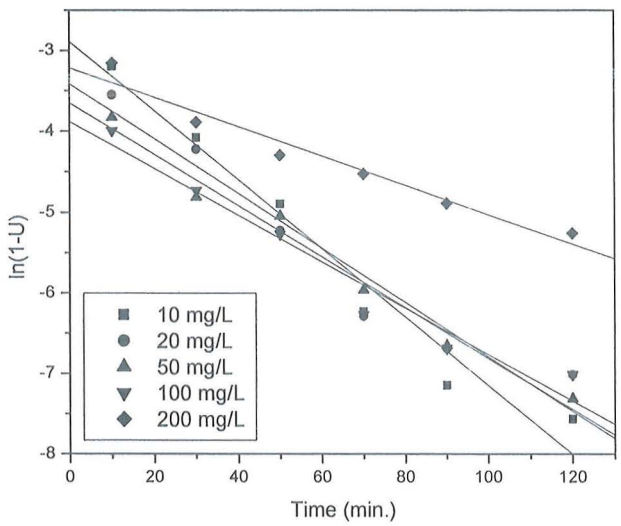

FIG. 7. First-order-reversible kinetic plots for copper (II) adsorption onto SDBS-modified-OPLP.

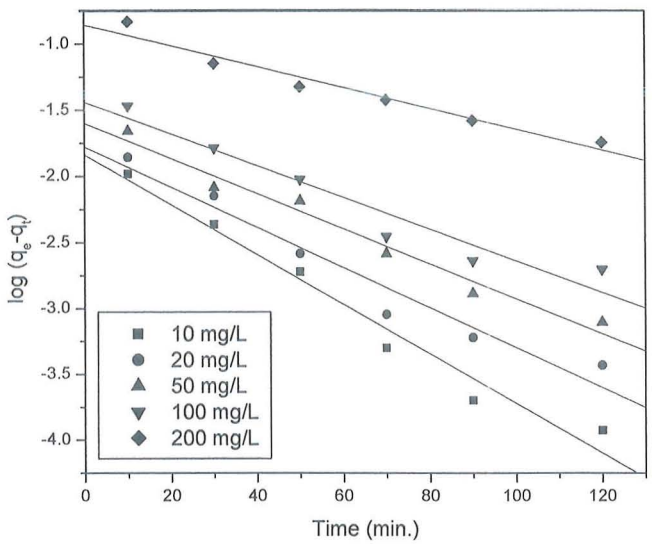

FIG. 8. Pseudo-first-order kinetic plots for copper (II) adsorption onto SDBS-modified-OPLP.

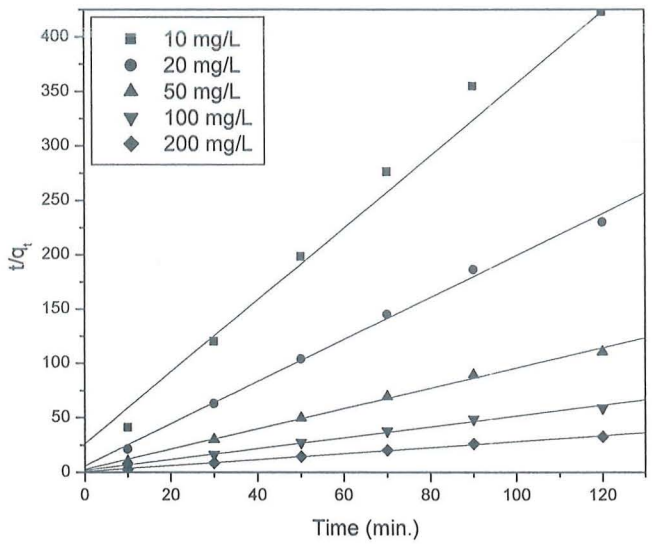

FIG. 9. Pseudo-second-order kinetic plots for copper (II) adsorption onto SDBS-modified-OPLP.

INTERNATIONAL JOURNAL OF CHEMICAL REACTOR ENGINEERING

Volume 8 2010 *Article* A108

Adsorption Equilibrium and Thermodynamic Studies of Copper (II) Ions from Aqueous Solutions by Oil Palm Leaves

Othman Sulaiman* Mohd Hazim Mohamad Amini† Mohd Rafatullah‡
Rokiah Hashim** Anees Ahmad††

*Universiti Sains Malaysia, othman@usm.my
†Universiti Sains Malaysia, ahjim120@yahoo.com
‡Universiti Sains Malaysia, mohd_rafatullah@yahoo.co.in
**Universiti Sains Malaysia, hrokiah@usm.my
††Universiti Sains Malaysia, anees@usm.my

ISSN 1542-6580

Adsorption Equilibrium and Thermodynamic Studies of Copper (II) Ions from Aqueous Solutions by Oil Palm Leaves*

Othman Sulaiman, Mohd Hazim Mohamad Amini, Mohd Rafatullah, Rokiah Hashim, and Anees Ahmad

Abstract

Oil palm leaf powders (OPLP), an agricultural waste material, were used as new non-conventional and low-cost adsorbents for the removal of copper (II) ions from aqueous solution. Batch studies were performed to evaluate and optimize the effects of various parameters such as contact time, pH of the solution, initial metal ion concentrations and adsorbent dosage. Langmuir, Freundlich and Temkin isotherms were used to analyze the equilibrium data at different temperatures. The experimental data fit well with the Langmuir adsorption isotherm, indicating thereby the mono layer adsorption of the copper (II) ions. The monolayer sorption capacity of OPLP for copper (II) ions was found to be 11.22 mg/g at 30 °C. The thermodynamic parameters like standard free energy, standard enthalpy, and standard entropy changes for the adsorption of copper (II) ions have also been computed and discussed. The heat of adsorption [ΔH° = -39.84 kJ/mol] implied that the adsorption was exothermic in nature.

KEYWORDS: oil palm leaf, adsorption, copper (II), isotherm, thermodynamic

*The authors acknowledged the Universiti Sains Malaysia (Short Term Research Grant Scheme (304/PTEKIND/639062), Fellowship to M. H. M. Amini and the Postdoctoral Fellowship to M. Rafatullah.

1. INTRODUCTION

Heavy metals are found in the wastewater streams of industrial processes, including textiles, metal plating to metal finishing, mining operations, tanneries, automotive, battery manufacturing, steel industries, paint manufacturing and electronic industries as well as improper disposal of metal based materials (Bryant et al., 1992; Nag, 1995; Shukla et al., 2002).

Copper was among the hazardous material that pollute the environment. Copper is used as a metal in machinery, construction, transportation and military weapons as well as an important component of white gold and other alloys used for imitation of jewellery. Containers involving copper materials may contaminate the products such as food, water or drink. Copper is essential to human life and health however, like all heavy metals, it is also potentially toxic. As an example, an intake of excessively large doses by man may lead to severe mucosal irritation, a central nervous system irritation, possible necrotic changes in the liver and kidney, etc. (Larous et al., 2005). The permissible limit of Cu is 2.5 mg/L in drinking water (Balkose and Baltacioglu, 1992).

In developed countries, removal of heavy metals from wastewater is normally achieved by advanced technologies such as ion exchange, chemical precipitation and electrochemical deposition (Jiang et al., 2009). But these technologies do not seem to be economically feasible because of their relatively high costs and that developing countries may not afford such technologies. Therefore, there is a need to look into alternatives to investigate a low-cost method, which is effective and economical. To overcome this difficulty there is a strong need to develop cheap adsorbents, which can be used in developing countries.

At present, there is growing interest in using low-cost, commercially available materials for the adsorption of heavy metals (Aydin et al., 2008). The use of agricultural wastes for the treatment of polluted water is also an attractive and promising option for the environment (Larous et al., 2005). A wide variety of agricultural waste materials such as modified bark (Gloaguen and Morvan, 1997), sawdust (Ajmal et al., 1998; Shukla et al., 2002; Rafatullah et al., 2009; Ahmad et al., 2009), orange peel (Feng et al., 2009), teak leaves powder (King et al., 2006), *Pinus sylvestris* biomass (Ucun et al., 2009) soybean straw (Zhu et al., 2008) bagasse (Jiang et al., 2009), pecan nutshell (Vaghetti et al., 2009), papaya wood (Saeed et al., 2005) and rubber tree leaf (Ngah and Hanafiah, 2008) are being used as low-cost alternatives to expensive adsorbents.

Attention was given to utilization of oil palm leaf as an adsorbent for removal of copper (II) ions from aqueous solution. Malaysia was the largest producer and exporter of palm oil in the world in 2006, comprising of 52 % or 26.3 million tonnes of the total world oil and fat production and the demand is

forecasted to be increasing each year, which means more and more waste will be produced (Sumathi et al., 2008). Leaf from oil palm tree could be easily obtained in large amount and at low cost. Further researches could open possibility of using oil palm leaf waste in industrial wastewater pollution management. The aim of this paper is to assess the potential of oil palm leaf powders (OPLP) for uptake of copper (II) ions from aqueous solutions. The effects of contact time, pH of metal solution, dosage of adsorbent and initial concentration of metal ion solution were studied. The adsorption isotherm and probable mechanism were explained. The thermodynamic parameters for the sorption of copper (II) ions have also been computed and discussed.

2. MATERIALS AND METHODS

2.1 Adsorbent

Oil palm leaves (*Elaeis guineensis*) were used as adsorbent for the sorption of copper (II) ions from aqueous solutions. It was collected from Kedah, Malaysia. Oil palm leaves were washed with deionized water to remove dust and soluble impurities. The leaves were dried, ground and sieved to a constant size of 250μ-500μ. OPLP was washed extensively again with distilled water for several times and dried in an oven at 60 ± 5^{0}C for 48 hours. The OPLP was placed in an airtight container for further use.

2.2 Adsorbate Solutions

Stock solution of metal ions were prepared by dissolving copper (II) nitrate hemipentahydrate ($Cu(NO_3)_2 \cdot 2.5H_2O$) into distilled water to a concentration of 1000mg/L. Stock solution was further diluted to different desired concentrations. All the chemicals used were of analytical reagent grade and were obtained from Sigma-Aldrich and Fluka (Germany).

2.3 Scanning Electron Microscopy, Fourier Transform Infrared Study and Surface Area Analysis

Scanning electron microscopy (Carl-Ziess SMT, Oberkochen, Germany) analysis was carried out on OPLP to study its surface morphology before and after adsorption of copper (II) ions. Fourier Transform Infrared (Nicolet, AVATAR FTIR-360) analysis was done on the natural OPLP and copper (II) adsorbed OPLP to determine the surface functional groups that might be involved in copper (II) ions sorption and the spectra were recorded from 4000 to 400 cm^{-1}. The

surface area of OPLP was determined using a Micromeritics ASAP 2010 gas adsorption surface analyzer.

2.4 Batch Adsorption Studies

Batch adsorption studies were carried out by shaking 0.5 g of the OPLP with 50 ml of the aqueous solutions of copper (II) in different conical flasks using a temperature-controlled shaker. The solution-adsorbents mixtures were stirred at 125 rpm and at the end of pre-determined time interval the reaction mixtures were filtered out and analyzed for its metal ion concentrations using Atomic Absorption Spectrometer, AAS (Analyst 100 Perkin Elmer). The adsorption experiments were also conducted to determine the equilibrium time (20, 40, 60, 80, 100, 120, 140, 160, 180, 200 and 240 min.), pH of the solution (1, 2, 3, 4, 5, 6, 7 and 8), initial concentrations (1, 10, 25, 50 and 100 mg/L),dosage of the adsorbent (0.1, 0.2, 0.3, 0.4, 0.5, 1.0, 1.5, 2.0, 2.5 and 3.0 g) and temperatures (25, 30, 40, 50 and 60 °C) for maximum adsorption. All the investigations were carried out in triplicate to avoid any discrepancy in experimental results. Metal solution controls were kept throughout the experiment to maintain quality control. The percentage of metal adsorption by the adsorbents was computed using the equation:

$$\% \text{ adsorption} = \{(Ci - Ce) / Ci\}\ 100 \qquad (1)$$

where Ci and Ce are the initial and equilibrium concentration of metal ion (mg/L) in the solution.

3. RESULTS AND DISCUSSION

3.1 Characterization of Adsorbent

The Brunauer-Emmett-Teller (BET) surface area and average pore diameter were determined. The value of BET surface area, under the detection level of the apparatus is 1.435 m^2g^{-1}. Pore sizes are classified in accordance with the classification adopted by the International Union of Pure and Applied Chemistry (IUPAC), that is, micropores (diameter (d) < 20Å), mesopores (20Å < d < 500Å), and macropores (d > 500Å). The average pore diameter determined by Barrett-Joiner-Halenda (BJH) method was 62.48 Å, suggesting that OPLP consists of mesopores.

The SEM micrograph of OPLP is shown in Figure 1. Figure 1a shows the OPLP possesses a surface morphology with pores of regular sizes. These pores

are useful to copper (II) ions adsorption. OPLP loaded with copper (II) ions Figure 1b, however, shows the surface of OPLP is covered with copper (II) ions. The surface of copper (II) loaded adsorbent is different from the surface of natural adsorbent.

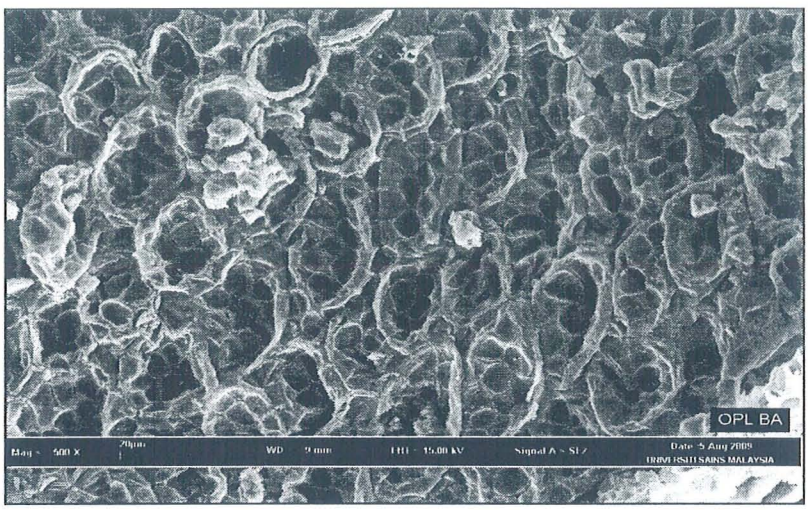

(a)

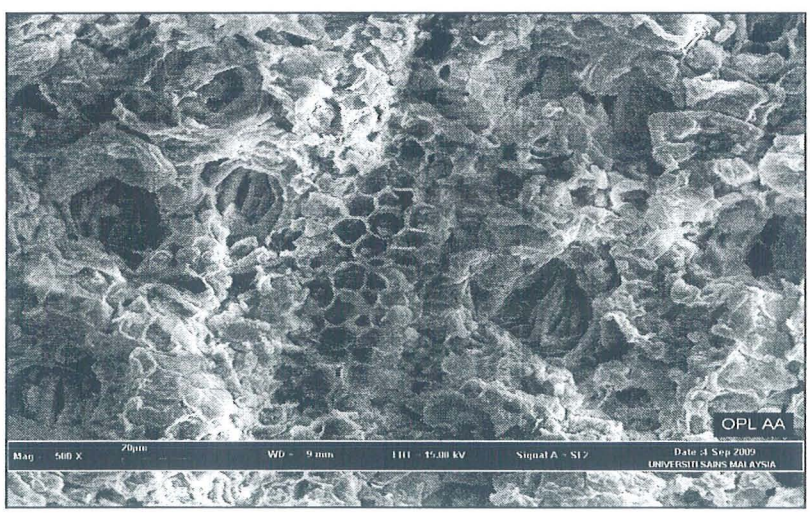

(b)

Figure 1. SEM micrographs of OPLP (magnification 500): (a) before adsorption and (b) after adsorption

The FTIR spectrum of OPLP before and after adsorption showed that some peaks were altered during the treatment (Figure 2 and Table 1). A peak at 3420 cm^{-1} was detected, representing O-H stretching of phenolic group of cellulose and lignin. Peaks at 2923 cm^{-1} and 2857 cm^{-1} showed presence of C-H stretching of aliphatic compounds. Peaks were also detected at 1732 cm^{-1}, 1649 cm^{-1} and 1513 cm^{-1} which indicates availability of C=O stretching, -C=C- stretching and N-O asymmetric stretching of aldehydes, alkenes and nitro compounds respectively. C-C stretching of aromatic compound was detected at 1458 cm^{-1} whereas CH_3 bending appeared at 1375 cm^{-1}. There is C-N stretching of aromatic amines at 1325 cm^{-1} while peaks at 1239 cm-1 and 1061 cm-1 might be C-O stretching of alcohols, carboxylic acids, esters and ethers (Rafatullah et al., 2009). Slight changes were detected within the peaks of FTIR spectrum after adsorption process as shown in Figure 2b. Changes in functional groups were believed due to involvement of them in sorption process either through chemical complexation or through physical Van der Waals forces. The characterization of the solid support showed that its morphology is represented by mesopores a fact which explain the moderate specific area. An elementary analysis by FTIR confirms the presence of the different identified functional groups which are responsible for this change.

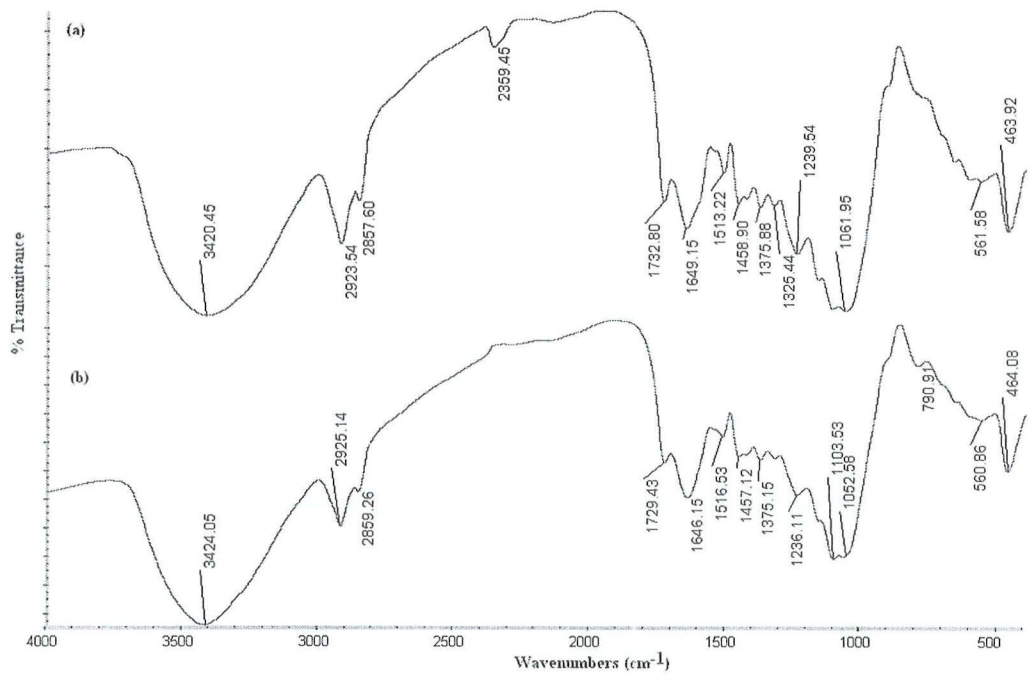

Figure 2. FTIR spectra of OPLP: (a) before adsorption and (b) after adsorption

Table 1. FTIR of OPLP

S. No.	Frequency (cm^{-1})		Differences	Assignment
	Before adsorption	After adsorption		
1	3420	3424	-4	O–H stretching
2	2923	2925	-2	C–H stretching
3	2857	2859	-2	C–H stretching
4	2359	-	-	N-H stretching
5	1732	1729	3	C=O stretching
6	1649	1646	3	–C=C– stretching
7	1513	1516	-3	N–O asymmetric stretch
8	1458	1457	1	C–C stretch (in–ring)
9	1375	1375	0	CH_3 bending
10	1325	-	-	C-N stretching
11	1239	1236	3	C–O stretch
12	-	1103	-	C–O stretch
13	1061	1052	9	C–O stretch

3.2 Effect of Contact Time and Initial Metal Concentration

The effect of time and amount of copper (II) ions adsorbed for different initial concentration by OPLP is shown in Figure 3. It can be seen from the figure that the adsorption at different concentrations is rapid in the initial stages and gradually decreases with the progress of adsorption until the equilibrium is reached. The adsorption of copper (II) ions increases with time and attain saturation in about 120-180 minutes. The adsorption capacity of copper (II) ions is rapid initially but it is constant with lapse of time. The figure reveals that maximum adsorption of copper (II) ions was attained after about 120 minutes. The rate of adsorption capacity is higher in the beginning due to larger surface area of the OPLP being available for the adsorption of the metal ions, and after a lapse of time the remaining vacant surface sites are difficult to be occupied due to repulsive forces between the solute molecules on the solid and bulk phases. For subsequent experiment, the contact time was thus maintained for 180 minutes to ensure that equilibrium could be achieved. On changing the initial concentration from 1 to 100 mg/L, the amount adsorbed increased from 5.82 to 11.23 mg/g. The plots are smooth and continuous, suggesting the possible monolayer adsorption of copper (II) ions on the surface of OPLP. Consequently, the concentration of copper (II) ions will greatly affect the extent and rate of copper (II) ions uptake onto surface of OPLP.

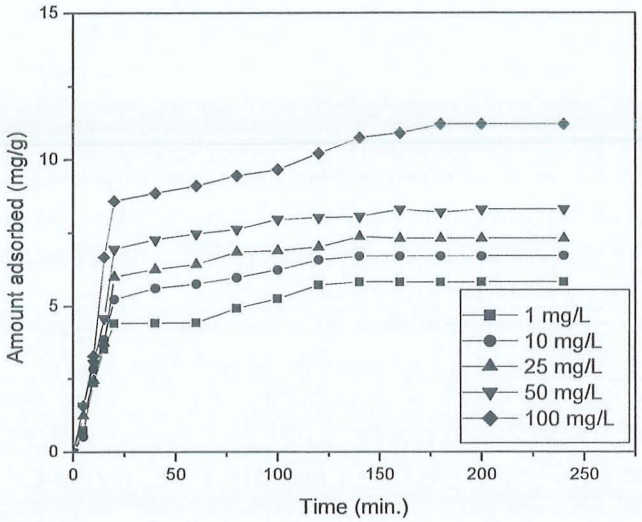

Figure 3. Effect of contact time and initial metal ions concentration on copper (II) ions adsorption: pH = 6, Temperature = 30 °C, Volume of solution = 50 ml, Adsorbent dosage = 10 g/L.

3.3 Point of Zero Charge (pH_{PZC}) Measurements and Effect of pH

The pH of the solutions has an important variable governing metal adsorption. In general, adsorption of cations is favoured at pH > pH_{PZC}. The effect of pH on the adsorption of copper (II) ions by OPLP was studied by varying pH of the solution over the range of 1-8 using different concentration. The determination of pH_{PZC} of OPLP was performed according to the solid addition method [Ngah and Hanafiah, 2008]. 50mL of 0.01M KNO_3 solution was placed in conical flasks in temperature controlled shaker. The initial pH of the solutions was adjusted to a value between 2 and 9 by adding 0.1M HCl or NaOH solutions. Then, 1 g of OPLP was added to each flask, strirred and the final pH of the solutions was measured after 24 h. The value of pH_{PZC} can be determined from the curve that cuts the pH_0 line of the plot ΔpH versus pH_0. The pH_{PZC} of an adsorbent is a very important characteristic that determines the pH at which the adsorbent surface has net electrical neutrality. At this value, the acidic or basic functional groups no longer contribute to the pH of the solution. The value of pH_{PZC} is close to the value of pH of aqueous slurry which is 5.9.

The effect of pH on the adsorption of copper (II) ions on OPLP is presented in Figure 4. It shows that the adsorption of the copper (II) ions in the pH range of 1 to 5 varies between 15 % and 65 %. The percentage removal of copper (II) ions was minimum at the pH 1 and increased with further increase in pH. At pH value lower than 3, the adsorption capacities were found to be low due

to the competitive adsorption of HO_3^+ ions and metal ions for the same active adsorption site (Shukla et al., 2002). As the pH increased, the adsorption surface become less positive and therefore electrostatic attraction between the metal ions and OPLP surface is likely to be increased (Rafatullah et al., 2009). At pH 6 there are three species present in solution as suggested by Elliot and Huang in 1981, (i) Cu^{2+} (in very small quantity) and (ii) $CuOH^+ = Cu(OH)_2$ (in large quantity), These species are adsorbed at the surface of adsorbent by ion exchange mechanism with the functional groups present in adsorbent or by hydrogen bonding as shown below:

$$\left.\begin{array}{r} 2\,(-\mathrm{ROH}) + \mathrm{M}^{2+} \rightarrow 2\,(\mathrm{RO})\,\mathrm{M} + 2\mathrm{H}^+ \\ -\mathrm{ROH} + \mathrm{M(OH)}^+ \rightarrow (-\mathrm{RO})\,\mathrm{M(OH)} + \mathrm{H}^+ \\ 2\,(-\mathrm{ROH}) + \mathrm{M\,(OH)_2} \rightarrow (-\mathrm{ROH})_2 + \mathrm{M(OH)_2\,H} \text{ — bonding} \end{array}\right\} \text{Ion- exchange}$$

where M represents the metal ions and R represents the matrix of OPLP, respectively.

However, at higher pH values of 6 to 8 the metal adsorption decreased. A decrease in adsorption at high pH is due to the formation of soluble hydroxyl complexes. The maximum sorption efficiency is around pH 6 (Ajmal et al., 1998). Therefore, pH 6 was selected to be the optimum pH for further studies.

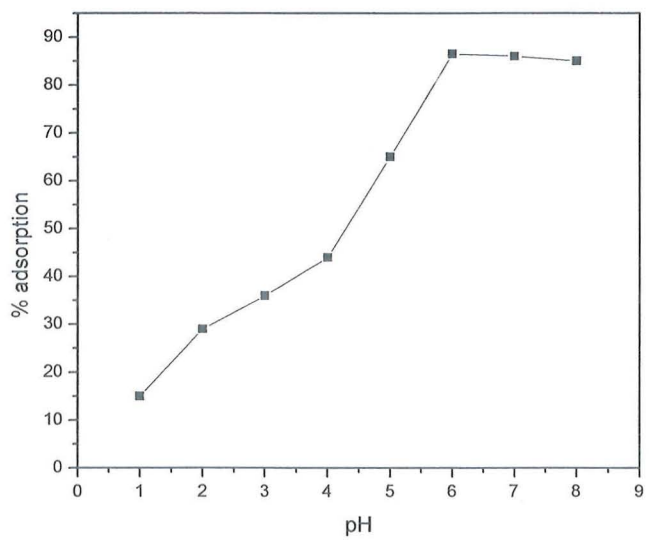

Figure 4. Effect of the solution pH on copper (II) ions adsorption: Contact time = 180 min., Initial concentration = 100 mg/L, Temperature = 30 °C, Volume of solution = 50 ml, Adsorbent dosage = 10 g/L.

3.4. Effect of Adsorbent Dosage

Adsorbent dosage is an important parameter because it determines the capacity of an adsorbent for a given concentration of the adsorbate. The adsorption studies of copper (II) ions on OPLP was done at 30°C temperature by varying the quantity of adsorbent from 0.1 g to 3.0 g while keeping the volume of the metal solutions constant at pH 6. When the adsorbent dosage was increased from 0.1 to 3.0 g the amount adsorbed per unit mass of adsorbent decreases considerably as shown in Figure 5. The decrease in unit adsorption with increase in the dose of adsorbent is due to the increase in active sites on the adsorbent and thus making easier penetration of the metal ions to the adsorption sites (Aydin et al., 2008).

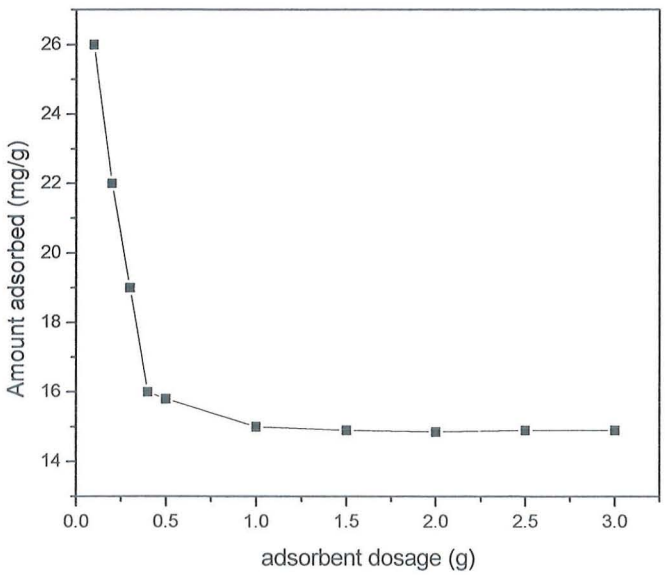

Figure 5. Effect of adsorbent dosage on copper (II) ions adsorption: Contact time = 180 min., pH = 6, Initial concentration = 100 mg/L, Temperature = 30 °C, Volume of solution = 50 ml.

3.5 Adsorption Behaviour of OPLP (Isotherm Studies)

To quantify the adsorption capacity of OPLP for the removal of copper (II) from aqueous solution, the Langmuir, Freundlich and Temkin isotherm models were used. A trial and error procedure was used to determine the three isotherms parameters by minimizing the respective coefficient of determination between experimental data and isotherms.

3.5.1 Langmuir Model

This model assumes that the adsorptions occur at specific homogeneous sites on the adsorbent and is used successfully in many monolayer adsorption processes (Langmuir, 1918). The data of the equilibrium studies for adsorption of copper (II) onto OPLP may follow the following form of Langmuir model:

$$Ce/A_m = (1/b)\,(1/K_L) + (1/b)\,(Ce) \qquad (2)$$

where Ce is the equilibrium concentration (mg/L) and A_m is the amount adsorbed per unit mass of adsorbent (mg/g), K_L is the Langmuir equilibrium constant that is related to the heat of adsorption and b is the monolayer capacity. The Langmuir type adsorption isotherm indicates surface homogeneity of the adsorbent and hint towards the conclusion that the surface of adsorbent is made up of small adsorption patches which are energetically equivalent to each other in respect to adsorption phenomenon. The correlation coefficient (R^2) values of 0.981 to 0.991 indicated that the adsorption data of copper (II) ions onto OPLP was well fitted to the Langmuir isotherm. The values of constants K_L and b were calculated and reported in Table 2.

3.5.2 Freundlich Model

The Freundlich model can be applied for non-ideal adsorption on heterogeneous surfaces and multilayer adsorption (Freundlich, 1906). According to this model:

$$A_m = (K_F)\,(Ce^{1/n}) \qquad (3)$$

$$\ln A_m = \ln K_F + 1/n \ln Ce \qquad (4)$$

where, K_F is the measure of sorption capacity, 1/n is sorption intensity and rest of the terms have the usual significance. The related parameters were calculated and reported in Table 2. The Freundlich type adsorption isotherm is an indication of surface heterogeneity of the adsorbent and thus is responsible for multilayer adsorption due to the presence of energetically heterogeneous adsorption sites.

3.5.3 Temkin Model

Temkin and Pyzhev (1934) considered the effects of indirect adsorbate/adsorbate interactions on adsorption isotherms. The Temkin isotherm has been used in the form as follows:

$$A_m = (RT/b) \ln (K_T Ce) \qquad (5)$$

This equation can be expressed in its linear form as

$$A_m = B \ln K_T + B \ln Ce \qquad (6)$$

where B = (RT/b), K_T is the Temkin equilibrium binding constants (L/mg) corresponding to the maximum binding energy and constant B is related to heat of adsorption. The heat of adsorption of all the molecules in the layer would decrease linearly with coverage due to adsorbate/adsorbate interactions. The constants K_T and B together with the R^2 values are shown in Table 2.

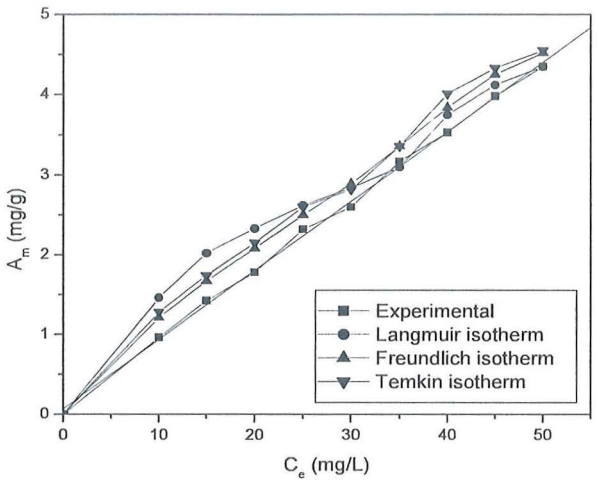

Figure 6. Adsorption isotherm plots for the adsorption of copper (II) ions at 30°C

Table 2. Adsorption isotherm constants and correlation coefficients for the adsorption of copper (II) ions on OPLP at 30°C

Adsorption isotherms	Parameters
Langmuir adsorption isotherm	
b (mg/g)	11.22
K_L (L/mg)	0.393
R^2	0.994
Freundlich adsorption isotherm	
K_F (mg/g)(L/mg)$^{1/n}$	01.63
1/n	0.080
R^2	0.966
Temkin adsorption isotherm	
K_T (L/mg)	0.089
B	18.66
R^2	0.989

From Table 2, the Langmuir adsorption isotherm model yielded best fit as indicated by the highest R^2 values at all temperatures compared to the Freundlich and Temkin adsorption isotherm models. Table 3 lists a comparison of maximum monolayer adsorption capacity of copper (II) ions on various agricultural waste adsorbents. OPLP is found to have a relatively good adsorption capacity of 11.22 mg/g and this indicates that it could be considered a promising material for the removal of copper (II) ions from aqueous solutions.

Table 3. Comparison of maximum adsorption capacities of different adsorbents for copper (II) ions

Adsorbents	Adsorption capacity (mg/g)	Contact time (h)	Concentration range (mg/L)	pH	Temp. range (K)	References
Shells of wheat	17.42	3	100-500	6	293 -333	Aydin et al., 2008
Shells of lentil	09.59	3	100-500	6	293-333	Aydin et al., 2008
Shells of rice	02.95	3	100-500	6	293-333	Aydin et al., 2008
sawdust	01.79	3	05-50	7	296	Yu et al., 2000
Rubber tree leaf	08.92	1	03-10	5	300-320	Ngah and Hanafiah, 2008
Meranti sawdust	32.05	2	01-200	6	303	Rafatullah et al., 2009
Modified meranti sawdust	37.17	1	25-250	6.6	303-333	Ahmad et al., 2009
Oil palm leaf powders (OPLP)	11.22	3	01-100	6	303-323	This study

3.6 Effect of Temperature

Temperature is a highly significant parameter in the adsorption processes. The adsorption of copper (II) ions from 25 to 60 °C with a maximum adsorption at 30 °C is shown in Figure 7. The enhanced adsorption might be due to the desolvation of the copper (II) ions, changes in the size of the pores and enhanced rate of intraparticle diffusion of copper (II) ions. However, after 30 °C, desorption of the copper (II) ions increases leading to a net decrease in adsorption from 30-50 °C. The percent adsorption decreases sharply above 30 °C due to enhanced rate of desorption. The decreasing trend of adsorption with temperature is mainly due to the weakening of adsorptive forces between the active sites of OPLP and the copper (II) ions (Helfferich, 1962). The extent of decrease in adsorption of solute of definite concentration with increase in temperature depends on the nature of the adsorbent-adsorbate system (Panday et al., 1986).

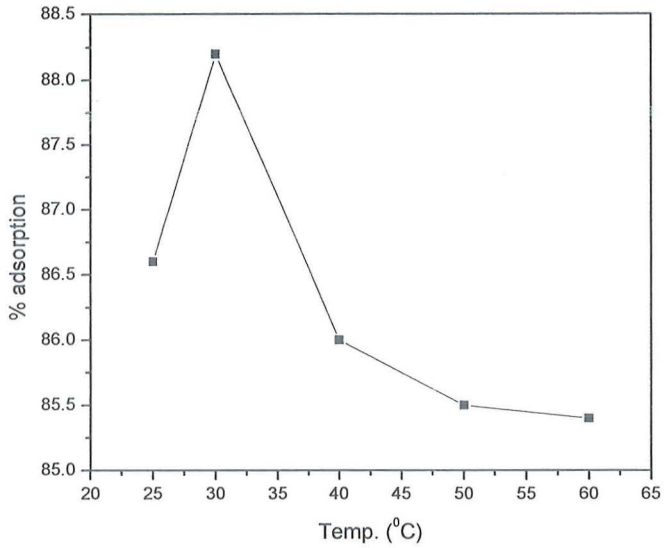

Figure 7. Effects of temperature on copper (II) ions adsorption: Contact time = 180 min., pH = 6, Initial concentration = 100 mg/L, adsorbent dosage = 10 g/L, Volume of solution = 50 ml.

3.7 Thermodynamic Study of Adsorption

The standard free energy change ($\Delta G°$) is the fundamental criterion of spontaneity of a process and can be determined using equilibrium constant as shown below:

$$\Delta G° = - RT \ln K_L \qquad (7)$$

where R is the universal gas constant (8.314 $Jmol^{-1}K^{-1}$) and T is the absolute temperature (K) and K_L is the equilibrium constant.

Similarly, the standard enthalpy change $\Delta H°$ from 303 to 323 K was computed from the following equation,

$$\ln K_L = \Delta S°/R - \Delta H°/RT \qquad (8)$$

A plot of $\ln K_L$ versus 1/T should be straight line. $\Delta H°$ and $\Delta S°$ values were obtained from the slope and intercept of this plot, respectively. The standard free energy change ($\Delta G°$), standard enthalpy change ($\Delta H°$), and standard entropy change ($\Delta S°$), were obtained from the Eq. (7, 8) and their values associated with

the adsorption of copper (II) ions onto OPLP are listed in Table 4. Negative values of $\Delta G°$ indicate the feasibility of the process and spontaneous nature of the adsorption with a high performance of copper (II) ions for OPLP. Negative value of $\Delta H°$ indicates the exothermic nature of the process, while negative value of $\Delta S°$ reflects the decrease in the randomness at the solid/liquid interface during the sorption process.

Table 4. Values of thermodynamic parameters for adsorption of copper (II) ions on OPLP

Temp. (K)	ΔG^o (kJmol^{-1})	ΔH^o (kJmol^{-1})	ΔS^o (kJmol^{-1}K^{-1})	R^2
303	-8.086			
313	-6.186	-39.84	-0.104	0.993
323	-4.844			

4. CONCLUSIONS

The present study showed that OPLP, an agricultural waste material, can be used as an adsorbent for the removal of copper (II) ions from aqueous solutions. Equilibrium data fitted very well in the Langmuir isotherm equation, confirming the monolayer adsorption capacity of copper (II) ions onto OPLP of 11.22 mg/g. The data obtained from adsorption isotherms at different temperatures were used to calculate thermodynamic parameters such as $\Delta G°$, $\Delta H°$, and $\Delta S°$ of adsorption. The results indicate that copper (II) ions adsorption onto OPLP is exothermic and spontaneous in nature. Taking into consideration of the above results, it can be concluded that the OPLP can be an alternative material for more costly adsorbents used for copper (II) ions removal in wastewater treatment processes.

REFERENCES

Ahmad A., Rafatullah M., Sulaiman O., Ibrahim M. H., Chii Y. Y., Siddique B. M., "Removal of Cu(II) and Pb(II) ions from aqueous solutions by adsorption on sawdust of meranti wood", Desalination, 2009, 247, 1-3, 636-646.

Ajmal M., Khan A. H., Ahmad S., Ahmad A., "Role of sawdust in the removal of copper(II) from industrial wastes", Water Research, 1998, 32, 10, 3085-3091.

Aydin H., Bulut Y., Yerlikaya C., "Removal of copper (II) from aqueous solution by adsorption onto low-cost adsorbents", Journal of Environmental Management, 2008, 87, 1, 37-45.

Balkose D., Baltacioglu H., "Adsorption of heavy metal cations from aqueous solutions by wool fibers", Journal of Chemical Technology and Biotechnology, 1992, 54, 4, 393-397.

Bryant P. S., Petersen J. N., Lee J. M., Brouns T. M., "Sorption of heavy metals by untreated red fir sawdust", Applied Biochemistry and Biotechnology, 1992, 34/35, 777-788.

Elliot H. A., Huang C. P., "Adsorption characteristics of some Cu(II) complexes on aluminosilicates", Water Research, 1981, 15, 849-855.

Feng, N., Guo, X., Liang. S., "Adsorption study of copper (II) by chemically modified orange peel", Journal of Hazardous Materials, 2009, 164, 2-3, 1286-1292.

Gloaguen V., Morvan H., "Removal of heavy metal ions from aqueous solution by modified barks", Journal of Environmental Science and Health, 1997, A32, 4, 901-912.

Helfferich F., "Ion Exchange", McGraw-Hill Book Company, 1962.

Jiang Y., Pang H., Liao B., "Removal of copper (II) ions from aqueous solution by modified bagasse", Journal of Hazardous Materials, 2009, 164, 1, 1-9.

King P., Srinivas P., Prasanna K.Y., Prasad V. S. R. K., "Sorption of copper (II) ion from aqueous solution by *Tectona grandis* 1.f. (Teak Leaves Powder)", Journal of Hazardous Materials, 2006, 136, 3, 560-566.

Larous S., Meniai, A. H. Lehocine M. B., "Experimental study of the removal of copper from aqueous solutions by adsorption using sawdust", Desalination, 2005, 185, 483-490.

Nag A., "Utilization of charred sawdust as an adsorbent of dyes, toxic salts and oil from water", Process Safety and Environmental Protection, 1995, 73, 4, 299-306.

Ngah W. S. W., Hanafiah M. A. K. M., "Adsorption of copper on rubber (*Hevea brasiliensis*) leaf powder: Kinetic, equilibrium and thermodynamic studies", Biochemical Engineering Journal, 2008, 39, 3, 521-530.

Panday K. K., Prasad G., Singh V. N., "Use of wollastonite for the treatment of Cu(II) rich effluents", Water Air Soil Pollution, 1986, 27, 287–296.

Rafatullah M., Sulaiman O., Hashim R., Ahmad A., "Adsorption of copper (II), chromium (II), nickel (II) and lead (II) ions from aqueous solutions by meranti sawdust", Journal of Hazardous Materials, 2009, 170, 2-3, 969-977.

Saeed A., Akhter M. W., Iqbal M., "Removal and recovery of heavy metals from aqueous solution using papaya wood as a new biosorbent", Separation and Purification Technology, 2005, 45, 1, 25-31.

Shukla A., Zhang Y., Dubey P., Margrave J. L., Shukla S. S., "The role of sawdust in the removal of unwanted materials from water", Journal of Hazardous Materials, 2002, 95, 1-2, 137-152.

Sumathi S., Chai S. P., Mohamed A. R., "Utilization of oil palm as a source of renewable energy in Malaysia", Renewable and Sustainable Energy Reviews, 2008, 12, 9, 2404-2421.

Ucun H., Aksakal O., Yildiz E., "Copper(II) and zinc(II) biosorption on *Pinus sylvestris* L.", Journal of Hazardous Materials, 2009, 161, 2-3, 1040-1045.

Vaghetti J. C. P., Lima E. C., Royer B., da Cunha B. M., Cardoso N. F., Brasil J. L., Dias S. L. P., "Pecan nutshell as biosorbent to remove Cu (II), Mn (II) and Pb (II) from aqueous solutions", Journal of Hazardous Materials, 2009, 162, 1, 270-280.

Yu B., Zhang Y., Shukla A., Shukla S. S., Dorris K. L., "The removal of heavy metal from aqueous solutions by sawdust adsorption-removal of copper", Journal of Hazardous Materials, 2000, B80, 33-42.

Zhu B., Fan T., Zhang D., "Adsorption of copper ions from aqueous solution by citric acid modified soybean straw", Journal of Hazardous Materials, 2008, 153, 1-2, 300-308.

Journal of Environmental Science and Health, Part C, 29:177–222, 2011
Copyright © Taylor & Francis Group, LLC
ISSN: 1059-0501 print / 1532-4095 online
DOI: 10.1080/10590501.2011.601847

Taylor & Francis
Taylor & Francis Group

Oil Palm Biomass–Based Adsorbents for the Removal of Water Pollutants—A Review

Tanweer Ahmad, Mohd Rafatullah, Arniza Ghazali, Othman Sulaiman, and Rokiah Hashim

School of Industrial Technology, Universiti Sains Malaysia, Penang, Malaysia

This article presents a review on the role of oil palm biomass (trunks, fronds, leaves, empty fruit bunches, shells, etc.) as adsorbents in the removal of water pollutants such as acid and basic dyes, heavy metals, phenolic compounds, various gaseous pollutants, and so on. Numerous studies on adsorption properties of various low-cost adsorbents, such as agricultural wastes and its based activated carbons, have been reported in recent years. Studies have shown that oil palm–based adsorbent, among the low-cost adsorbents mentioned, is the most promising adsorbent for removing water pollutants. Further, these bioadsorbents can be chemically modified for better efficiency and can undergo multiple reuses to enhance their applicability at an industrial scale. It is evident from a literature survey of more than 100 recent papers that low-cost adsorbents have demonstrated outstanding removal capabilities for various pollutants. The conclusion is been drawn from the reviewed literature, and suggestions for future research are proposed.

Keywords: adsorption; pollutants; heavy metals; dyes; phenols; low-cost adsorbents; oil palm biomass

1. INTRODUCTION

Water is a major source for survival on this planet. Comprising more than 70% of the Earth's surface, water is undeniably the most valuable natural resource existing on our planet. Without this invaluable compound, the life on the Earth would be non-existent. Water is an important and essential component of this universe and plays a vital role in the proper functioning of the Earth's ecosystems. Despite this, safe drinking water is not available in some parts of the world. The quality of water resources is deteriorating exponentially because

Address correspondence to M. Rafatullah, School of Industrial Technology, Universiti Sains Malaysia, 11800 Penang, Malaysia. E-mail: mohd_rafatullah@yahoo.co.in; mrafatullah@usm.my

of their contamination [1–3]. The ever-growing population, unplanned urbanization, rapid industrialization, and unskilled utilization of natural water resources have led to the destruction of water quality in many parts of the world. In many developing countries, groundwater provides drinking water for more than half of the nation's population and is the sole source of drinking water for many rural communities and some large cities. However, due to industrial, agricultural, and domestic activities, a variety of chemicals can pass through the soil and potentially contaminate the natural water resources and reservoirs. In recent years, various toxic chemicals have been widely detected at dangerous levels in drinking water in many parts of the world, posing a variety of serious health risks to human beings [4]. Industrial waters and even natural waters are often contaminated by toxic or sometimes carcinogenic impurities, causing ecological disequilibrium and severe public health problem [5–8]. In general, contaminants come under two broad classes: viz. organic and inorganic. Some organic pollutants include industrial solvents, volatile organic compounds, insecticides, pesticides, and food processing wastes. Inorganic pollutants include gaseous pollutants such as nitrogen oxide, sulphur dioxide, hydrogen sulfide, ammonia and ammonium compounds, toxic metals, fertilizers, and industrial discharges [2]. Many organic and inorganic pollutants have been reported in water along with microbial populations. Among these, certain organic and inorganic pollutants are dangerous because of their highly toxic and carcinogenic nature [9]. Moreover, some organics and heavy metal ions are not biodegradable or biotransformable and, hence, persist in the environment for a long time. Most toxic organic pollutants are pesticides, polynuclear aromatic hydrocarbons (PAHs), polychlorinated biphenyls (PCBs), polybrominated diphenyl ethers (PBDEs), plasticizers, phenols, and drug residues whereas toxic metal ions include arsenic, cadmium, chromium, zinc, lead, copper, mercury, and nickel, among others [3, 10–12].

A number of technologies are available with varying degree of success to control the pollution, such as chemical precipitation, oxidation, reduction, coagulation, ion exchange, reverse osmosis, solvent extraction, flocculation, membrane separation, filtration, evaporation, electrolysis, and adsorption, which have been used to remove and recover toxic contaminants from industrial effluents [13–24]. However, the shortcomings of most of these methods are high operational and maintenance costs, generation of toxic sludge, and the complicated procedure involved in the treatment. Comparatively, adsorption process is considered better in water treatment because of convenience, ease of operation, and simplicity of design [25]. Moreover, it is universal in nature since it can be applied for the removal of soluble and insoluble contaminants and biological pollutants with removal efficiency of 90% to 99%. Activated carbon is undoubtedly considered as a universal adsorbent for effluent treatment and is commonly used for the removal of various pollutants [26]. However, its widespread use in wastewater treatment is sometimes restricted due to its

higher cost. A large variety of non-conventional adsorbents have been examined for their ability to remove various types of pollutants from water and wastewater and have been reviewed extensively [4, 27–44]. It has been found that various low-cost adsorbents developed from different origins show little or poor adsorption potential for the removal of various pollutants as compared to commercial activated carbon. Therefore, the search for the development of low-cost materials as adsorbents as well as the precursor for the production of activated carbon is ongoing.

Among several agricultural wastes studied as adsorbents for the removal of pollutants, oil palm biomass has been of great importance as various parts such as trunks, fronds, leaves, empty fruit bunches, and shells have been extensively studied as adsorbents for the removal of diverse types of pollutants. Oil palm–based agricultural wastes have gained wide attention as effective adsorbents due to low-cost and significant adsorption potential for the removal of various pollutants. The oil palm (*Elaeis guineensis*) comprises two species of the *Arecaceae*, or palm family. Oil palm grows well in the wet and humid tropics, in bands of land extending 10° to the north and also to the south of the Equator [45], with a fair amount of sunshine and hot climate coupled with temperature averages of 25°C and a high rainfall rate (2.0 mm of rain) well distributed throughout the year [46]. The oil palm originates from West Africa where it grows in the wild and later was developed into an agricultural crop. They are produced mainly in South East Asia (Malaysia, Indonesia, and Thailand), Africa (Nigeria and Cameroon), America, and several southern provinces of China. It was introduced to Malaysia, then Malaya, by the British in early 1870s as an ornamental plant. In 1917, the first commercial planting took place in Tennamaran Estate in Selangor. Today, 4.49 million hectares of land in Malaysia is under oil palm cultivation, producing 17.73 million tons of palm oil and 2.13 tons of palm kernel oil. Malaysia is one of the largest producers and exporters of palm oil in the world, accounting for 11% of the world's oils and fats production and 27% of export trade of oils and fats. The industry provides employment to more than half a million people and livelihood to an estimated one million people. Over the past few decades, the Malaysian palm oil industry has grown to become a very important agriculture-based industry. The palm oil industry is an important contributor to the country's gross domestic product [45]. With the growth of palm oil production in Malaysia, the amount of residues generated also shows a corresponding increase. The type of biomass produced from the oil palm industry includes trunks, fronds, leaves, empty fruit bunches, and shells [47]. In Malaysia, oil palm industries are producing huge quantities of non-oil palm biomass of about 90 million tons of lignocellulosic biomass each year, of which about 40 million tons are in the form of empty fruit bunches, trunks, and fronds [48]. The empty fruit bunches represents about 9% of this total solid waste production. At present, 65% of the empty fruit bunches generated is incinerated and the bunch ash is recycled

back to the plantation as fertilizer. Palm shells are generated in great quantities in this economy sector, along with other wastes that are mostly disposed without further utilization. It is only in recent years that the interest to palm shell has increased, mainly due to the research findings that this material can be an excellent source of high-quality and low-cost activated carbon [49]. At present, the biomass is either left at the plantation to provide organic nutrients to the oil palm trees or is burned illegally or used as solid fuel in the boiler to generate steam or electricity at the mills [50]. In addition, oil palm biomass or ash derived from it can be converted into adsorbents for the adsorption of toxic gases and heavy metals and other pollutants. Some researchers have studied the use of oil palm ash as an absorbent for removing pollutant gasses such as sulfur dioxides and nitrogen oxides. Oil palm ash is produced after combustion of oil palm fiber and shell as boiler fuel to produce steam for palm oil mill consumption. The oil palm ash was found to contain high amount of silica, calcium, potassium, and alumina that can be utilized to synthesize active compounds that are responsible for adsorption of various pollutants on the surface of adsorbents [51–54]. The application of these biomasses for value-added purposes such as in the removal of various water pollutants has been explored and needs further investigation. The abundance and cheap supply of the biomasses will justify their use as potential adsorbents for different pollutants [55].

No previous review is available where researchers can get an overview of the adsorption capacities of various oil palm biomass–based adsorbents used for the adsorption of different pollutants. Herein, we provide the first review article that provides researchers an overview of the adsorption capacities of various oil palm biomass–based adsorbents for the removal of different pollutants (acid and basic dyes, heavy metals, phenolic compounds, various gaseous pollutants, etc.). We have incorporated most of the valuable available literature on adsorption process utilizing various oil palm biomass–based adsorbents. This review provides the recent literature demonstrating the usefulness of oil palm biomass–based adsorbents in the adsorption of various pollutants. A summary of relevant published data (in terms of adsorption capacities, applicable adsorption isotherm models, and kinetic models) with some of the latest important results have been discussed. The authors recommend that the reported adsorption capacities be taken as a specific set of conditions rather than as maximum adsorption capacities. The reader is strongly encouraged to refer to the original research papers for information on experimental conditions.

2. CHEMICAL COMPOSITION OF OIL PALM BIOMASS

Oil palm is a lignocellulosic material rich in carbohydrates in the form of starch and sugar and containing cellulose, hemicelluloses, and lignin. The chemical compositions of different parts of oil palm biomass are presented in

Table 1: Chemical Composition of Different Parts of Oil Palm Biomass

Parts of Oil Palm Biomass	Extractives	Chemical Composition (%)		
		Holocellulose	Cellulose	Lignin
Bark	10.00	77.82	18.87	21.85
Leaves	20.60	47.70	44.53	27.35
Frond	3.50	83.13	47.76	20.15
Shells	—	47.70	29.70	53.40
Mid-part of trunk	14.50	72.60	50.21	20.15
Core-part of trunk	9.10	50.73	43.06	22.75
Empty fruit bunch	3.21	80.09	50.49	17.84
Hardwood	0.1–7.7	71–89	31–64	14–34
Softwood	0.2–8.5	60–80	30–60	21–37

Table 1 [56]. Lignocellulosic substances contain three main structural components: hemicellulose, cellulose, and lignin. It also contains extractives. Generally, three main components have high molecular weights and contribute much mass, while the extractives are of small molecular size and are available in little quantity. Hemicellulose consists of different monosaccharide units. The polymer chains of hemicellulose have short branches and are amorphous. Because of the amorphous morphology, hemicellulose is partially soluble or swellable in water. Hemicellulose is derived mainly from chains of pentose sugars and act as the cement material holding together the cellulose and fibers [57]. The backbone of the chains of hemicellulose can be a homopolymer (generally consisting of single sugar repeat unit) or a heteropolymer (mixture of different sugars). Hemicellulose is largely soluble in alkali and, as such, is more easily hydrolyzed [58, 59]. Cellulose is a linear polymer chain that is formed by joining the anhydroglucose units into glucose chains [60]. These anhydroglucose units are bound together by β-(1, 4)-glycosidic linkages. Due to this linkage, cellobiose is established as the repeat unit for cellulose chains. By forming intramolecular and intermolecular hydrogen bonds between OH groups within the same cellulose chain and the surrounding cellulose chains, the chains tend to be arranged parallel and form a crystalline supramolecular structure. Cellulose is insoluble in most solvents and has a low accessibility to acid and enzymatic hydrolysis. Chemical modification of cellulose is a promising technique for modifying its physical and chemical properties to improve the adsorption property toward removal of various pollutants [33]. Lignin is a polymer of aromatic compounds. It is a natural polymer, which together with hemicelluloses, acts as a cementing agent matrix of cellulose fibers in the structures of plants. Their functions are to provide structural strength, provide sealing of water conducting system that links roots with leaves, and protect plants against degradation [61]. Lignin is a macromolecule that consists of alkyl phenols and has a complex three-dimensional structure. The

basic chemical phenyl propane units of lignin (primarily syringyl, guaiacyl, and p-hydroxy phenol) are bonded together by a set of linkages to form a very complex matrix. This matrix comprises a variety of functional groups, such as hydroxyl, methoxyl, and carbonyl, which impart a high polarity to the lignin macromolecule [62, 63]. Cellulose and lignin structures were extensively investigated in the earlier studies [64–66]. Extractives are the organic substances that have low molecular weight and are soluble in neutral solvents. Resin (terpenes, lignans, and other aromatics), fats, waxes, fatty acids and alcohols, terpentines, tannins, and flavonoids are categorized as extractives [67]. Oil palm biomass is now considered to be one of the most promising non-wood lignocellulosic raw materials as adsorbents for the removal of various pollutants.

3. REVIEW ON ADSORPTION OF WATER POLLUTANTS THROUGH DIFFERENT PARTS OF OIL PALM BIOMASS

Although many review articles have been published on the importance of low-cost adsorbents in environmental pollution control [27–44], many of them are generally either adsorbate-specific or adsorbent-specific. Studies have shown that various parts of oil palm biomass can be used as promising adsorbents for removing different water pollutants. Not only is oil palm biomass abundant but it is actually an efficient adsorbent that is effective to many types of pollutants, such as dyes, heavy metals, phenolic compounds, and various gaseous pollutants. To make better utilization of these cheap and abundant wastes, it is proposed to convert them into value-added products. Since the price of commercial activated carbon has dropped continually over the past decade or so, interest is growing in the use of other low-cost and abundantly available lignocellulosic materials as precursors for the preparation of activated carbon [68].

3.1. Adsorption of Dyes Through Oil Palm Biomass

Dyes are important water pollutants that are generally present in the effluents of textile, leather, paper, and dye manufacturing industries. The high level of worldwide production and extensive use of dyes generate colored wastewaters that cause water pollution. The colored dye effluents are generally considered to be highly toxic to the aquatic biota and affect the symbiotic process by disturbing the natural equilibrium through reduced photosynthetic activity due to the coloration of water in streams. Some dyes are reported to cause allergy, dermatitis, skin irritation, and cancer in humans [33]. Therefore, removal of such dyes before discharging them into natural water streams is essential. Oil palm biomass–based adsorbents have been widely explored for the removal of different classes of dyes.

Oil palm biomass was converted into activated carbon for the treatment of dyeing industry wastewater by Tan and colleagues [69]. Batch experiments were carried out to study the adsorption isotherm and kinetics at 30°C, with the initial concentration of 50–500 mg/L and solution pH of 6.5. Equilibrium data were fitted to Langmuir, Freundlich, Temkin, and Dubinin-Radushkevich isotherm models. It was found that the equilibrium data were best represented by the Langmuir isotherm model, with maximum monolayer adsorption capacity of 243.90 mg/g at 30°C. The adsorption process was shown to be exothermic in nature. The kinetic data were fitted to pseudo-first–order, pseudo-second–order and intraparticle diffusion models, and it was found to follow closely the pseudo-second–order model.

Chemically modified, activated carbon oil palm shell was used for the removal of methylene blue by Tan and associates [70]. The activated carbon was treated with hydrochloric acid to enhance the adsorption of methylene blue. The Fourier transform infrared spectroscopy (FTIR) measurements showed that the surface of the activated carbon had more acidic groups such as carboxylic and ether. Adsorption equilibrium data were fitted to the Langmuir, Freundlich, and Dubinin–Radushkevich isotherm models. The equilibrium data for both the untreated and hydrochloric acid treated activated carbons were best represented by the Langmuir isotherm. The adsorption capacity of treated activated carbon was 303.03 mg/g, which was 24.24% higher compared to the untreated activated carbon. The kinetic data were found to follow closely the pseudo-second–order model for both activated carbons. The adsorption of methylene blue on the treated activated carbon was found to be endothermic in nature and was favored by using a higher solution pH.

Equilibrium and kinetic studies on basic dye adsorption by oil palm fiber activated carbon was studied by Tan and colleagues [71]. Oil palm fiber was used to prepare activated carbon by physiochemical activation method. The Brunauer-Emmett-Teller (BET) surface area of the prepared activated carbon was 1354 m^2/g. Scanning electron microscopy (SEM) study showed that the activated carbon of oil palm fiber was porous with well-developed pores. The main surface functional groups present in the derived activated carbon were quinone and aromatic rings. The effects of various parameters such as contact time, initial methylene blue concentration, and temperature were investigated at solution pH of 6.5. The adsorption capacity was found to increase with an increase in the three parameters studied. Equilibrium data were fitted to Langmuir, Freundlich, Temkin, and Dubinin–Radushkevich isotherms. The equilibrium data were best fitted by the Langmuir isotherm, with maximum monolayer adsorption capacity of 277.78 mg/g at 30°C. The adsorption kinetics was found to follow the pseudo-second–order kinetic model. The positive ΔH° value indicated the endothermic nature of the adsorption interaction, whereas the positive ΔS° value showed increased randomness at the solid-solution interface during the adsorption process. The negative value of ΔG° indicated

the feasibility and the spontaneous nature of the adsorption of methylene blue onto the prepared activated carbon.

Optimization of basic dye removal by oil palm fiber-based activated carbon using response surface methodology was investigated [72]. Activated carbon was prepared by using physiochemical activation method, which consisted of potassium hydroxide treatment and carbon dioxide gasification. The effects of three preparation variables—the activation temperature, activation time, and chemical impregnation ratio—on methylene blue uptake from aqueous solutions and activated carbon yield were investigated. Based on the central composite design, a quadratic model and a two factor interaction model were respectively developed to correlate the preparation variables to the methylene blue uptake and carbon yield. From the analysis of variance (ANOVA), the significant factors on each experimental design response were identified. The optimum activated carbon prepared from oil palm fiber was obtained by using activation temperature of 862°C, activation time of 1 h and chemical impregnation ratio of 3:1. The optimum activated carbon showed methylene blue uptake of 203.83 mg/g and activated carbon yield of 16.50%. The equilibrium data for adsorption of methylene blue on the optimum activated carbon were well represented by the Langmuir isotherm, giving maximum monolayer adsorption capacity as high as 400 mg/g at 30°C.

Activated carbons were prepared from the biomass of oil palm wood via two stages—an environmentally friendly pyrolysis pilot plant and an activation pilot plant [73]. Experimental results showed that pyrolysis and activation conditions leading to various final average temperatures had significant effect on the properties of activated carbons prepared. Suitable pyrolysis operating conditions of 7 m^3/h airflow rate for 4 hrs until final average pyrolysis temperature 390°C and activation conditions of 7.45 kg limestone calcined with airflow rate 202.4 mL/s for 3.5 hrs until final average activation temperature of 806°C produced an activated carbon yield of 13.7%, 68.3% fixed carbon, 16.9% volatile matters, 4.3% ash, 10.6% moisture, 1084 m^2/g BET surface area, and a micropore surface area of 931.6 m^2/g. Maximum adsorption capacity of methylene blue was found to be 90.9 mg/g. The high micropore fraction, nitrogen gas adsorption isotherm and SEM showed that these activated carbons possessed intricate pore network comprising micropores and narrow mesopores. FTIR characterization indicated that pyrolysis and activation temperatures affected the surface functional groups and maximum methylene blue adsorption was dependent on BET surface area.

The effect of temperature on the sorption of methylene blue from aqueous solutions onto palm kernel fiber was investigated [74]. Batch kinetics and isotherm studies were performed at temperatures ranging from 299 to 339 K. The kinetic data were studied in terms of the pseudo-first–order and pseudo-second–order kinetic models and the Bangham and intraparticle diffusion models. The pseudo-second–order model best described the sorption process

and was employed in predicting the rate constant. In addition activation energy of sorption has also been determined based on the pseudo-second–order rate constant. The isotherm data were analyzed by the Langmuir and Freundlich isotherms. Palm kernel fiber was found to have a Langmuir monolayer capacity of 233.41 mg/g at 299 K. The adsorption is endothermic at ambient temperature and the computation of the thermodynamic parameters, ΔH°, ΔS°, and ΔG° indicates that the sorption was favorable at all temperatures.

The kinetics and mechanism of methylene blue sorption from aqueous solution using palm kernel fiber as adsorbent was investigated [75]. Batch kinetic experiments were performed and system variables investigated included pH and initial dye concentration. Increases in the dye concentration resulted in an increase in the amount of dye adsorbed per unit mass of adsorbent for all sorbent/dye combination. The initial uptake of dye was found to be rapid from solutions with lower concentration. The kinetic data were fitted to the pseudo-first, pseudo-second, intraparticle diffusion and mass transfer models. The pseudo-first–order reaction kinetics fitted to the experimental data only in the first 5 min of sorption and then deviated, while the pseudo-second–order kinetic model was found to fit the experimental data for the entire sorption period with high coefficient of determination. Equations were developed using the pseudo-second–order model, which predicts the amounts of methylene blue at any contact time and initial concentration within the given range. This suggests that the sorption of methylene blue onto palm kernel fiber follows a chemical activation mechanism. Mass transfer was found to be favored at high concentrations while intraparticle diffusion was favored at low concentrations.

The adsorption of two reactive dyes, reactive black 5 (RB 5) and reactive red E (RR E), onto activated carbon prepared by palm kernel shell (PKSAC) was studied by Nourouzi and colleagues [76]. The adsorption capacity of PKSAC for RB 5 was higher than that for RR E. It was found that in binary system, due to competitive condition, the adsorption capacity of PKSAC for both dyes is lower than that in a single system. Adsorption of reactive dyes for single system can be represented by the Freundlich and Redlich-Peterson models. For binary systems, the equilibrium was described successfully by the modified extended Freundlich model. The rates of adsorption in the single system were found to agree well with the pseudo-second–order kinetic model. Finally, the chemical oxygen demand (COD) of the treated reactive dye solutions from single and binary systems showed that a minimum 4 g/L dosage of PKSAC was needed to reduce the COD to an acceptable level.

The rate of adsorption of two reactive dyes, RB 5 and RR E, onto palm kernel shell-based activated carbon was studied [77]. The results showed that the external coefficients of mass transfer decreased with increasing initial adsorbate concentration. In addition, it was found that the adsorption process was better described by using the two resistance models— film-surface diffusion.

The removal of Remazol Black 5 (RB 5) from the synthetic wastewater using PKSAC was investigated by Zawani and associates [78]. The optimum pH was found at acidic range, pH 2. The results of this study indicated that PKSAC can be successfully used for the adsorption of RB 5 from aqueous solutions. Freundlich isotherm fit well with the equilibrium data for adsorption of RB 5 dye, and the maximum adsorption capacity was determined to be 58.8, 96.7, and 98.6 mg/g at 30, 40, and 50°C, respectively. Two simplified kinetic models, pseudo-first order and pseudo-second order, were tested. The pseudo-first–order kinetic model fit very well with the dynamical adsorption behavior of RB 5 dye. The negative values of ΔG° and ΔH° obtained indicated that the RB 5 dye adsorption process is spontaneous and exothermic.

Palm kernel fiber was investigated for its ability to perform as a suitable sorbent for anionic dye from aqueous solution [79]. The effect of sorbent dose and temperature was investigated using a batch sorption technique. The isotherm data were closely fitted to the Langmuir equation, and the dye sorption capacity of palm kernel fiber increased as the sorbent dose decreased. Maximum saturated monolayer sorption capacity of palm kernel fiber for 4-bromoaniline-azo-1,8-dihydronaphthalene-3,6-disodiumsulphate was 38.6 mg/g. The thermodynamic analysis indicated that the system is spontaneous and exothermic, and up to 66.4% of the dye sorbed can be desorbed with distilled water. The results revealed the potential of palm kernel fiber as a low-cost sorbent for the anionic dye.

The ability of palm kernel coat (PKC) to abstract Congo Red (CR), an anionic dye, from an aqueous system was studied in a batch adsorption system [80]. The two process variables were optimized: the initial dye concentration and adsorbent dosage. Studies on the effect of initial concentration on the dynamics of the adsorption process showed that an increase in dye concentration resulted in an increase in the amount of dye sorbed per unit mass of adsorbent. The initial uptake of dye was found to be rapid at the inception of the sorption reaction. It slows down with time as the sorption process proceeds and equilibrium is attained. The results obtained when the PKC dosage was optimized showed that the amount of CR sorbed per unit (g) of PKC decreased with an increase in PKC dosage, while the amount of CR (%) sorbed increased with an increase in PKC dosage. An equation was developed using the pseudo-second–order model, which predicts the amount of CR at any contact time and initial concentration within the given range. The rate-limiting step of the sorption reaction was also determined using the intraparticle diffusion, liquid film diffusion, and Boyd kinetic models. The results obtained showed that intraparticle diffusion becomes rate controlling at low concentration, while at high concentration film diffusion is the main rate-controlling parameter. The results of the batch desorption studies showed that chemisorption played a prominent role in the sorption process. The elution curve obtained from the continuous

desorption studies showed that the elution rate was fast and high elution efficiency could be obtained with 0.1 M CH_3COOH as an eluting solvent.

Oil palm trunk fiber (OPTF) was successfully utilized as a low-cost alternative adsorbent for the removal of hazardous dye malachite green (MG) [81]. The operating variables studied were contact time, initial dye concentration, and solution pH. Equilibrium adsorption data were analyzed by three isotherms, namely the Freundlich isotherm, the Langmuir isotherm, and the multilayer adsorption isotherm. The best fit to the data was obtained with the multilayer adsorption. The monolayer adsorption capacity of OPTF was found to be 149.35 mg/g at 30°C. Adsorption kinetic data were modeled using the Lagergren pseudo-first–order, Ho's pseudo-second–order and Elovich models. It was found that the Lagergren's model could be used for the prediction of the system's kinetics. The overall rate of dye uptake was found to be controlled by external mass transfer at the beginning of adsorption and then for initial MG concentrations of 25, 50, 100, 150, and 300 mg/L. The rate-control changed to intraparticle diffusion at a later stage, but for initial MG concentrations 200 and 250 mg/L no evidence was found of intraparticle diffusion at any period of adsorption. It was found that with increasing the initial concentration of MG, the pore-diffusion coefficient increased while the film-diffusion coefficient decreased.

Ahmad and colleagues [82] used oil palm ash as an adsorbent for the removal of direct blue 71 from aqueous solutions. The experimental data were analyzed by the Langmuir and Freundlich models of adsorption. Equilibrium data fit well with Freundlich model in the range of 50–600 mg/L. The equilibrium adsorption capacity of the palm ash was determined with the Langmuir equation and was found to be 400.01 mg/g at 30°C. The rates of adsorption were found to conform to the pseudo-second–order kinetics with good correlation.

In the laboratory-scale studies conducted by Isa and associates [83], palm ash was effectively used for the removal of disperse blue and disperse red dyes from aqueous solutions. The adsorption capacities of the ash for the dyes removal were found to be affected by the solution's pH, with lower pH favoring adsorption. This was attributed to the presence of excess positive charge on its surface. More than 99% removal was achieved for both the dyes at pH 2. The amount of disperse dyes adsorbed increased with the increase in contact time and initial dye concentrations. The equilibrium time for both the dyes was 60 min. Adsorption of the disperse dyes could be described by both the Langmuir and Freundlich isotherms, with the former yielding somewhat better fits. The adsorption kinetics followed the pseudo-second–order model indicating that chemisorption was the rate-controlling step in the adsorption of the dyes. Column plugging was the main problem encountered due to the fine particle size of the ash. Pelletisation of ash using calcium oxide and calcium sulfate was not successful.

A summary of adsorption capacities of oil palm biomass–based adsorbents for different dyes have been presented in Table 2.

3.2. Adsorption of Heavy Metals Through Oil Palm Biomass

Heavy metal pollution is one of the most important environmental problems today. The pollution of water resources due to the indiscriminate disposal of metal ions has been causing worldwide concern. Wastewater from many industries such as metallurgical, tannery, chemical manufacturing, mining, and battery manufacturing industries contains one or more toxic metal ions. It is therefore, necessary to remove these metal ions from the wastewaters before releasing into the environment because there is the possibility that these metal ions could enter into the food chain through waste discharges into water bodies. Oil palm biomass has been extensively investigated as adsorbents for the removal of diverse metal ions from water and wastewater by different researchers.

The ability of modified soda lignin (MSL) extracted from oil palm empty fruit bunches (EFB) in removing lead (II) ions from aqueous solutions was studied by Ibrahim and associates [84]. The effect of contact time, point zero charge (pHpzc), and pH of the solution, initial metal ion concentration, and adsorbent dosage on the removal process were investigated. The amount of lead (II) ions uptake (mg/g) was found to increase with increase in contact time, pH, and initial metal ion concentration. Equilibrium data fit very well in the Langmuir isotherm equation, confirming the monolayer adsorption capacity of lead (II) ions onto MSL with a monolayer adsorption capacity of 46.72 mg/g at 47°C. The rate of adsorption was found to follow to pseudo-second–order kinetics with a good correlation. As the concentration of desorbing solutions (HCl, HNO_3, and EDTA) increases, more lead (II) ions were able to be desorbed. More than 80% of lead (II) ions were able to be desorbed from MSL using 0.02 mol/L HCl, HNO_3, and EDTA solutions. This result showed that the test adsorbent could be reused without significant losses in its initial adsorption capacity.

The continuous adsorption of lead ions from aqueous solution on unpretreated palm shell activated carbon (PSAC) was studied by Issabayeva and associates [49]. It was found that the breakthrough period was shorter at pH 3 than at pH 5. Increase of the flow rate from 0.5 up to 2.0 L/h accelerated the PSAC saturation time at both pHs. Presence of malonic and boric acids did not improve adsorption of lead on palm shell–activated carbon. Moreover, presence of malonic acids resulted in a shorter breakthrough period at pH 5, compared to single lead system.

Palm shell–activated carbon was impregnated with polyethyleneimine (PEI) and the effect of impregnation on batch adsorption of Ni^{2+}, Cd^{2+}, or Pb^{2+} as well as the equilibrium behavior of adsorption of metal ions on PEI-impregnated activated carbon were investigated [85]. PEI impregnation

Table 2: Adsorption Capacities Of Oil Palm Biomass–Based Adsorbents for the Adsorption of Dyes

Adsorbents	Adsorbates	Adsorption Capacities (mg/g)	References
Oil palm shells activated carbon	Methylene blue	243.90	(69)
Chemically modified oil palm shells activated carbon	Methylene blue	303.03	(70)
Oil palm fiber activated carbon	Methylene blue	277.78	(71)
Oil palm fiber–based activated carbon	Methylene blue	400.00	(72)
Oil palm wood activated carbon	Methylene blue	90.90	(73)
Oil palm kernel fiber	Methylene blue	233.41	(74)
Oil palm kernel shell activated carbon	Reactive black 5	81.34	(77)
	Reactive red E	42.37	
Oil palm kernel shell activated carbon	Remazol black 5	58.80–98.60	(78)
Oil palm kernel fiber	4-bromoaniline-azo-1,8-dihydronaphthalene-3,6-disodiumsulphate	38.60	(79)
Palm kernel coat	Congo red	66.23	(80)
Oil palm trunk fiber	Malachite green	149.35	(81)
Oil palm ash	Direct blue 71	400.01	(82)
Oil palm ash	Disperse blue	49.50	(83)
	Disperse red	61.35	

increased the single metal adsorption capacities of Ni^{2+} or Cd^{2+} except for Pb^{2+}, where its adsorption capacities were reduced by 16.67% and 19.55% for initial solution pH of 3 and 5, respectively. This suggested that PEI-impregnated activated carbon could be used for selective separation of Pb^{2+} ions from other metal ions. The adsorption data of all the metal ions on both virgin and PEI-impregnated activated carbon for both initial solution pH of 3 and 5 generally fitted the Langmuir and Redlich-Peterson isotherms considerably better than the Freundlich isotherm.

Pseudo-second–order model for lead ion sorption from aqueous solutions onto palm kernel fiber was studied by Ho and Ofomaja [86]. The batch sorption model, based on a pseudo-second–order mechanism, was applied to predict the rate constant of sorption, the equilibrium capacity, and the initial sorption rate with the effects of the initial solution pH and fiber dose. Equilibrium concentrations were evaluated with the equilibrium capacity obtained from the pseudo-second–order rate equation. An isotherm was obtained by changing fiber doses using the equilibrium concentration and the equilibrium capacity obtained based on the pseudo-second–order constants.

The kinetics of sorption of a mono-solute of lead ions and of a bi-solute of lead and calcium ions onto palm kernel fiber was investigated in a batch system [87]. The experimental data were analyzed based on an intraparticle diffusion equation and a pseudo-second–order mechanism, in both the mono- and bi-solute sorption systems, in order to predict the rate constant of sorption, the equilibrium capacity, and the initial sorption rate. The results indicate that the sorption mechanism is described by a pseudo-second–order equation. Intraparticle diffusion was significant in the lower-concentration systems. In addition, a modified intraparticle diffusion equation was applied to the sorption systems. The sorption capacity of lead and the initial sorption rate decreased with an increase in calcium concentration. Calcium appears to enhance hydrogen release from the surface of the sorbent.

Abia and Asuquo [88] examined the sorption kinetics of Pb(II) and Cd(II) ions from aqueous solutions using unmodified and chemically (mercaptoacetic acid) modified oil palm fruit fiber (MOPF). The results indicated that different kinetic parameters were obtained from the four forms of pseudo-second–order equations. The chemical modification of the adsorbent increased the equilibrium sorption capacity with maximum values of 5.579 mg/g for Pb(II) and 7.980 mg/g for Cd(II) for the 1.0 MOPF adsorbents. The kinetics of sorption indicated that the pseudo-second–order model can be used to describe the mechanism of sorption of Pb(II) and Cd(II) ions.

Lead (II) and nickel (II) adsorption kinetics from aqueous metal solutions using chemically modified and unmodified oil palm fruit fiber (UOPF) adsorbents was studied [89]. The adsorbent was chemically modified with 0.5 M and 1.0 M mercaptoacetic acid (0.5 MOPF and 1.0 MOPF). The removal of the two metals was found to increase with an increase in chemical modification, the

sequence being 1.0 MOPF > 0.5 MOPF > UOPF. The adsorption of nickel (II) was higher than that of lead (II). The kinetics of the adsorption of both metals was rapid in the initial stage followed by a slow rate. The adsorption data indicated the applicability of the intraparticle diffusion model for lead (II) removal. However, the kinetics of nickel (II) sorption did not follow the intraparticle diffusion model.

Removal of mercury, lead, and copper from an aqueous solution by activated carbon of palm oil empty fruit bunch (OPEFB) was studied by Wahi and colleagues [90]. The study indicated that the OPEFB-activated carbon produced through chemical activation by using NaOH as the activating agent could be used as an effective adsorbent material for the removal of Hg(II) and Pb(II) from wastewater. However, Cu(II) can only be removed at lower percentage. From the calculation based on Langmuir isotherm, Hg(II) shows the highest adsorption capacity of 52.67 mg/g, followed by Pb(II) and Cu(II) with adsorption capacity of 48.96 mg/g and 0.84 mg/g, respectively. The study also showed that the adsorption of Hg(II), Pb(II), and Cu(II) by OPEFB-activated carbon is dependent on the dosage of adsorbent and the initial metals concentration.

Removal of Cr (VI) from aqueous solutions using treated oil palm fiber was examined by Isa and associates [91]. Adsorption of Cr (VI) by sulphuric acid and heat-treated oil palm fiber was conducted using batch tests. The influence of pH, contact time, initial chromium concentration, and adsorbent dosage on the removal of Cr (VI) from the solutions was investigated. The Cr (VI) adsorption capacity of treated oil palm fiber was favored at low pH, which was attributed to the presence of excess positive charge on its surface. Complete removal of Cr (VI) was achieved at pH 1.5. The removal efficiency was found to correlate with the initial Cr (VI) concentration, adsorbent dosage, and the contact time between Cr (VI) and the adsorbent. Adsorption of chromium could be adequately described by both Freundlich and Langmuir adsorption isotherms. The Freundlich model presented a slightly better fit. Desorption of Cr (VI) was difficult and suggested that treated oil palm fiber may be efficiently employed as a single-use adsorbent and may not be suitable for economic regeneration.

Removal of chromium metal ion from industrial wastewater using chitosan-coated oil palm shell charcoal was studied [92]. A new composite adsorbent has been prepared by coating chitosan onto acid-treated oil palm shell charcoal (AOPSC). Chitosan loading on the AOPSC support is about 21% by weight. The shape of the adsorbent is nearly spherical with particle diameter ranging 100–150 μm. The adsorption capacity of the composite biosorbent was evaluated by measuring the extent of adsorption of chromium metal ions from water under equilibrium conditions at 25°C. Using the Langmuir isotherm model, the equilibrium data yielded the following ultimate capacity

values for the coated biosorbent on a per gram basis of chitosan: 154 mg/g. Bioconversion of Cr (VI) to Cr (III) by chitosan was also observed. After the biosorbent was saturated with the metal ions, the adsorbent was regenerated with 0.1 M sodium hydroxide. The influence of several operational parameters such as dose of adsorbent, agitation speed, initial pH, and contact time was investigated. pH is an important parameter for adsorption of metal ions from aqueous solution because it affects the solubility of the metal ions, concentration of the counter ions on the functional groups of the adsorbent, and the degree of ionization of the adsorbate during reaction. The pHpzc value of acid treated OPSC was found to be around 4.7.

Adsorption characteristics of Cr(III) on palm oil fuel ash (POFA) were investigated by Chu and Hashim [93]. The equilibrium and kinetic properties of Cr(III) are studied in batch stirred-tank experiments. The extent of Cr(III) sorption increases on raising solution pH. This occurs as a result of competition between Cr(III) and protons for binding sites on the surface of POFA. The maximum equilibrium uptake capacity at pH 6 is 0.31 mmol/g. A Langmuir isotherm model with pH-dependent parameters accounts very well for the measured equilibrium data. Modeling studies using a second-order irreversible reaction model and a pseudo-first–order kinetic model indicated that transient profiles obtained experimentally for a range of initial metal concentrations and sorbent dosages are in good agreement with calculated curves of both models. The variations in the rate coefficients of the two models with the initial metal concentration and sorbent dosage are believed to be brought about by the heterogeneous nature of the POFA sorbent and are consistent with the interpretation that the sorption of Cr(III) on the exterior surface of POFA is the rate-limiting step. From an engineering viewpoint, either one of the two models could be used for an optimization of contact times in a batch Cr(III) removal process provided the dependence of the rate coefficient of the model on system variables is properly correlated.

Oil palm leaf powder (OPLP) was used as a low-cost adsorbent for the removal of copper (II) ions from aqueous solution by Sulaiman and associates [94]. Batch studies were performed to evaluate and optimize the effects of various parameters such as contact time, pH of the solution, initial metal ion concentrations, and adsorbent dosage. Langmuir, Freundlich, and Temkin isotherms were used to analyze the equilibrium data at different temperatures. The experimental data fit well with the Langmuir adsorption isotherm, indicating the mono layer adsorption of the copper (II) ions. The monolayer sorption capacity of OPLP for copper (II) ions was found to be 11.22 mg/g at 30°C. The data obtained from adsorption isotherms at different temperatures were used to calculate thermodynamic parameters such as ΔG°, ΔH°, and ΔS° of adsorption. The results indicated that copper (II) ions adsorption onto OPLP is exothermic and spontaneous in nature.

The adsorption of Cu(II) ions from aqueous solutions by soda lignin as an absorbent using a batch adsorption system was examined by Ibrahim and colleagues [95]. The soda lignin used in this study was extracted from black liquor derived from oil palm empty fruit bunches (EFB) using 20% v/v sulfuric acid. The effects of varying experimental parameters such as pH value, adsorbent dosage, different concentrations of Cu(II) ions, and agitation period were investigated. The results revealed that the optimum adsorption of Cu(II) onto soda lignin was recorded at a pH of 5.0 at an adsorbent dosage of 0.5 g soda lignin and an agitation period of 40 min. The adsorption capacity for Cu(II) ions using soda lignin was 7.95 mg/g. The results indicate that the adsorption isotherms could be well fitted by the Freundlich equation (based on sorption on a heterogeneous surface) while the kinetic experimental data was well correlated with the pseudo-second–order kinetic model, implying that the chemical sorption is the rate-limiting step.

Ho and Ofomaja [96] studied the kinetics of copper ion adsorption on palm kernel fiber. Batch kinetics studies were carried out based on the assumption of the pseudo-second–order kinetic model, which was developed to predict the rate constant of adsorption, the equilibrium adsorption capacity, and initial adsorption rate with the effect of initial copper concentration and reaction temperature. It was also revealed that the copper ions and palm kernel fiber interaction is endothermic with activation energy higher than 22 kJ/mol, indicating that adsorption is chemical in nature.

Equilibrium studies of copper ion adsorption onto palm kernel fiber were studied by Ofomaja [97]. Batch equilibrium studies were carried out such as solution pH, sorbent dose, and sorption temperature. The equilibrium sorption data were then analyzed using the Langmuir, Freundlich, Dubinin-Radushkevich (D-R), and Temkin isotherms. The results revealed that sorption was pH-dependent and increased with increasing solution pH above the pH_{PZC} of the palm kernel fiber with an optimum dose of 10 g/dm^3. The equilibrium data were found to fit the Langmuir isotherm model best, with a monolayer capacity of 3.17×10^{-4} mol/g at 339 K. The sorption equilibrium constant increased with increasing temperature, indicating that bond strength between sorbate and sorbent increased with temperature and sorption was endothermic. This was confirmed by the increase in the values of the Temkin isotherm constant with increasing temperature. Using the Dubinin-Radushkevich (D-R) isotherm parameter, free energy was in the range of 15.7–16.7 kJ/mol, suggesting that the sorption mechanism was ion exchange. Desorption studies showed that a high percentage of the copper was desorbed from the adsorbent using acid solutions (HCl, HNO_3, and CH_3COOH) and the desorption percentage increased with acid concentration. Desorption of copper ions from palm kernel fiber was more efficient using the strong acids and CH_3COOH, and this efficiency increased with acid concentration confirming that sorption mechanism is mainly by chemical ion exchange. The thermodynamics of the copper ions

and palm kernel fiber system indicate that the process is spontaneous and endothermic.

Chu and Hashim [98] presented a surface reaction rate model that can be used to describe the batch adsorption of metal ions on oil palm ash. Kinetic data of Cu(II) and Ni(II) adsorption on oil palm ash were compared with prediction of the theoretical model following determination of its parameters from small-scale experiments. Any batch adsorption systems employing adsorbent that exhibits Langmuir-type adsorption can therefore be simulated effectively with this model. The model can be used to assess the effects of alteration of operational parameters without the need to carry out extensive experimental work.

The efficiency of palm pressed fibers (PPF) in removing nickel(II) and copper(II) ions from solutions was investigated in column experiments by Tan and associates [99]. Column studies showed that the sorption of nickel(II) and copper(II) ions are flow rate and bed depth dependent and can be regenerated at least four times without affecting the sorption efficiency of the column. Bed depth service time (BDST) studies at various constant flow rates of PPF column showed that Hutchin's BDST model for activated carbon column can be applied to the system studied. Based on this model, PPF column can be reliably scaled up without running a pilot test on a large column. PPF could also be placed in the landfill to enhance the immobilization of nickel(II) and copper(II) ions in the soil system of the landfill area.

Salamatinia and associates [55] evaluated the efficiency of oil palm bark (OPB), oil palm frond (OPF), and empty fruit bunch (EFB) as low-cost adsorbents for the removal of Cu and Zn from water. The sorption processes were performed in a batch mode with 250 mL Cu and Zn solutions at 100 mg/L using between 0.5 and 1.0 g of sorbent. The samples were tested every 24 hrs up to 168 hrs in normal room temperature. No diffusion limitation was observed in the sorption process. Zinc removal efficiency of 51.5% and 46.0% with 1.0 g of OPF and EFB, respectively, was observed while OPB showed the lowest removal efficiency. For copper, the removal was achieved at 54% for 1.0 g OPF and 56.5% using 1.0 g of EFB. Copper showed better sorption on the three biomasses. The OPB and EFB introduced excessive amounts of soluble organics into the water. The experimental data obtained with OPF sorbent could fit Freundlich isotherm model better. The result suggested the heterogeneous binding sites in the biomass.

The use of NaOH-treated oil palm frond (OPF) sorbent for Cu and Zn removal and its subsequent regeneration process was reported by Salamatinia and colleagues [100]. The regeneration of the spent sorbent was achieved by desorbing the metals in 0.1M NaOH, ethylenediaminetetraacetic acid (EDTA), hydrochloric acid (HCl), and nitric acid (HNO_3) solutions. The reusability study of the sorbent was conducted using 100 mg/L of Cu and Zn at a pH of 4.5 and 5.5, respectively for 1 h. The results were correlated with the mechanism

of the metal uptake. The sorption process data satisfactorily fit the Freundlich isotherm to suggest heterogeneity in the sorption sites. Because of its relatively weaker interactions with sorbent, Zn showed better regeneration efficiency of up to 88%. HCl was the best regenerating agent and the same trend was shared by both heavy metals. The isotherm and desorption results suggested that ion exchange was the main mechanism for the uptake of those metals. The desorption efficiency dropped by about 20% while the sorption capacity experienced a drastic drop after reuse for the fourth cycle. The damage that occurred on the heavy metal binding sites by the strong acid was responsible for this drop.

Activated carbons derived from oil palm empty fruit bunches (EFB) were investigated to find the suitability of its application for removal of zinc through adsorption process by Alam and associates [101]. The activated carbon produced was at optimum activation temperature of 1000°C and at a time of 30 minutes. The SEM showed the presence of pores with estimated pore size between 2.57 to 7.46 μm. The statistical analysis and batch adsorption test were done to optimize the activation conditions for activated carbon production. The results indicated that activated carbon derived from 1000°C and for 30 minutes has maximum adsorption capacity (1.63 mg/g) for the removal of zinc (98%) in the aqueous solutions.

Sugawara and colleagues [102] prepared an adsorbent for the heavy metals from palm shell with a simple two-step process using pyrolysis and sulfur impregnation. Palm shell was pyrolyzed with three different methods—rapid pyrolysis, slow pyrolysis, and KOH pyrolysis—and the prepared char with high specific surface area was sulfurized with H_2S impregnation to obtain the sulfur-impregnated char with the adsorption ability of heavy metals. The pyrolysis char with high specific surface area can be obtained by KOH pyrolysis, which was pre-treated with KOH solution before slow pyrolysis, and then added sulfur into KOH pyrolysis char using H_2S gas. The sulfur content of sulfur-impregnated char increased with increasing the time of H_2S treatment, and increased the adsorption amount of Pb^{2+} from aqueous solution. The sulfur-impregnated char was more effective for Pb^{2+} and Zn^{2+} adsorption than commercial charcoal.

Kinetics of Cd^{2+} and Cr^{3+} adsorption from aqueous solutions using mercaptoacetic acid modified and unmodified oil palm fruit fiber adsorbents were studied by Abia and Asuquo [103]. Iqbal and associates [104] studied the very new adsorbent petiolar felt-shealth of palm for the removal of Pb^{2+}, Ni^{2+}, Cd^{2+}, Cu^{2+}, Cr^{3+}, and Zn^{2+} from contaminated water. Real-time determination of kinetics of adsorption of Pb(II) onto palm shell–based activated carbon using ion selective electrode was studied by Aroua and colleagues [105]. Palm kernel shell and palm kernel husk, two readily available agricultural waste products, have been used as low-cost potential adsorbents to remove Cr and Pb from drill cuttings by Iyagba and Opete [106]. Chu and Hashim [107] studied the adsorption and desorption characteristics of zinc on ash particles derived from

Table 3: Adsorption Capacities of Oil Palm Biomass–Based Adsorbents for the Adsorption of Heavy Metals

Adsorbents	Adsorbates	Adsorption Capacities (mg/g)	References
Oil palm frond	Zn(II)	13.00	(55)
	Cu(II)	13.80	
Oil palm bark	Zn(II)	06.40	(55)
	Cu(II)	08.60	
Oil palm empty fruit bunch	Zn(II)	13.20	(55)
	Cu(II)	14.10	
Modified soda lignin of oil palm empty fruit bunch	Pb(II)	46.72	(84)
Oil palm shell activated carbon impregnated with polyethyleneimine	Ni(II)	05.43–09.65	(85)
	Cd(II)	07.57–13.05	
	Pb(II)	31.75–55.87	
Oil palm fruit fiber	Pb(II)	04.87	(88)
	Cd(II)	07.20	
Chemically modified oil palm fruit fiber	Pb(II)	05.58	(88)
	Cd(II)	07.98	
Oil palm empty fruit bunch activated carbon	Hg(II)	52.67	(90)
	Pb(II)	48.96	
	Cu(II)	0.84	
Chitosan coated oil palm shell charcoal	Cr(VI)	52.68	(92)
Oil palm fuel ash	Cr(III)	16.12	(93)
Oil palm leaf powders	Cu(II)	11.22	(94)
Soda lignin from oil palm fruit empty bunch	Cu(II)	07.95	(95)
Oil palm kernel fiber	Cu(II)	20.12	(97)
Oil palm ash	Zn(II)	04.71–10.66	(107)

oil palm waste. A summary of adsorption capacities of oil palm biomass based adsorbents for different heavy metal ions has been presented in Table 3.

3.3. Adsorption of Phenolic Compounds Through Oil Palm Biomass

Phenolic compounds are considered to be hazardous wastes when released into the aquatic environment by industries such as coke ovens in steel plants, petroleum refineries, petrochemical, phenolic resin, pharmaceutical, and chemical and dye industries [108]. The discharge of phenolic waste into waterways may adversely affect human health as well as that of flora and fauna. It is imperative to remove phenol up to regulatory standards from wastewater before being discharged into waterways. Oil palm biomass–based adsorbents have also been explored for the removal of phenolic pollutants from water and wastewater.

Steam-activated carbons from oil-palm shells were prepared and used in the adsorption of phenol by Lua and Jia [109]. The BET surface area of the

activated carbon was 1183 m^2/g and a total pore volume of 0.69 cm^3/g using N_2 adsorption at 77 K. The phenol adsorption capacity of the activated carbon is a function of the solution temperature. The adsorption capacity of the oil palm shell–activated carbons decreased from 319 to 157 mg/g when the solution temperature increased from 298 to 323 K, respectively. The adsorption isotherms could be described by both the Langmuir-Freundlich and the Langmuir equations. The overall enthalpy change of the adsorption process based on the oil palm shell–activated carbons was –27 kJ/mol, indicating that adsorption is an exothermic process. A new multipore model was proposed that takes into account a concentration-dependent surface diffusion coefficient within the particle. This model is an improvement to the traditional branched pore model. The theoretical concentration versus time curve generated by the proposed model fitted the experimental data for phenol adsorption reasonably well.

Jia and Lua [110] presented a model that takes into account a concentration-dependent intra-particle effective surface diffusion coefficient in the branched pore kinetic model. This model was applied to adsorption data obtained from the adsorption of phenol solution by activated carbons prepared from oil palm shells. The Langmuir equilibrium isotherm is more accurate than the Freundlich isotherm equations to describe the adsorption of aqueous phenol onto oil palm shell–activated carbons. The concentration-dependent branched pore kinetic model has been shown to be applicable and accurate for a wide range of experimental conditions prevailing in the adsorption system tested. The fraction of non-micropore structure has a fundamental and important effect on the adsorption process. The validity of the model proves that the effective surface diffusion coefficient is a concentration-dependent parameter.

Steam-activated carbons from oil palm shells were pyrolysed under vacuum condition as well as in a nitrogen stream by Jia and Lua [111]. For fixed steam activation conditions of 900°C and 1 h hold time, the optimum pyrolysis conditions under vacuum was 675°C and 2 hrs hold time in which the BET and non-micropore surface areas were 988 m^2/g and 273 m^2/g, respectively. However, when pyrolysed in a nitrogen stream, the activated carbons yielded BET and non-micropore surface areas of 794 m^2/g and 157 m^2/g, respectively, for a pyrolysis temperature of 750°C and a hold time of 2 hrs. Under a vacuum environment, the volatiles released from the oil palm shells during pyrolysis can be quickly removed to reduce pore blockage to steam during the subsequent activation process. Using the former activated carbons, the maximum phenol adsorption capacity was 166 mg/g of activated carbon. For all the phenol adsorption tests conducted, the adsorption capacity was found to be linearly proportional to the BET surface area of the activated carbon.

The factors affecting the performance of activated carbon prepared from oil palm empty fruit bunches for adsorption of phenol were evaluated by Alam and colleagues [112]. The activation temperature of the powdered activated

carbon (PAC) produced was found to have the most significant effect on the yield and adsorption of phenol compared to the activation time and CO_2 gas flow rate. The preparation conditions of 900°C activation temperature, 15 min activation time, and 0.1 L/min CO_2 gas flow rate gave the best quality PAC with higher adsorption capacity and yield. Characterization of PAC produced showed that the activation conditions would find good-quality adsorbent with the BET surface area of 345.1 m^2/g and well-forming pores distribution.

Alam and associates [113] studied the removal of phenol by activated carbons prepared from palm oil mill effluent sludge (POME). Four types of activated carbon were produced from POME sludge: three from thermal activation (300, 500, and 800°C) and one from boiling treatment at 150°C. Among the activated carbons, the POME at 800°C showed good adsorption capacity with very low content of phenol released in aqueous solution. A contact time of 6 hrs was needed for the adsorption of phenol in equilibrium. It was observed that the adsorption capacity was higher at lower values of pH 2–3 and higher value of initial concentration of phenol 200–300 mg/L. The data were well fit by Freundlich isotherm and pseudo-second–order kinetic compared to Langmuir isotherm and pseudo-first–order kinetic.

Activated carbons derived from oil palm empty fruit bunches (EFB) were investigated to find the suitability of its application for removal of phenol in aqueous solution through adsorption process [114]. Three activated carbons were derived from thermal activation at 300, 500, and 800°C and one from physical activation (boiling treatment at 150°C). The results revealed that the activated carbons at thermal activation of 500 and 800°C showed good adsorption capacity with very low content of phenol released in aqueous solution compared to others. It was observed that the adsorption capacity was higher at lower values of pH (2–3) and higher value of initial concentration of phenol (200–300 mg/L). The correlation coefficient showed that the Freundlich isotherm and pseudo-second–order kinetic were better fitted than the Langmuir isotherm and pseudo-first–order kinetic.

Ling and colleagues [115] prepared porous carbons from the potassium hydroxide (KOH) treated self-adhesive carbon grains (SAGC) of the precarbonized oil palm empty fruit bunch for the removal of phenol. The SACG were treated with KOH at different percentages (0%–70% by weight). The treated SACG was carbonized at 700°C in nitrogen environment using a multisteps heating profile. Characterization by nitrogen adsorption isotherm at 77 K showed that the surface area and pore volume of the carbon powders increased as the percentages of KOH increased—they are dominated by micropores. The maximum surface area of 432 m^2/g was obtained for the sample treated with KOH 70 wt%. Batch adsorption was carried out at room temperature to determine the adsorption of phenols by the carbon powders. Percentages removal of phenols by the carbon powders using adsorption isotherms was found to be

increased as the surface area and pore volume increased. The percentages removal of phenol for sample treated with KOH 70 wt% is 72%, which is only 22% inferior to the commercial carbon. The experimental data of the removal equilibrium were correlated by the Freundlich and Langmuir equations, and the result showed that the phenol adsorption isotherm of all samples shown to fit the Freunlich and Langmuir adsorption isotherm model satisfactorily and indicated that the adsorption condition is favorable.

The potential feasibility of activated carbon derived from oil palm empty fruit bunch for the removal of 2, 4-dichlorophenol (2, 4-DCP) from aqueous solution was studied by Shaarani and Hameed [116]. The activated carbon was prepared via chemical activation with phosphoric acid. The effect of contact time, initial concentration (25–250 mg/L), temperature (30–50°C), and pH (2–12) were investigated. The experimental data were analyzed by the Langmuir and Freundlich isotherm models. The equilibrium data were best represented by Langmuir isotherm model, with a maximum monolayer adsorption capacity of 232.56 mg/g at 30°C. The adsorption kinetics was well described by the pseudo-second–order kinetic model.

The adsorption characteristics of 2, 4, 6-trichlorophenol (TCP) on activated carbon prepared from oil palm empty fruit bunch were evaluated by Tan and colleagues [117]. Adsorption of TCP was found to increase with an increase in agitation time, TCP initial concentration, and solution temperature. Acidic solution pH was proved to be more favorable for adsorption of TCP on the activated carbon. The equilibrium data were best described by the Freundlich and Redlich-Peterson isotherm models. The kinetics of the adsorption process was found to follow the pseudo-second–order kinetic model. Boyd plot revealed that the adsorption of TCP on the activated carbon was mainly governed by particle diffusion. The positive ΔH° value indicated that the adsorption process was endothermic in nature. Ethanol desorption technique was shown to be a promising way to regenerate the spent activated carbon prepared in this study by giving relatively high TCP desorption of 99.6%.

Tan and associates [118] investigated the adsorption potential of oil palm shell–based activated carbon to remove 2, 4, 6-trichlorophenol from aqueous solution using fixed-bed adsorption column. The effects of 2, 4, 6-trichlorophenol inlet concentration, feed flow rate, and activated carbon bed height on the breakthrough characteristics of the adsorption system were determined. The ethanol desorption technique applied was found to be highly efficient in regenerating the spent oil palm shell–based activated carbon, showing TCP desorption of 96.25%.

The effects of three preparation variables—(i) CO_2 activation temperature, (ii) CO_2 activation time, and (iii) KOH and char impregnation ratio on the 2, 4, 6-trichlorophenol (TCP) uptake and carbon yield of the activated carbon prepared from oil palm empty fruit bunch—were investigated by Hameed and associates [119]. Based on the central composite design, two quadratic models

were developed to correlate the three preparation variables to the two responses. The activated carbon preparation conditions were optimized using response surface methodology by maximizing both the TCP uptake and activated carbon yield within the ranges studied. The optimum conditions for preparing activated carbon from EFB for adsorption of TCP were as follows: CO_2 activation temperature of 814°C, CO_2 activation time of 1.9 hrs and impregnation ratio of 2.8, which resulted in 168.89 mg/g of TCP uptake and 17.96% of activated carbon yield. The textural characterization results revealed that the BET surface area of the EFB-based activated carbon prepared was 1141 m^2/g, with total pore volume of 0.6 cm^3/g and average pore diameter of 2.5 nm, indicating that the activated carbon was mesoporous in nature. The activated carbon produced demonstrated homogeneous pore size distribution with the pores arranged in an array of honeycombed structures.

The adsorption of 4-chloroguaiacol (4CG) onto activated carbon prepared from the oil palm shell (OPSAC) was studied by Hamad and colleagues [120]. The adsorbent was prepared from oil palm shell raw material impregnated in sodium hydroxide (NaOH) solution followed by the pyrolysis and activation process at 800°C in N_2 and CO_2 gas separately. The effects of solution pH, agitation time, and initial concentration of 4CG were evaluated. 4CG adsorption uptake was found to increase with increase in contact time and initial concentration, while the high adsorption was obtained in an acidic medium at pH = 2. The high BET surface area and the average pore diameter were equal to 2247 m^2/g and 2.68 nm, respectively. The surface morphology and functional groups of the activated carbon were determined by using scanning electron microscopy and Fourier transform infrared analysis. The adsorption equilibrium data were analyzed by Langmuir, Freundlich, and Temkin isotherm models. Adsorption data of 4CG from the activated carbon were in agreement with Langmuir isotherm, with a maximum monolayer adsorption capacity of 454.45 mg/g. Adsorption kinetics was found to follow the pseudo-second–order model with good correlation coefficients for 4CG. From the results of this study, it is concluded that OPSAC is an efficient adsorbent for removing 96.03% of 30 mg/L of 4CG from aqueous solution.

Statistical optimization of adsorption processes for removal of 2,4-dichlorophenol by activated carbon derived from oil palm empty fruit bunches were investigated by Alam and associates [121]. The activated carbon produced from empty fruit bunch at 800°C showed a good adsorption capacity of 2,4-dichlorophenol. The equilibrium time observed for the activated carbon was 8 hrs. The adsorption capacity was observed to be higher at lower pH of 4 and at higher concentration (250 mg/L) of 2,4-dichlorophenol solution with a moderate agitation speed of 100 r/min. The regression coefficient showed that Langmuir isotherm fits the results better than the Freundlich isotherm.

Panumati and colleagues [122] studied the adsorption of phenol from diluted aqueous solutions by activated carbons obtained from oil palm shell, and

the adsorption of phenol from polluted water was studied by Salim and associates [123] through modified oil palm shell. A summary of adsorption capacities of oil palm biomass based adsorbents for the different phenolic pollutants is presented in Table 4.

3.4. Adsorption of Gaseous Pollutants through Oil Palm Biomass

The contamination of the atmosphere is one of the most important environmental problems and is known to be caused by the progressive industrialization of the planet. One of the major contributors in atmospheric contamination is the emission of sulfur dioxides (SO_x) and nitrogen oxides (NO_x), which result in acid rain and ground-layer ozone formation. Fuel combustion processes and power plants are the largest contributor of these gases in the form of flue gas. Due to its high toxicity and negative impact in the environment, interest in reducing the emissions of these gases has been increasing. Oil palm biomass–based activated carbon can be used as an adsorbent for the removal of gaseous pollutants.

Adsorption of sulfur dioxide (SO_2) onto activated carbons prepared from oil-palm shells was investigated by Lua and Guo [124]. Experimental results showed that the adsorption temperature and SO_2 concentration significantly determined the amount of SO_2 adsorbed and the equilibrium time. However, sample particle size had minimum effect on the equilibrium time. For the SO_2 concentration of 2000 ppm, the adsorption activation energy and frequency factor were found to be 12.6 kJ/mol and 3.4×10^3 min^{-1}, respectively. A linearly proportional relationship between the BET surface area and the adsorptive capacity of the activated carbon from oil-palm shells was observed. This indicates that the adsorptive capacity of the activated carbon is mainly determined by its textural characteristics. Higher SO_2 concentration also resulted in the commencement of adsorption for the activated carbon with a lower BET surface area. An intraparticle Knudsen diffusion model based on a Freundlich isotherm was developed for predicting the amount of SO_2 adsorbed and the SO_2 concentration profile within the particle. Based on the estimated isotherm parameters and diffusion coefficients by experimental data fitting, this model could predict the amount adsorbed under different concentrations very well. However, this model was unsuitable for the activated carbon prepared from oil-palm shells by chemical activation because of the occurrence of chemisorption, which was related to the nature of the sample surface functional groups.

Oil palm shells pretreated with KOH were used for the preparation of activated carbon for the adsorption of SO_2 [125]. Experimental results showed that SO_2 concentration and adsorption temperature significantly affected the amount of SO_2 adsorbed and the equilibrium time. Higher SO_2 concentration and lower adsorption temperature were favorable for adsorption. Sample

Table 4: Adsorption\capacities of Oil Palm Biomass–Based Adsorbents for the Adsorption of Phenolic Compounds

Adsorbents	Adsorbates	Adsorption Capacities (mg/g)	References
Oil palm shell activated carbon	Phenol	319.00	(109)
Oil palm shell activated carbon	Phenol	166.00	(111)
Oil palm empty fruit bunch activated carbon	Phenol	04.87	(112)
Palm oil mill effluent sludge activated carbon	Phenol	12.08	(113)
Oil palm empty fruit bunch activated carbon	Phenol	13.11	(114)
Oil palm empty fruit bunch activated carbon	Phenol	89.29–91.74	(115)
Oil palm empty fruit bunch activated carbon	2,4-dichlorophenol	232.56	(116)
Oil palm empty fruit bunch activated carbon	2,4,6-trichlorophenol	588.24	(117)
Oil palm empty fruit bunch activated carbon	2,4,6-trichlorophenol	168.89	(119)
Oil palm shell activated carbon	4-chloroguaiacol	454.45	(120)
Oil palm empty fruit bunch activated carbon	2,4-dichlorophenol	27.25	(121)

particle size only had an effect on the equilibrium time due to the effect of the diffusion rate. Desorption at the same temperature for adsorption and a higher temperature of 200°C confirmed the presence of chemisorption. Compared with the activated carbon pretreated with 30% phosphoric acid (H_3PO_4) that had larger BET and micropore surface areas, the sample impregnated with 10% KOH had a higher adsorptive capacity for SO_2, which was closely related to the surface organic functional groups of the sample.

Microporous activated carbons prepared from palm shell by thermal activation and their applications to sulfur dioxide adsorption were studied by Guo and Lua [126]. The effects of activation temperature on the textural properties of the palm shell–activated carbons—namely BET surface area, porosity, and microporosity—were investigated. The activated carbons prepared from palm shell possessed well-developed porosity (predominantly microporosity), leading to potential applications in gas-phase adsorption for air pollution control. During the CO_2 activation process, as the activation temperature increased the sample weight loss was due to the release of volatile matters in a continual carbonization process and carbon burn-off through carbon-CO_2 weak oxidation, resulting in the development of porosity. The maximum BET surface area of the palm shell–activated carbon was 1366 m^2/g. Static and dynamic adsorption tests for sulfur dioxide (SO_2), a common gaseous pollutant, were carried out in a thermogravimetric analyzer and a packed column configuration, respectively. The effects of adsorption temperature, adsorbate inlet concentration, and adsorbate superficial velocity on the adsorptive performance of the prepared activated carbons were studied. Microporous oil palm shell–activated carbons prepared by physical activation for gas phase adsorption were investigated by Luo and Guo [127]. The effects of CO_2 activation conditions on the characteristics of the activated carbon, such as composition, porosity, hardness, and internal pore surface area, were investigated in order to optimize preparation parameters. The activation temperature and hold time were found to have important influences on the BET and micropore surface areas of the activated carbon. For the parameters investigated, the optimum conditions for CO_2 activation to derive maximum BET surface area were found to be at an activation temperature of 1173 K and a hold time of 30 min, with a heating rate of 10 K/min and a CO_2 flow rate of 100 cm^3/min. Under these conditions, the largest BET surface area for the oil palm shell–activated carbon was 1366 m^2/g. For the kinetic study of the carbon-CO_2 reaction, theoretical predictions using the random pore model agreed very well with the data from thermogravimetric analyses. The activation reaction rate was found to be dependent on both the initial pore structure of the char and the transient pore structure, which was progressively developing during the activation process. When SO_2 gas was used as the adsorbate, a linear relationship between the specific pore surface area and the adsorptive capacity of the adsorbent was observed. This could be elucidated by the neutral (or slightly acidic) nature of the surface

functional groups, as detected by Fourier transform infrared spectroscopy, on the oil palm shell–activated carbon.

Adsorptions of sulphur dioxide onto activated carbon prepared from oil palm shells with and without pre-impregnation were studied by Guo and Luo [128]. The effects of fixed-bed length, SO_2 gas superficial velocity, adsorbent particle size, and internal pore structure on fixed-bed performance were investigated. Some characteristic parameters such as the breakthrough time, exhaustion time, length of mass transfer zone, adsorptive capacity, and adsorption rate constant were derived from the breakthrough curves. Tests of SO_2 adsorption onto activated carbons prepared from oil palm shells pre-impregnated with potassium hydroxide (KOH) and phosphoric acid (H_3PO_4) of different concentrations were also carried out. It was found that the fixed-bed performance was not only dependent on the operating conditions and the textural properties of the adsorbent but was also influenced by the surface chemistry of the adsorbent, which was related to the type and concentration of the impregnating agent.

Preparation and characterization of activated carbons from oil palm stones for gas-phase adsorption were studied [129]. Ultimate and proximate analyses, pycnometry, mercury porosimetry, surface area and porosimetry, and transmission electron microscopy were carried out to evaluate the textural properties of the activated carbons. The activation temperature and the hold time were found to have important influences on the surface area and pore size distribution of the activated carbon. The optimum conditions for CO_2 activation to derive maximum BET surface area were found to be at an activation temperature of 900°C and a hold time of 30 min. with a heating rate of 10°C min^{-1} and CO_2 flow rate of 100 cm^3/min. Under these conditions, the largest BET surface area for the oil palm stone-activated carbon was 1366 m^2/g. For chemical characterization, an x-ray diffractometer and an FTIR spectroscope were used to identify the inorganic components and surface organic functional groups of the activated carbons, respectively. The activation temperature and hold time had significant effects on the surface functional groups. For the determination of the adsorptive capacity of the activated carbons, adsorption of sulphur dioxide was carried out using thermogravimetric analyses.

Sumathi and colleagues [130] examined the impregnated carbon-based sorbents for simultaneous removal of SO_2 and NOx from simulated flue gas. The carbon-based sorbents were prepared using PSAC impregnated with several metal oxides (Ni, V, Fe, and Ce). The removal of SO_2 and NOx from the simulated flue gas was investigated in a fixed-bed reactor. The results showed that PSAC impregnated with CeO_2 (PSAC-Ce) reported the highest sorption capacity among other impregnated metal oxides for the simultaneous removal of SO_2 and NOx. PSAC-Ce showed the longest breakthrough time of 165 and 115 min for SO_2 and NOx, respectively. The properties of the pure and impregnated PSAC were analyzed by BET, FTIR, and XRF. The physical–chemical

features of the PSAC-Ce sorbent indicated a catalytic activity in both the sorption of SO_2 and NOx. The formation of both sulfate (SO_4^{2-}) and nitrate (NO_3^-) species on spent PSAC-Ce further prove the catalytic role played by CeO_2.

The preparation, optimization, and activity of the active adsorbent prepared from oil palm ash for the removal of SO_2 in the flue gas from the combustion systems were investigated [131]. The adsorbent was prepared from oil palm ash, $Ca(OH)_2$, and $CaSO_4$ using a water hydration process. A central composite design was used to study the influence of various adsorbent preparation variables: hydration period, amount of oil palm ash, and amount of $CaSO_4$ on the BET specific surface area of the resulting adsorbent. The surface areas of the adsorbents obtained were in the range of 18.7 to 147.2 m^2/g. An empirical model was then developed to correlate the three adsorbent preparation variables to the BET surface area. Based on the empirical model, a maximum specific surface area of 128.6 m^2/g existed with a hydration period of 10 hrs, amount of oil palm ash 15.0 g, and amount of $CaSO_4$ 2.7 g. The predicted values were found to agree very well with the experimental result. The desulfurization activity of the adsorbent derived from oil palm ash/$Ca(OH)_2/CaSO_4$ was found to be significantly higher than that of its starting materials.

Zainudin and associates [51] studied the oil palm ash (OPA) as an active adsorbent for flue gas desulfurization using hydration process. Active adsorbents for dry-type flue gas desulfurization were prepared from OPA, CaO, $Ca(OH)_2$, and $CaSO_4$ using water hydration process. A central composite design was used to develop an empirical model that correlates the adsorbent surface area with the adsorbent preparation variables. The maximum surface area of adsorbent obtained in this study were adsorbent 120.5 m^2/g and 126.0 m^2/g. Higher hydration period (30 hrs), ratio of OPA to $CaO/Ca(OH)_2$ (3:1), and the use of $Ca(OH)_2$ instead of CaO as the starting materials ($Ca(OH)_2$) were found to give a positive effect on the adsorbent BET surface area. The use of $Ca(OH)_2$ instead of CaO as the starting material produced adsorbent with a higher surface area. The adsorbent with maximum surface area of 134.2 m^2/g was prepared from $Ca(OH)_2$ as the starting material. Activity tests showed that the desulfurization activity of adsorbent prepared by hydrating OPA with $CaO/Ca(OH)_2/CaSO_4$ was much higher compared to the desulfurization activity of the starting materials. The x-ray diffraction analysis showed that the reactive species in the adsorbent were a complex compound containing calcium silicate hydrate or calcium aluminum silicate hydrate. The adsorbent prepared from $OPA/CaSO_4/CaO$ or $Ca(OH)_2$ was also found to be composed of porous structure contributing to its high BET surface area. The potassium ions in OPA were found to form reactive species and were probably involved in the adsorption of SO_2 together with calcium ions. The reactive species in the adsorbent were complex compounds containing Ca, K, Si, Al, O ions, and hydrated water, which have a porous structure.

The preparation of activated carbons from extracted oil palm fibers for the reduction of nitric oxide was studied [132]. Experimental results showed that it was feasible to produce activated carbons from extracted oil palm fibers by a two-step procedure involving either physical activation or chemical activation with KOH impregnation. The activated carbon with the highest BET surface area was obtained by pyrolysis at 750°C for 2 hrs, followed by activation with CO_2 at 850°C for 30 min from the fibers impregnated with 0.10 M KOH for 24 hrs. The results from the thermogravimetric study on the reduction of nitric oxide showed that activated carbons prepared from extracted oil palm fibers could reduce NO*x* appreciably either by reaction with NO at high temperatures or by simultaneous reaction and adsorption for a mixture of NO and O_2. These activated carbons can be potentially used for NO*x* reduction in flue-gas streams from high-temperature combustors or downstream of electrostatic precipitators and in some chemical plants operating at room temperature.

The simultaneous occurrence of adsorption and reaction of nitrogen monoxide on activated carbon in the presence of oxygen and water vapor in a fix-bed reactor has been studied by Klose and Rincon [133]. The study was based on the measurement of breakthrough curves at temperatures between 100 and 150°C and on the subsequent thermal desorption in a fix-bed reactor. The experimental results showed that the reactions on this system include the simultaneous adsorption, reduction, and catalytic oxidation of NO together with the adsorption of created NO_2. During desorption, NO_2 reacts to NO through a reductive desorption process. An acceleration of the NO oxidation occurs when the saturation level of the adsorbed NO is reached, resulting in a maximum on the breakthrough curve. Different adsorbed NO species are formed during the process: one thermal unstable NO and three thermal stable NO species—NO_2, NO, and $(NO)_2$ dimers, respectively.

Effect of surface chemistry on gas-phase adsorption by activated carbon prepared from oil palm stone with pre-impregnation was investigated by Guo and Luo [134]. Experimental results showed that activated carbons with sufficient hardness, fairly high BET surface area, and well-developed microporosities can be prepared from oil palm stones pre-impregnated with various solutions ($ZnCl_2$, H_3PO_4, or KOH). Chemical characterization showed that impregnation significantly affected the surface functional groups. The samples pretreated with H_3PO_4 presented acidic groups such as phenols and carboxylic acids, whereas those with KOH impregnation showed basic groups likely to be pyrones (cyclic ketone) and other keto-derivatives of pyran. From adsorption tests of NO_2 and NH_3 it was found that the activated carbons pretreated with KOH could adsorb more NO_2 but less NH_3 than those pretreated with H_3PO_4 even though they had almost identical BET surface areas. This indicated that the adsorptive capacity of the activated carbon was not only determined by its textural characteristics but was also related to the surface chemistry, which

was relevant to the type of impregnating agent, concentration of impregnation solution, and activation temperature.

Adsorption of ammonia (NH_3) onto activated carbons prepared from palm shells impregnated with sulfuric acid (H_2SO_4) was investigated by Guo and colleagues [135]. The effects of activation temperature and acid concentration on pore surface area development were studied. The relatively large micropore surface areas of the palm shell–activated carbons prepared by H_2SO_4 activation suggest their potential applications in gas adsorption. Adsorption experiments at a fixed temperature showed that the amounts of NH_3 adsorbed onto the chemically activated carbons, unlike those prepared by CO_2 thermal activation, were not solely dependent on the specific pore surface areas of the adsorbents. Adsorption and desorption tests also suggested combined physisorption and chemisorption of NH_3 for the chemically activated carbons. The adsorptive capacity of chemisorption increased with the amounts of oxygen, which were present in the form of surface oxygen functional groups as detected by FTIR. The main oxygen functional groups of the palm shell–activated carbons were presumably phenols, carboxylic acids (or carboxylic anhydrides), and carbonyl groups (either isolated or arranged in quinone-like fashion). Hydrogen atoms of NH_3 can strongly interact with oxygen in the form of hydroxyl (H–O) and carbonyl (C=O) groups on the adsorbents. NH_3 can therefore adsorb onto active adsorption sites provided by oxygen functional groups via hydrogen bonding.

Characterization of adsorbent prepared from oil palm shell by CO_2 activation for removal of gaseous pollutants was studied by Guo and Lua [136]. The effects of activation temperature on the textural and chemical properties of the activated carbon were studied. It was found that significant weight losses occurred during the activation process due to continual release of volatile matter and carbon burn-off through weak carbon–CO_2 oxidation, resulting in an increase of solid density and a decrease of apparent density. Hence, the activated carbons prepared from oil palm shells possessed well-developed porosities and predominant microporosities, which were verified by SEM and transmission electron microscopy, respectively. The predominant micropore development in oil palm shell–activated carbons will lead to applications in gas-phase adsorption for the removal of air pollutants. The relationship between the adsorptive capacity for NO_2 or NH_3 and the BET surface area was found to be linearly proportional. This was due to the neutral (or slightly acidic) surface functional groups of the oil palm shell–activated carbon as detected by the FTIR.

Adsorption of hydrogen sulphide (H_2S) onto activated carbons derived from oil palm shell by thermal or chemical activation method was investigated by Guo and colleagues [137]. The activated carbons prepared by KOH and H_2SO_4 activation had better dynamic adsorption performances due to longer breakthrough times, prolonged exhaustion times, and relatively short mass transfer zone. Therefore, the corresponding adsorption capacities were also larger.

An intra-particle Knudsen diffusion model based on a Freundlich isotherm was developed for predicting the amount of H_2S adsorbed. Desorption tests at the same temperature as adsorption (298 K) and at an elevated temperature (473 K) were carried out to confirm the occurrence of chemisorption and oxidation of H_2S on the activated carbon. Surface chemistries of the palm shell–activated carbons were characterized by FTIR and Boehm titration. It was found that uptaking H_2S onto the palm shell–activated carbons was due to different mechanisms; e.g., physisorption, chemisorptions, and/or H_2S oxidation, depending on the activation agent and activation method.

Activated carbons with relatively high densities and well-developed porosity were prepared from oil palm stones pretreated with H_2SO_4 and KOH impregnations for the removal of SO_2 and NH_3 [138]. The effects of impregnation concentration and soaking time on the textural properties, such as adsorption isotherm, porosity, surface area, and pore size distribution, were investigated. A reasonably high BET surface area and predominant microporosity of the oil palm stone carbons suggested their potential applications in gas-adsorbing processes. From adsorption tests of SO_2 and NH_3, it was found that the activated carbons pretreated with KOH could adsorb more SO_2 but less NH_3 than those pretreated with H_2SO_4, even though they had almost identical BET and micropore surface areas. This indicated that the adsorptive capacity of the activated carbon was not only determined by its textural characteristics but also related to the surface chemistry. Chemical characterization showed that impregnation significantly affected the surface chemistry, i.e. inorganic component and surface organic functional group. For organic functional groups, the samples pretreated with H_2SO_4 presented acidic groups such as phenols and carboxylic acids, whereas those with KOH impregnation showed alkaline groups suggested to be pyrones (cyclic ketone) and other keto-derivatives of pyran.

Oil palm shell adsorbents prepared by phosphoric acid (H_3PO_4) and potassium hydroxide (KOH) activation and their effect on the adsorption capacity of nitrogen dioxide (NO_2) and ammonia (NH_3) gases were investigated by Guo and Lua [139]. The surface areas were increased with the increase of both the concentration of the impregnating solution and the soaking time due to extended action of the impregnating agent. However, the BET surface area decreased when 40% KOH solution was used due to overgasification of the precursor, resulting in detrimental effects on pore evolution. Adsorption and desorption tests of nitrogen dioxide (NO_2) and ammonia (NH_3) gases were used to evaluate the adsorptive capacities of the oil palm shell adsorbents. From the experimental results, it was found that surface functional groups, which were determined by the concentration of impregnation solution and the soaking time, had a significant influence on the adsorptive capacity due to the occurrence of chemisorption. Moreover, mechanisms of chemical activation of oil

palm shell using H_3PO_4 and KOH for the evolution of porosity and the formation of surface functional groups were also proposed based on the phenomena observed.

Lua and Guo [140] studied the feasibility of activated carbon prepared from oil palm stone by one-step CO_2 activation for gaseous pollutant removal. Guo and associates [141] also studied the feasibility of activated carbon prepared from extracted flesh fiber and seed shell of a palm oil processing mill. Tan and Ani [142] studied the oil palm shell–based carbon molecular sieves for air separation. Later Ahmad and associates [143] studied the adsorption kinetics of O_2, N_2, CO_2, and CH_4 in carbon molecular sieves produced by oil palm shell. Niya and colleagues [144] used the activated carbon prepared from oil palm shell impregnated with $ZnCl_2$ for methane adsorption. Jia and coauthors [145] studied the separation of ethane gas by adsorption onto oil palm shell–based activated carbon

3.5. Adsorption of Miscellaneous Pollutants Through Oil Palm Biomass

Salman and Hameed [146] investigated the potential of oil palm fronds–activated carbon on the adsorption of bentazon from aqueous solutions. Oil palm fronds (OPF) were used to prepare activated carbon (OPFAC) using the physiochemical activation method, which consisted of potassium hydroxide (KOH) treatment and carbon dioxide gasification. The effects of the preparation variables, which were activation temperature, activation time, and chemical impregnation ratios (KOH:char by weight), on the carbon yield and bentazon removal were investigated. Based on the central composite design, two-factor interaction and quadratic models were, respectively, employed to correlate the OPFAC preparation variables to the bentazon removal and carbon yield. From the analysis of variance (ANOVA), the most influential factor on each experimental design response was identified. The optimum conditions for preparing activated carbon from OPF were: (i) activation temperature of 850°C, (ii) activation time of 1 h, and (iii) KOH and char ratio of 3.75 and 1. The predicted and experimental results for removal of bentazon and yield of OPFAC were 99.85%, 20.5% and 98.1%, 21.6%, respectively.

Lim and colleagues [147] studied the removal of α and β endosulfan from water using oil palm shell–activated carbon. They found that removal of β endosulfan was significantly more efficient than that of α endosulfan. Kinetic equilibrium for β endosulfan adsorption onto oil palm shell–activated carbon was achieved after 30 min of contact time with a very high capacity of 418 mg/g. The adsorption kinetics data fitted the pseudo-second–order model well implying that chemisorption was the rate-controlling step. Equilibrium adsorption data for oil palm shell–activated carbon fitted the Freundlich isotherm better

Table 5: Adsorption Isotherm and Kinetic Studies of Different Pollutants onto Oil Palm Biomass–Based Adsorbents

Adsorbents	Adsorbates	Applicable Isotherm Models	Applicable Kinetic Models	References
Oil palm shells activated carbon	Methylene blue	Langmuir	Pseudo-second–order	(69)
Chemically modified oil palm shells activated carbon	Methylene blue	Langmuir	Pseudo-second–order	(70)
Oil palm fiber activated carbon	Methylene blue	Langmuir	Pseudo-second–order	(71)
Oil palm fiber–based activated carbon	Methylene blue	Langmuir	—	(72)
Oil palm wood activated carbon	Methylene blue	Langmuir	—	(73)
Oil palm kernel fiber	Methylene blue	Langmuir	Pseudo-second–order	(74)
Oil palm kernel fiber	Methylene blue	—	Pseudo-second–order	(75)
Oil palm kernel shell activated carbon	Reactive black 5 Reactive red E	Freundlich and Redlich-Peterson	Pseudo-second–order	(76)
Oil palm kernel shell activated carbon	Reactive black 5 Reactive red E	—	Film surface pore diffusion	(77)
Oil palm kernel shell activated carbon	Remazol black 5	Freundlich	Pseudo-first–order	(78)
Oil palm kernel fiber	4-bromoaniline-azo-1,8-dihydronaphthalene-3,6-disodiumsulphate	Langmuir	—	(79)
Palm kernel coat	Congo red	—	Pseudo-second–order	(80)
Oil palm trunk fiber	Malachite green	Multilayer adsorption	Lagergren pseudo-first–order	(81)
Oil palm ash	Direct blue 71	Freundlich	Pseudo-second–order	(82)
Oil palm ash	Disperse blue Disperse red	Langmuir	Pseudo-second–order	(83)
Oil palm frond	Zn(II) Cu(II)	Freundlich	—	(55)
Oil palm bark	Zn(II) Cu(II)	Freundlich	—	(55)

Oil palm empty fruit bunch	Zn(II) Cu(II)	Freundlich	—	(55)
Modified soda lignin of oil palm empty fruit bunch	Pb(II)	Langmuir	Pseudo-second–order	(84)
Oil palm shell activated carbon impregnated with polyethyleneimine	Ni(II) Cd(II) Pb(II)	Langmuir and Redlich-Peterson	—	(85)
Oil palm fruit fiber	Pb(II) Cd(II)	—	Pseudo-second–order	(88)
Chemically modified oil palm fruit fiber	Pb(II) Cd(II)	—	Pseudo-second order	(88)
Oil palm empty fruit bunch activated carbon	Hg(II) Pb(II) Cu(II)	Langmuir and Freundlich	—	(90)
Chitosan coated oil palm shell charcoal	Cr(VI)	Langmuir	—	(92)
Oil palm fuel ash	Cr(III)	Langmuir	Pseudo-first–order and second-order irreversible reaction	(93)
Oil palm leaf powders	Cu(II)	Langmuir	—	(94)
Soda lignin from oil palm fruit empty bunch	Cu(II)	Freundlich	Pseudo-second–order	(95)
Oil palm kernel fiber	Cu(II)	Langmuir	—	(97)
Mercaptoacetic acid modified oil palm fruit fiber	Cd(II) and Cr(III)	—	Intraparticle diffusion	(103)
Oil palm shell activated carbon	Pb(II)	—	Pseudo-second–order and Elovic	(105)
Palm kernel shell activated carbon	Cr(III) and Pb(II)	Freundlich	—	(106)
Palm kernel husk activated carbon	Cr(III) and Pb(II)	Freundlich	—	(106)

(Continued on next page)

Table 5: Adsorption Isotherm and Kinetic Studies of Different Pollutants onto Oil Palm Biomass–Based Adsorbents *(Continued)*

Adsorbents	Adsorbates	Applicable Isotherm Models	Applicable Kinetic Models	References
Oil palm ash	Zn(II)	Langmuir and extended Langmuir-Freundlich	First-order	(107)
Oil palm shell activated carbon	Phenol	Langmuir and Langmuir-Freundlich	Concentration-dependent branched pore	(109)
OPS activated carbon	Phenol	Langmuir	Concentration-dependent branched pore	(110)
Palm oil mill effluent sludge activated carbon	Phenol	Langmuir and Freundlich	Pseudo-second-order	(113)
Oil palm empty fruit bunch activated carbon	Phenol	Freundlich	Pseudo-second-order	(114)
Oil palm empty fruit bunch activated carbon	Phenol	Langmuir and Freundlich	—	(115)
Oil palm empty fruit bunch activated carbon	2,4-dichlorophenol	Langmuir	Pseudo-second–order	(116)
Oil palm empty fruit bunch activated carbon	2,4,6-trichlorophenol	Freundlich and Redlich-Peterson	Pseudo-second–order	(117)
Oil palm shell activated carbon	4-chloroguaiacol	Langmui	Pseudo-second–order	(119)
Oil palm empty fruit bunch activated carbon	2,4-dichlorophenol	Langmuir	—	(121)
Oil palm shell activated carbon	Phenol	Freundlich	—	(122)
Modified oil palm shell	Phenol	Freundlich	—	(123)
Oil palm shell activated carbon	Endosulfan	Freundlich	Pseudo-second–order	(147)

than the Langmuir adsorption isotherm, suggesting the existence of multilayer adsorption of endosulfan on a relatively heterogeneous oil palm shell–activated carbon surface. Adinata and associates [148] studied the palm shell-based activated carbon in the production of carbon molecular sieves by the chemical vapor deposition method using benzene as a depositing agent. They investigated the influences of deposition temperature, time, and flow rate of benzene on pore development of carbon molecular sieve and methane adsorption capacity.

Tables 5 sums up various adsorption isotherm models and kinetic models for different pollutants onto oil palm biomass–based adsorbents. Some well-known isotherms such as Freundlich, Langmuir, Redlich-Paterson, Temkin, and Dubinin-Radushkevich as well as several adsorption kinetic models were established to understand the adsorption kinetics and rate-limiting step. These include pseudo-first–order and pseudo-second–order, first-order reversible reaction, external mass transfer, Elovich's model, and Film surface pore diffusion models. The pseudo-first–order and pseudo-second–order kinetic models are the most well liked to study the adsorption kinetics of various pollutants.

4. CONCLUSIONS AND FUTURE DIRECTIONS

In recent years, increasing costs and environmental considerations have led to the use of new low-cost adsorbents derived from renewable resources. In this review, applications of oil palm biomass–based adsorbents for the removal of a diverse type of pollutants have been reviewed based on a substantial number of relevant articles published. The use of oil palm biomass as low-cost adsorbents for removing various pollutants from water and wastewater presents many attractive features, especially their contribution in the reduction of costs for waste disposal, therefore contributing to environmental protection. Although the amount of available literature data for the application of oil palm biomass–based adsorbents in water and wastewater treatment is increasing at a tremendous pace, there are still several gaps which need more attention.

The conditions for the production of low-cost adsorbents after surface modification for higher uptake of pollutants need to be optimized. Mechanistic studies need to be performed in detail to propose a correct binding mechanism of aquatic pollutants with low-cost adsorbents. The potential of low-cost adsorbents under multicomponent pollutants needs to be assessed. This would make a significant impact on the potential commercial application of low-cost adsorbents to industrial system. As evident from the literature survey, no report is available reporting the removal of anions and radionuclides by oil palm biomass–based adsorbents. It is therefore necessary to examine the potential of oil palm biomass–based adsorbents for different anions and radionuclides. Few reports are available on the removal of pesticides by oil palm biomass–based

adsorbent, which needs to be explored in more detail. There is scarce data available for the competitive adsorption of pollutants (metal ions adsorption in presence of phenols, dyes, and other contaminants and vice-versa). Therefore, more research should be conducted in this direction. It is further suggested that the research should not be limited to only lab scale batch studies, but pilot-plant studies should also be conducted utilizing low-cost adsorbents to check their feasibility on a commercial scale.

Little efforts seem to have been made to carry out a cost comparison between activated carbon and various non-conventional adsorbents. This aspect needs to be investigated further in order to promote large-scale use of non-conventional adsorbents. Despite the scarcity of consistent cost information, the widespread uses of low-cost adsorbents in industries for wastewater treatment applications today are strongly recommended due to their local availability, technical feasibility, engineering applicability, and cost-effectiveness. Despite various drawbacks and challenges that currently exist, a widespread and great progress in this area can be expected in the future.

Finally, we wish to comment on zero waste strategy of adsorption process. There is a bigger scope of research of utilization of used adsorbents for further treatment processes. Another possibility of exploration is the recovery cum reuse of adsorbed substances. All future researches might be accompanied by adsorption/desorption and/or adsorption/re-adsorption process so that there is no net sludge generation and, if any, it should be minimum. Such a strategy will fulfill the goal of zero waste.

ACKNOWLEDGMENTS

The authors acknowledge the research grant provided by the Universiti Sains Malaysia under the Short Term Grant Scheme (Project No. 304/PTEKIND/639062) and Research University (RU) Scheme (Project No. 1001/PTEKIND/814048).

REFERENCES

1. Ambashta RD, Sillanpaa M. Water purification using magnetic assistance: A review. *J Hazard Mater*. 2010; 180:38–49.

2. Vijayaraghavan K, Yun YS. Bacterial biosorbents and biosorption. *Biotechnol Adv*. 2008; 26:266–291.

3. Ali I, Gupta VK. Advances in water treatment by adsorption technology. *Nat Protoc*. 2006; 1:2661–2667.

4. Bhatnagar A, Vilar VJP, Botelho CMS, Boaventura RAR. Coconut-based biosorbents for water treatment—A review of the recent literature. *Adv Colloid Interface Sci*. 2010; 160:1–15.

5. Peternele WS, Winkler-Hechenleitner AA, Gomez Pineda EA. Adsorption of Cd(II) and Pb(II) onto functionalized formic lignin from sugar cane bagasse. *Bioresour Technol.* 1999; 68:95–100.

6. Shibi IG, Anirudhan TS. Polymer-grafted banana (*Musa paradisiaca*) stalk as an adsorbent for the removal of lead(II) and cadmium(II) ions from aqueous solutions: kinetic and equilibrium studies. *J Chem Technol Biotechnol.* 2006; 81:433–444.

7. Karnitz Jr O, Gurgel LVA, Perin de Melo JC, Botaro VR, Sacramento Melo TM, de Freitas Gil RP, Gil LF. Adsorption of heavy metal ion from aqueous single metal solution by chemically modified sugarcane bagasse. *Bioresour Technol.* 2007; 98:1291–1297.

8. Gurgel LVA, de Freitas RP, Gil LF. Adsorption of Cu(II), Cd(II), and Pb(II) from aqueous single metal solutions by sugarcane bagasse and mercerized sugarcane bagasse chemically modified with succinic anhydride. *Carbohyd Polym.* 2008; 74: 922–929.

9. Ali I, Aboul-Enein HY. *Chiral pollutants: Distribution, toxicity and analysis by chromatography and capillary electrophoresis.* John Wiley & Sons, Hoboken, NJ; 2004.

10. Moore JW, Ramamoorthy S. *Heavy metals in natural waters: Applied monitoring and impact assessment.* Springer, New York; 1984.

11. Dich J, Zahm SH, Hanberg A, Adami HO. Pesticides and cancer. *Cancer Causes Control.* 1997; 8:420–443.

12. Brusick D. Genotoxicity of phenolic antioxidants. *Toxicol Indust Health.* 1993; 9:223–230.

13. Parekh BS. *Reverse osmosis technology: Applications for high purity water production.* New York: Marcel Dekker; 1988.

14. Nemerow N, Dasgupta A. *Industrial and hazardous waste treatment.* New York: Van Nostrand Reinhold; 1991.

15. Ali I, Jain CK. *Water encyclopedia: Domestic, municipal, and industrial water supply and waste disposal.* New York: John Wiley & Sons; 2005.

16. Gupta VK, Ali I. *Encyclopaedia of surface and colloid science.* New York: Marcel Dekker; 2003.

17. Wojnarovits L, Foldvary Cs M, Takacs E. Radiation-induced grafting of cellulose for adsorption of hazardous water pollutants: A review. *Radiation Phy Chem.* 2010; 79:848–862.

18. Dabrowski A. Adsorption-from theory to practice. *Adv. Colloid Interface Sci.* 2001; 93:135–224.

19. Rafatullah M, Sulaiman O, Hashim R, Ahmad A. Adsorption of Copper (II) onto Different Adsorbents. *J Disp Sci Tech.* 2010; 31:918–930.

20. Ahmad A, Rafatullah M, Danish M. Sorption studies of Zn(II)- and Cd(II)ions from aqueous solution on treated sawdust of sissoo wood. *Holz als Roh- und Werkstoff.* 2007; 65:429–436.

21. Ahmad A, Rafatullah M, Sulaiman O, Ibrahim MH, Chii YY, Siddique BM. Removal of Cu(II) and Pb(II) ions from aqueous solutions by adsorption on sawdust of Meranti wood. *Desalination.* 2009; 247:636–646.

22. Rafatullah M, Sulaiman O, Hashim R, Ahmad A. Adsorption of copper (II), chromium (III), nickel (II) and lead (II) ions from aqueous solutions by Meranti sawdust. *J Hazard Mater.* 2009; 170:969–977.

23. Ahmad A, Rafatullah M, Sulaiman O, Ibrahim MH, Hashim R. Scavenging behaviour of Meranti sawdust in the removal of methylene blue from aqueous solution. *J Hazard Mater*. 2009; 170:357–365.

24. Danish M, Sulaiman O, Rafatullah M, Hashim R, Ahmad A. Kinetics for the removal of paraquat dichloride from aqueous solution by activated date (phoenix dactylifera) stone carbon. *J Disp Sci Tech*. 2010; 31:248–259.

25. Faust SD, Aly OM. *Adsorption process for water treatment*. Stoneham: Butterworths Publishers, Massachusetts; 1987.

26. Bansal RC, Goyal M. *Activated carbon adsorption*. CRC Press, New York; 2005.

27. Miguel GS, Lambert SD, Graham NJD. A practical review of the performance of organic and inorganic adsorbents for the treatment of contaminated waters. *J Chem Technol Biotechnol*. 2006; 81: 1685–1696.

28. Mohan D, Pittman Jr CU. Arsenic removal from water/wastewater using adsorbents—A critical review. *J Hazard Mater*. 2007; 142: 1–53.

29. Ahmaruzzaman M. Adsorption of phenolic compounds on low-cost adsorbents: A review. *Adv Colloid Interface Sci*. 2008; 143: 48–67.

30. Sud D, Mahajan G, Kaur MP. Agricultural waste material as potential adsorbent for sequestering heavy metal ions from aqueous solutions—A review. *Bioresour Technol*. 2008; 99: 6017–6027.

31. Lin SH, Juang RS. Adsorption of phenol and its derivatives from water using synthetic resins and low-cost natural adsorbents: A review. *J Environ Manage*. 2009; 90:1336–1349.

32. Bhatnagar A, Sillanpää M. Applications of chitin- and chitosan-derivatives for the detoxification of water and wastewater—A short review. *Adv Colloid Interface Sci*. 2009; 152: 39.

33. Demirbas A. Agricultural based activated carbons for the removal of dyes from aqueous solutions: A review. *J Hazard Mater*. 2009; 167:1–9.

34. Gupta VK, Suhas. Application of low-cost adsorbents for dye removal—A review. *J Environ Manage*. 2009; 90:2313–2342.

35. Rafatullah M, Sulaiman O, Hashim R, Ahmad A. Adsorption of methylene blue on low-cost adsorbents: A review. *J Hazard Mater*. 2010; 177:70–80.

36. Foo KY, Hameed BH. Insights into the modeling of adsorption isotherm systems. *Chem Eng J*. 2010; 156: 2–10.

37. Srinivasan A, Viraraghavan T. Decolorization of dye wastewaters by biosorbents: A review. *J Environ Manage*. 2010; 91: 1915–1929.

38. Ahmaruzzaman M. A review on the utilization of fly ash. *Progress in Energy Combustion Sci*. 2010; 36:327–363.

39. Farooq U, Kozinski JA, Khan MA, Athar M. Biosorption of heavy metal ions using wheat based biosorbents—A review of the recent literature. *Bioresour Technol*. 2010; 101:5043–5053.

40. Miretzky P, Cirelli AF. Cr(VI) and Cr(III) removal from aqueous solution by raw and modified lignocellulosic materials: A review. *J Hazard Mater*. 2010; 180: 1–19.

41. Bhatnagar A, Sillanpaa M. Utilization of agro-industrial and municipal waste materials as potential adsorbents for water treatment—A review. *Chem Eng J*. 2010; 157:277–296.

42. Gupta VK, Carrott PJM, Ribeiro Carrott MML, Suhas. Low-cost adsorbents: Growing approach to wastewater treatment—A review. *Critical Rev Environ Sci Technol*. 2010; 39:783–842.

43. Kailash D, Dharmendra P. Low cost adsorbents for heavy metal removal from wastewater: A review. *Res J Chem Environ*. 2010; 14:100–103.

44. Ahmad T, Rafatullah M, Ghazali A, Sulaiman O, Hashim R, Ahmad A. Removal of pesticides from water and wastewater by different adsorbents: A review. *J Environ Sci Health, Part C—Environ Carcinog & Ecotoxic Revs*. 2010; 28: 231–271.

45. Yusoff S. Renewable energy from palm oil-innovation on effective utilization of waste. *J Cleaner Prod*. 2006; 14: 87–93.

46. Chuah TG, Wan Azlina AGK, Robiah Y, Omar R. Biomass as the renewable energy sources in Malaysia: An overview. *Int J Green Energy*. 2006; 3:323–346.

47. Shuit SH, Tan KT, Lee KT, Kamaruddin AH. Oil palm biomass as a sustainable energy source: A Malaysian case study. *Energy*. 2009; 34:1225–1235.

48. MPOB (Malaysian Palm Oil Board), 2003. Latest development and commercialization of oil palm biomass. Seminar on Business Opportunity in Oil Palm Biomass, 21 August, 2003, Selangor, Malaysia.

49. Issabayeva G, Aroua MK, Sulaiman NM. Continuous adsorption of lead ions in a column packed with palm shell activated carbon. *J Hazard Mater*. 2008; 155:109–113.

50. Jaafar M, Sukaimi J. The future of palm oil in the new millennium in Malaysia. *J Burotrop Bulletin*. 2001; 16:10–21.

51. Zainudin NF, Lee KT, Kamaruddin AH, Bhatia S, Mohamed AR. Study of adsorbent prepared from oil palm ash (OPA) for flue gas desulfurization. *Separ Purif Technol*. 2005; 45:50–60.

52. Mohamed AR, Zainudin NF, Lee KT, Kamaruddin AH. Reactivity of absorbent prepared from oil palm ash for flue gas desulfurization: Effect of SO_2 concentration and reaction temperature. *Stud Surf Sci Catal*. 2006; 159: 449–452.

53. Ghazali A, Daud WRW, Law KN. Alkaline Peroxide Mechanical Pulping (APMP) of oil palm lignocellulosics: Part 2. Empty Fruit Bunch (EFB) responses to pretreatments. *Appita J*. 2006; 59: 65–70.

54. Ghazali A, Daud WRW, Law KN. Pre-treatment of oil palm biomass for alkaline peroxide pulping. *Cellulose Chem Technol*. 2009; 43: 331–338.

55. Salamatinia B, Kamaruddin AH, Abdullah AZ. Removal of Zn and Cu from wastewater by sorption on oil palm tree-derived biomasses. *J Appl Sci*. 2007; 7:2020–2027.

56. Hashim R, Nadhari WNAW, Sulaiman O, Kawamura F, Hiziroglu S, Sato M, Sugimoto T, Seng TG, Tanaka R. Characterization of raw materials and manufactured binderless particleboard from oil palm biomass. *Mater Design*. 2011; 32:245–254.

57. Theander O. In: Overand RP, Mile TA, Mudge LK, eds. *Fundamentals of thermochemical biomass conversion*. New York: Elsevier Applied Science Publisher; 1985.

58. Unal H, Alibas K. Agricultural residues as biomass energy. *Energy Sour Part B*. 2007; 2:123–140.

59. Demirbas A. Recent progress in biorenewable feedstocks. *Energy Educ Sci Technol*. 2008; 22:69–95.

60. Balat M. Mechanisms of thermochemical biomass conversion processes. Part 1. Reactions of pyrolysis. *Energy Sour Part A*. 2008; 30:620–635.

61. Glasser WG, Sarkanen S., eds. *Lignin: Properties, materials*. Washington DC: American Chemical Society; 1989.

62. Hashem A, Akasha RA, Ghith A, Hussein DA. Adsorbent based on agricultural wastes for heavy metal and dye removal: A review. *Energy Educ Sci Technol*. 2007; 19:69–86.

63. Balat M. Mechanisms of thermochemical biomass conversion processes. Part 3. Reactions of liquefaction. *Energy Sour Part A*. 2008; 30:649–659.

64. Mohan D, Pittman Jr CU, Steele PH. Pyrolysis of wood/biomass for bio-oil: A critical review. *Energy Fuels*. 2006; 20:848–889.

65. Young RA. Structure, swelling and bonding of cellulose fibers. In: *Cellulose: Structure, modification, and hydrolysis*. New York: Wiley and Sons; 1986:9.

66. Garcia-Valls R, Hatton TA. Metal ion complexation with lignin derivatives. *Chem Eng J*. 2003; 94:99–105.

67. Gong R, Liu X, Feng M, Liang J, Cai W, Li N. Comparative study of methylene blue sorbed on crude and monosodium glutamate functionalized sawdust. *J Health Sci*. 2008; 54:623–628.

68. Guo J, Gui B, Xiang SX, Bao XT, Hu-ji Zhang, Aik Chong L. Preparation of activated carbons by utilizing solid wastes from palm oil processing mills. *J Porous Mater*. 2008; 15:535–540.

69. Tan IAW, Ahmad AL, Hameed BH. Adsorption of basic dye using activated carbon prepared from oil palm shell: batch and fixed bed studies. *Desalination*. 2008; 225:13–28.

70. Tan IAW, Ahmad AL, Hameed BH. Enhancement of basic dye adsorption uptake from aqueous solutions using chemically modified oil palm shell activated carbon. *Colloids Surf A*. 2008; 318:88–96.

71. Tan IAW, Hameed BH, Ahmad AL. Equilibrium and kinetic studies on basic dye adsorption by oil palm fibre activated carbon. *Chem Eng J*. 2007; 127:111–119.

72. Hameed BH, Tan IAW, Ahmad AL. Optimization of basic dye removal by oil palm fibre-based activated carbon using response surface methodology. *J Hazard Mater*. 2008; 158:324–332.

73. Ahmad AL, Loh MM, Aziz JA. Preparation and characterization of activated carbon from oil palm wood and its evaluation on Methylene blue adsorption. *Dyes Pigm*. 2007; 75:263–272.

74. Ofomaja AE. Sorption dynamics and isotherm studies of methylene blue uptake on to palm kernel fibre. *Chem Eng J*. 2007; 126:35–43.

75. Ofomaja AE. Kinetics and mechanism of methylene blue sorption onto palm kernel fibre. *Process Biochem*. 2007; 42:16–24.

76. Nourouzi MM, Chuah TG, Choong TSY. Equilibrium and kinetic study on reactive dyes adsorption by palm kernel shell-based activated carbon: In single and binary systems. *J Environ Eng*. 2009; 135:1393–1398.

77. Nourouzi MM, Chuah TG, Choong TSY. Adsorption of reactive dyes by palm kernel shell activated carbon: Application of film surface and film pore diffusion models. *E-J Chem*. 2009; 6:949–954.

78. Zawani Z, Luqman CA, Thomas SYC. Equilibrium, kinetics and thermodynamic studies: Adsorption of remazol black 5 on the palm kernel shell activated carbon (PKS-AC). *Eur J Sci Res*. 2009; 37:67–76.

79. Ofomaja AE, Ho YS, Equilibrium sorption of anionic dye from aqueous solution by palm kernel fibre as sorbent. *Dyes Pigm.* 2007; 74:60–66.

80. Oladoja NA, Akinlabi AK, Congo red biosorption on palm kernel seed coat. *Ind Eng Chem Res.* 2009; 48:6188.

81. Hameed BH, Khaiary El MI. Batch removal of malachite green from aqueous solutions by adsorption on oil palm trunk fibre: Equilibrium isotherms and kinetic studies. *J Hazard Mater.* 2008; 154:237–244.

82. Ahmad AA, Hameed BH, Aziz N. Adsorption of direct dye on palm ash: Kinetic and equilibrium modeling. *J Hazard Mater.* 2007; 141:70–76.

83. Isa MH, Lang LS, Asaari FAH, Aziz HA, Ramli NA, Dhas JPA. Low cost removal of disperse dyes from aqueous solution using palm ash. *Dyes Pigm.* 2007; 74: 446–453.

84. Ibrahim MNM, Ngah WSW, Norliyana MS, Daud WRW, Rafatullah M, Sulaiman O, Hashim R. A novel agricultural waste adsorbent for the removal of lead (II) ions from aqueous solutions. *J Hazard Mater.* 2010; 182;377–385.

85. Yin CY, Aroua MK, Daud WMAW. Enhanced adsorption of metal ions onto polyethyleneimine-impregnated palm shell activated carbon: Equilibrium studies. *Water Air Soil Pollut.* 2008; 192:337–348.

86. Ho YS, Ofomaja AE. Pseudo-second-order model for lead ion sorption from aqueous solutions onto palm kernel fiber. *J Hazard Mater.* 2006; B 129:137–142.

87. Ho YS, Ofomaja AE. Effects of calcium competition on lead sorption by palm kernel fibre. *J Hazard Mater.* 2005; B 120:157–162.

88. Abia AA, Asuquo ED. Sorption of Pb(II) and Cd(II) ions on chemically unmodified and modified oil palm fruit fiber absorbent: Analysis of pseudo second order kinetics models. *Ind J Chem Tech.* 2008; 15:341–348.

89. Abia AA, Asuquo ED. Lead (II) and nickel (II) adsorption kinetics from aqueous metal solutions using chemically modified and unmodified agricultural adsorbents. *African J Biotechnol.* 2006; 5:1475–1482.

90. Wahi R, Ngaini Z, Jok VU. Removal of mercury, lead and copper from aqueous solution by activated carbon of palm oil empty fruit bunch. *World Appl Sci J.* 2009; 5: 84–91.

91. Isa MH, Ibrahim N, Aziz HA, Adlan MN, Sabiani NHM, Zinatizadeh AAL, Kutty SRM. Removal of chromium (VI) from aqueous solution using treated oil palm fibre. *J Hazard Mater.* 2008; 152:662–668.

92. Nomanbhay SM, Palanisamy K. Removal of heavy metal from industrial wastewater using chitosan coated oil palm shell charcoal. *Electronic J Biotechnol.* 2005; 8:43–53.

93. Chu KH, Hashim MA. Adsorption characteristics of trivalent chromium on palm oil fuel ash. *Clean Techn Environ Policy.* 2002; 4:8–15.

94. Sulaiman O, Amini MHM, Rafatullah M, Hashim R, Ahmad A. Adsorption equilibrium and thermodynamic studies of copper (II) ions from aqueous solutions by oil palm leaves. *Int J Chem Reac Eng.* 2010; 8:1–16.

95. Ibrahim MNM, Ngah WSW, Norliyana MS, Daud WRW. Copper(II) Biosorption on soda lignin from oil palm empty fruit bunches (EFB). *Clean.* 2009; 37:80–85.

96. Ho YS, Ofomaja AE. Kinetic studies of copper ion adsorption on palm kernel fibre. *J Hazard Mater.* 2006; B 137:1796–1802.

97. Ofomaja AE. Equilibrium studies of copper ion adsorption onto palm kernel fibre. *J Environ Manag.* 2010; 91:1491–1499.

98. Chu KH, Hashim MA. Kinetic studies of Copper(II) and Nickel(II) adsorption by oil palm ash. *J Ind Eng Chem*. 2003; 9:163–167.

99. Tan WT, Lee CK, Ng KL. Column studies of Copper(II) and Nickel(II) ions sorption on palm pressed fibres, environmental technology. *Environ Technol*. 1996; 17:621–628.

100. Salamatinia B, Kamaruddin AH, Abdullah AZ. Regeneration and reuse of spent NaOH-treated oil palm frond for copper and zinc removal from wastewater. *Chem Eng J*. 2010; 156;141–145.

101. Alam MZ, Muyibi SA, Kamaldin N. Twelfth International Water Technology Conference, IWTC12 2008, 373–383, Alexandria, Egypt.

102. Sugawara K, Wajima T, Kato T, Sugawara T. Preparation of carbonaceous heavy metal adsorbent from palm shell using sulfur impregnation. *Ars Separatoria Acta*. 2007; 5:88–98.

103. Abia AA, Asuquo ED. Kinetics of Cd^{2+} and Cr^{3+} sorption from aqueous solutions using mercaptoacetic acid modified and unmodified oil palm fruit fibre (*Elaeis guineensis*) adsorbents. *Tsinghua Sci Technol*. 2007; 12:485–492.

104. Iqbal M, Saeed A, Akhtar N. Pettiolar felt- shealth of palm: A new biosorbent for the removal of heavy metals from contaminated water. *Bioresour Technol*. 2002; 81:151–153.

105. Aroua MK, Leong SPP, Teo LY, Yin CY, Daud WMAW. Real-time determination of kinetics of adsorption of lead(II) onto palm shell-based activated carbon using ion selective electrode. *Bioresour Technol*. 2008; 99:5786–5792.

106. Iyagba ET, Opete OSE. Removal of chromium and lead from drill cuttings using activated palm kernel shell and husk. *African J Environ Sci Technol*. 2009; 3:171–179.

107. Chu KH, Hashim MA. Adsorption and desorption characteristics of zinc on ash particles derived from oil palm waste. *J Chem Technol Biotechnol*. 2002; 77:685–693.

108. Zumriye A, Yener J. A comparative adsorption/biosorption study of monochlorinated phenols onto various sorbents. *Waste Manag*. 2001; 21:695–702.

109. Lua AC, Jia Q. Adsorption of phenol by oil-palm-shell activated carbons. *Adsorption*. 2007; 13:129–137.

110. Jia Q, Lua AC. Concentration-dependent branched pore kinetic model for aqueous phase adsorption. *Chem Eng J*. 2008; 136:227–235.

111. Jia Q, Lua AC. Effects of pyrolysis conditions on the physical characteristics of oil-palm-shell activated carbons used in aqueous phase phenol adsorption. *J Anal Appl Pyrolysis*. 2008; 83:175–179.

112. Alam MZ, Ameem ES, Muyibi SA, Kabbashi NA. The factors affecting the performance of activated carbon prepared from oil palm empty fruit bunches for adsorption of phenol. *Chem Eng J*. 2009; 155:191–198.

113. Alam MZ, Muyibi SA, Mansor MF, Wahid R. Removal of phenol by activated carbons prepared from palm oil mill effluent sludge. *J Environ Sci*. 2006; 18:446–452.

114. Alam MZ, Muyibi SA, Mansor MF, Wahid R. Activated carbons derived from oil palm empty-fruit bunches: Application to environmental problems. *J Environ Sci*. 2007; 19:103–108.

115. Ling YY, Deraman M, Jumali MH, Omar R, Aziz AA, Abdelrahman AE, Peng TH, Meihua JT, Muslimin M, Mohtar M. Preparation and phenols adsorption property of porous carbon from oil palm empty fruit bunches. *Solid State Sci Technol*. 2005; 13:170–178.

116. Shaarani FW, Hameed BH. Batch adsorption of 2, 4-dichlorophenol onto activated carbon derived from agricultural waste. *Desalination*. 2010; 255:159–164.

117. Tan IAW, Ahmad AL, Hameed BH. Adsorption isotherms, kinetics, thermodynamics and desorption studies of 2, 4, 6-trichlorophenol on oil palm empty fruit bunch-based activated carbon. *J Hazard Mater*. 2009; 164:473–482.

118. Tan IAW, Ahmad AL, Hameed BH. Fixed-bed adsorption performance of oil palm shell-based activated carbon for removal of 2, 4, 6-trichlorophenol. *Bioresour Technol*. 2009; 100:1494–1496.

119. Hameed BH, Tan IAW, Ahmad AL. Preparation of oil palm empty fruit bunch-based activated carbon for removal of 2, 4, 6-trichlorophenol: Optimization using response surface methodology. *J Hazard Mater*. 2009; 164:1316–1324.

120. Hamad BK, Noor AM, Afida AR, Asri MNM. High removal of 4-chloroguaiacol by high surface area of oil palm shell-activated carbon activated with NaOH from aqueous solution. *Desalination*. 2010; 257:1–7.

121. Alam MZ, Muyibi SA, Toramae J. Statistical optimization of adsorption processes for removal of 2,4-dichlorophenol by activated carbon derived from oil palm empty fruit bunches. *J Environ Sci*. 2007; 19:674–677.

122. Panumati S, Chudecha K, Vankhaew P, Choolert V, Chuenchom L, Innajitara W, Sirichote O. Adsorption of phenol from diluted aqueous solutions by activated carbons obtained from bagasse, oil palm shell and pericarp of rubber fruit. *Songklanakarin J Sci Technol*. 2008; 30:185–189.

123. Salim MR, Othman F, Ali MI, Patterson J, Hardy T. Application of locally available materials for the treatment of organic polluted water. *Water Sci Technol*. 2002; 46:339–346.

124. Lua AC, Guo J. Adsorption of sulfur dioxide on activated carbon from oil-palm waste. *J Environ Eng*. 2001; 127:895–901.

125. Guo J, Lua AC. Adsorption of sulfur dioxide onto activated carbons prepared from oil-palm shells impregnated with potassium hydroxide. *J Chem Technol Biotechnol*. 2000; 75:971–976.

126. Guo J, Lua AC. Activated carbons prepared from palm shell by thermal activation and their application to sulfur dioxide adsorption. *J. Colloid Interface Sci*. 2002; 251;242–247.

127. Lua AC, Guo J. Microporous oil-palm-shell activated carbon prepared by physical activation for gas-phase adsorption. *Langmuir*. 2001; 17;7112–7117.

128. Guo J, Lua AC. Adsorption of sulphur dioxide onto activated carbon prepared from oil-palm shells with and without pre-impregnation. *Sep Purif Technol*. 2003; 30:265–273.

129. Lua AC, Guo. Preparation and characterization of activated carbons from oil-palm stones for gas-phase adsorption. *Colloids Surf A*. 2001; 179:151–162.

130. Sumathi S, Bhatia S, Lee KT, Mohamed AR. Selection of best impregnated palm shell activated carbon (PSAC) for simultaneous removal of SO_2 and NOx. *J Hazard Mater*. 2010; 176:1093–1096.

131. Mohamed AR, Lee KT, Noor NM, Zainudin NF. Oil palm ash/Ca(OH)2/CaSO4 adsorbent for flue gas desulfurization. *Chem Eng Technol*. 2005; 28:339–345.

132. Lua AC, Guo J. Activated carbons prepared from extracted-oil palm fibers for nitric oxide reduction. *Energy Fuels*. 1998; 12;1089–1094.

133. Klose W, Rincon S. Adsorption and reaction of NO on activated carbon in the presence of oxygen and water vapour. *Fuel*. 2007; 86:203–209.

134. Guo J, Lua AC. Effect of surface chemistry on gas-phase adsorption by activated carbon prepared from oil-palm stone with pre-impregnation. *Sep Purif Technol*. 2000; 18:47–55.

135. Guo J, Xu WS, Chen YL, Lua AC. Adsorption of NH_3 onto activated carbon prepared from palm shells impregnated with H_2SO_4. *J Colloid Interface Sci*. 2005; 281:285–290.

136. Guo J, Lua AC. Characterization of adsorbent prepared from oil-palm shell by CO_2 activation for removal of gaseous pollutants. *Mater Lett*. 2002; 55:334–339.

137. Guo J, Luo Y, Lua AC, Chi R, Chen YL, Bao XT, Xiang SX. Adsorption of hydrogen sulphide (H_2S) by activated carbons derived from oil-palm shell. *Carbon*. 2007; 45: 330–336.

138. Guo J, Lua AC. Textural and chemical characterisations of activated carbon prepared from oil-palm stone with H_2SO_4 and KOH impregnation. *Microporous Mesoporous Mater*. 1999; 32:111–117.

139. Guo J, Lua AC. Surface functional groups on oil-palm-shell adsorbents prepared by H_3PO_4 and KOH activation and their effects on adsorptive capacity. *Trans IChemE Part A*. 2003; 81:585–590.

140. Lua AC, Guo J. Activated carbon prepared from oil palm stone by one-step CO_2 activation for gaseous pollutant removal. *Carbon*. 2000; 38:1089–1097.

141. Guo J, Gui B, Xiang S, Bao X, Zhand H, Lua AC. Preparation of activated carbons by utilizing solid wastes from palm oil processing mills. *J Porous Mater*. 2008; 15:535–540.

142. Tan JS, Ani FN. Carbon molecular sieves produced from oil palm shell for air separation. *Sep Purif Technol*. 2004; 35:47–54.

143. Ahmad MA, Daud WMAW, Aroua MK. Adsorption kinetics of various gases in carbon molecular sieves (CMS) produced from palm shell. *Colloids Surf A*. 2008; 312:131–135.

144. Niya AA, Daud WMAW, Mjalli FS. Using granular activated carbon prepared from oil palm shell by $ZnCl_2$ and physical activation for methane adsorption. *J Anal Appl Pyrolysis*. 2010; 89: 197–203.

145. Jia G, Guang HU, Chong LUAA, Heslop MJ. Separation of ethane gas by adsorption onto various biomass-derived activated carbons. *Adv Mater Res*. 2010; 113–114:1896–1899.

146. Salman JM, Hameed BH. Effect of preparation conditions of oil palm fronds activated carbon on adsorption of bentazon from aqueous solutions. *J Hazard Mater*. 2010; 175;133–137.

147. Lim YN, Shaaban MG, Yin CY. Removal of endosulfan from water using oil palm shell activated carbon and rice husk ash. *J Oil Palm Res*. 2008; 20:527–532.

148. Adinata D, Daud WMAW, Aroua MK. Production of carbon molecular sieves from palm shell based activated carbon by pore sizes modification with benzene for methane selective separation. *Fuel Process Technol*. 2007; 88:599–605.

SOUVENIR & ABSTRACTS

INTERNATIONAL CONFERENCE ON CHEMISTRY: FRONTIERS AND CHALLENGES

[Under SAP (DRS-I)]

5 - 6 March, 2011

CENTENARY CELEBRATIONS (1911-2011)

DEPARTMENT OF CHEMISTRY

[H.R.H. Prince of Wales Chemical Laboratory-1911]

ALIGARH MUSLIM UNIVERSITY

ALIGARH-202002 (U.P.) INDIA

CSIR

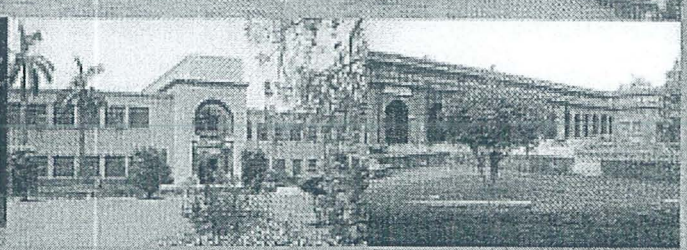

PP-9

Structure Stabilization of α-Chymotrypsin by Polyols

Awanish Kumar, P. Madhusudhana Reddy and P. Venkatesu*

Department of Chemistry, University of Delhi, Delhi 110 007, India

nfluence of polyols on the structure and stability of α-chymotrypsin (CT) have been explored by using ntial scanning calorimeter (DSC), circular dichroism (CD) and fluorescence spectroscopy. We have predicted rmodynamic folding properties [transition temperature (T_m), enthalpy change (ΔH), heat capacity change (ΔC_p) ibbs free energy change (Δg_n)] from DSC to understand the clear picture of folding/unfolding of CT. These explicitly explain that stabilizing polyols are preferentially excluded from the surface of CT, since water has a tendency toward favorable interactions with functional groups of the CT than with polyols. Our results reveal e T_m, ΔH, and ΔG_n of CT in polyols increase linearly with polyol concentration. Among different types of s studied, trehalose acts as the best CT stabilizer under various stress conditions. Additionally, herein, we have terized the counteracting effects of trehalose on the deleterious effect of urea on CT through DSC at a 1:2 ratio alose and urea, as well as various urea concentrations (up to 6 M) in the presence of 1 M trehalose. Our parallel mental results explicitly elucidate that trehalose strongly offset the deleterious actions of urea on CT at 1:2 atio of trehalose and urea only.

PP-10

Adsorption behaviour of methyl orange from aqueous solutions using oil palm leaf powder

Mohd Rafatullah, Othman Sulaiman, Rokiah Hashim and Anees Ahmad

School of Industrial Technology, Universiti Sains Malaysia, 11800 Penang, Malaysia
E-mail address: mrafatullah@gmail.com; mrafatullah@usm.my (M. Rafatullah)

n leaf powder (OPLP), an abundant agricultural by-product in Malaysia, was used as an adsorbent for the l of methyl orange (MO) from aqueous solutions. Batch experiments were conducted to study the main ters under various conditions such as contact time, solution pH, adsorbent dosage and initial metal ion tration on sorption of MO. The results showed that the optimum pH value for maximum sorption determined Morphological changes observed in scanning electron micrographs of untreated and treated OPLP confirmed nomenon of sorption. Fourier transform infrared spectroscopy (FT-IR) confirmed the MO and OPLP ions responsible for adsorption. The Langmuir and Freundlich adsorption isotherm constants were calculated heir applicability for the system and the results were being discussed. The thermodynamic parameters such as rgy, enthalpy and entropy changes for the sorption of MO were computed to predict the nature of sorption . The kinetics data obtained were modeled by pseudo-first-order, pseudo-second-order, and Weber-Morris n models, respectively. The process of adsorption follows a pseudo-second-order rate model. In conclusion, P was found possible to be used as a low cost adsorbent for removal of MO from aqueous solutions.

Proceedings International Conference on Environmental Research and Technology (ICERT 2010)

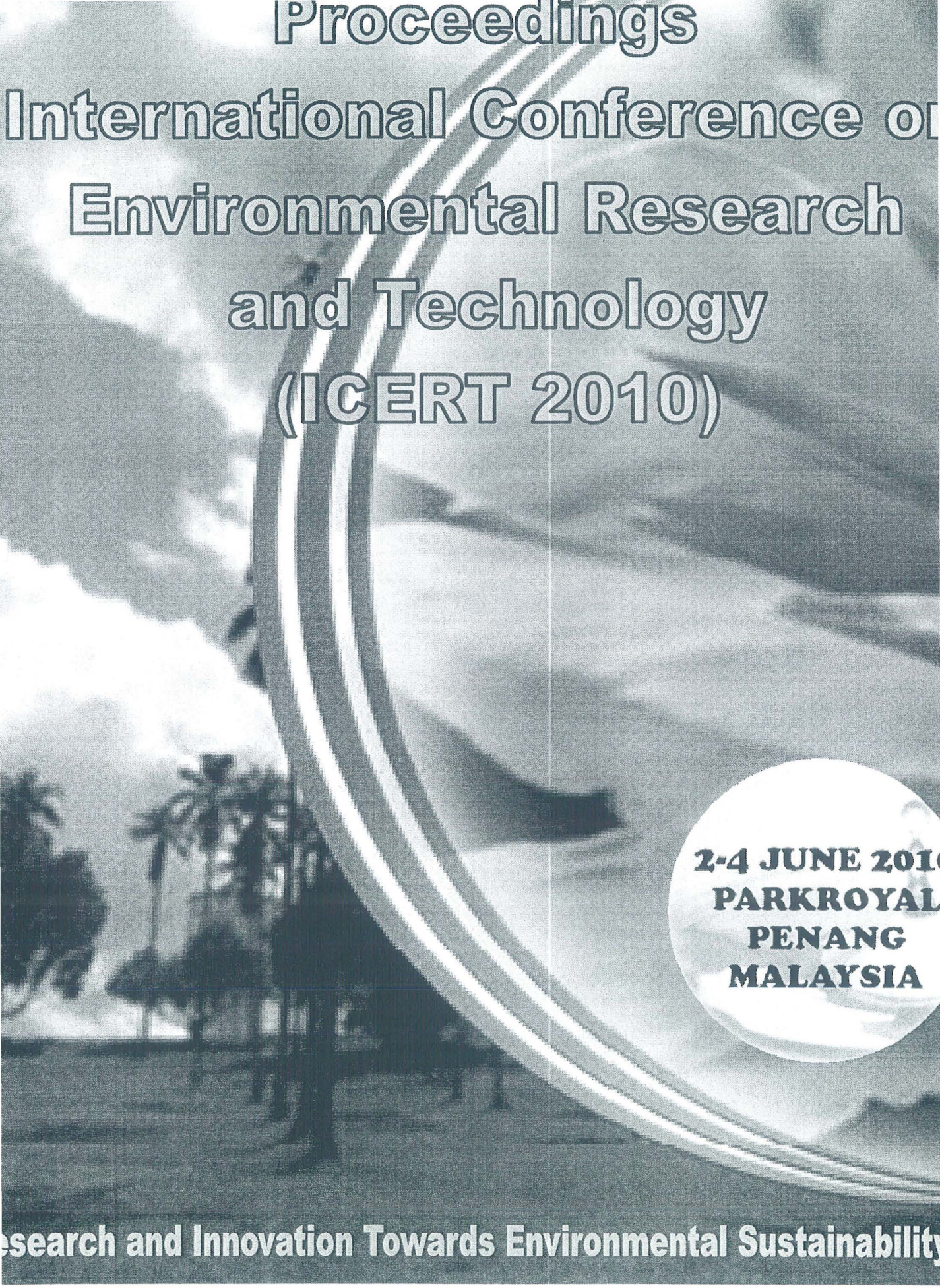

esearch and Innovation Towards Environmental Sustainability

UNIVERSITI SAINS MALAYSIA

Edito
Teng Tjoon T
Yusri Yu

BIOSORPTION OF COPPER (II) IONS FROM AQUEOUS SOLUTION BY OIL PALM LEAVES

M. H. M. Amini[1]*, M. Rafatullah[1], O. Sulaiman[1], R. Hashim[1], A. Ahmad[2]
[1]Division of Bioresource, Paper and Coatings Technology, School of Industrial Technology, Universiti Sains Malaysia, 11800 Penang, Malaysia
[2]Division of Environmental Technology, School of Industrial Technology, Universiti Sains Malaysia, 11800 Penang, Malaysia
E-mail: hazimamini@yahoo.com

ABSTRACT
A novel adsorbent, oil palm leaves were used to remove copper (II) ions from aqueous solutions. Oil palm leaves were dried, grounded, washed using distilled water and sieved into different sizes. The effects of different system variables, viz, contact time, pH, dosage of adsorbent, size of adsorbent particles and initial metal ion concentration on biosorption of copper (II) ions were studied. The results showed that the optimum pH value for maximum biosorption determined was 6.0 for copper (II) ions. The Langmuir, Freundlich and Temkin adsorption isotherm constants were calculated to find their applicability for the system and the results were being discussed. The thermodynamic parameters such as free energy, enthalpy and entropy changes for the biosorption of copper (II) ions were computed to predict the nature of biosorption process. In conclusion, the oil palm leaves particles were found possible to be used as a low cost adsorbent for removal of copper (II) ions from aqueous solution.

Key words: Biosorption , Copper (II), Isotherm , Oil palm leaf, Thermodynamic.

INTRODUCTION
Heavy metals pollution is among global problems exist nowadays. Copper was among the hazardous material that pollute the environment which is used as metal in machinery, construction, transportation and military weapons. Consuming food and beverages contaminated with copper will affect the liver badly continued by hemolysis and damage to renal tubules, the brain, and other organs (Gaetke and Chow, 2003). Therefore, water or waste water should be treated to remove this hazardous material.

The use of agricultural wastes for the treatment of polluted water is also an attractive and promising option for the environment. A wide variety of agricultural waste materials such as orange peel (Feng et al., 2009), soybean hull (Ucun et al., 2009), pecan nut shell (Veghetti et al., 2009), meranti sawdust (Rafatullah et al., 2009) and soybean straw (Zhu et al., 2008) are being used as low-cost alternatives to expensive adsorbents.

Attention was given to utilization of oil palm leaf as biosorbent for removal of copper (II) ions from aqueous solution. The objective of this paper is to assess the potential of oil palm leaf particles for uptake of copper (II) ions from aqueous solutions. The effect of temperature, contact time, pH of metal solution, dosage of biosorbent, size of biosorbent particles and initial concentration of metal ion solution was investigated. The biosorption isotherm and probable mechanism are explained. The thermodynamic parameters for the biosorption of copper (II) ions have also been computed and discussed.

MATERIALS AND METHODS
Biosorbent and adsorbate solution
Oil palm leaves (*Elaeis guineensis*) were used as biosorbent and were obtained from Kedah, Malaysia. They were washed with distilled water and left to air dried before cutting it into smaller pieces. Leaves were grounded using grinder into smaller particles, washed using distilled water and dried in an oven at 60±5^{0}C for 48 hours (Hameed, 2009). Copper (II) nitrate hemipentahydrate 98% (Sigma-aldrich, Cu(NO3)2·2.5H2O) was used in preparing adsorbate solution by diluting 1g of the chemical with 1000ml of distilled water. Stock solution was further diluted to different desired concentrations.

Batch biosorption studies
Batch biosorption studies were done according to Ahmad et al. (2007). 50 ml of five different concentrations of Cu (II) ion solution was mixed with 0.5 mg oil palm leaf particles in stoppered conical flask, agitated in water bath shaker for different length of times at constant revolution of 125rpm at 30^{0}C. Then mixtures were filtered and filtrate solutions were analysed using atomic absorption spectrometer for their final concentration. Different parameters were being studied including the equilibrium time (20, 40, 60, 80, 100, 120, 140, 160, 180, 200 and 240 min.), pH of the solution (2, 3, 4, 5, 6, 7 and 8), dosage of the adsorbent (0.1, 0.2, 0.3, 0.4, 0.5, 1.0, 1.5, 2.0, 2.5 and 3.0 g), size of adsorbent particles (0.53µm-125µm, 125µm-250µm, 250µm-500µm and 500µm-1mm) and

initial concentrations (1, 10, 25, 50 and 100 mg/L) for maximum adsorption. Three replicates were done for each study to ensure data reliability. Biosorption was expressed in percentage, using the formula;

$$\text{Biosorption, \%} = (Ci - Ce) / Ci \times 100 \quad (1)$$

where, Ci and Ce are the initial and equilibrium concentration of metal ions (mg/L) in the solution.

RESULTS AND DISCUSSION

Effect of initial metal concentrations and contact time

The effects of different contact times on biosorption of Cu (II) ions were investigated. Contact times between 20 to 240 minutes were chosen and a graph of biosorption percentage versus contact time was plotted. Fig. 1 showed biosorption percentage increases gradually as longer contact time was provided until it reaches equilibrium around 120^0C to 180^0C. Degradation of particles could be possible reason to explain desorption activity after about 180 minutes of contact time. Yu et al., (2003) reported the same phenomenon in his work to remove metal ions from aqueous solution using maple sawdust. Fig. 1 also showed the effect of increasing initial concentration of metal ions on biosorption percentage. Biosorption was most efficient at lower initial concentrations and gradually decreases as the initial concentrations were increased. As concentrations go higher, percentage of adsorption become lower as the amount of adsorption sites on the surface of adsorbent was limited to a certain amount.

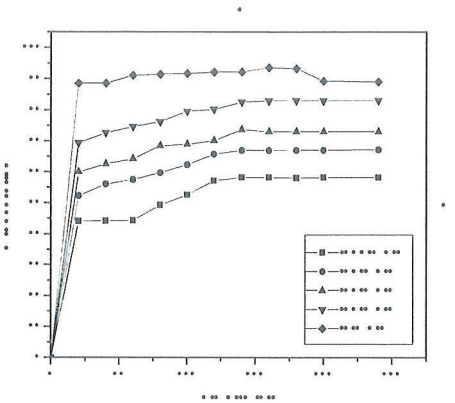

Figure 1 Effect of initial concentrations and contact time

Effect of pH on biosorption

Effect of pH of adsorbate solution is shown in Fig. 2. It shows that the adsorption of the metal in the pH range of 1 to 5 varies between 15 % and 65 %. The percentage removal of copper (II) ions was minimum at the pH 1 and increased with increasing pH. Biosorption efficiency was higher with higher pH value while at low pH value, H^+ ions were rivalling with copper cations for biosorption sites in the system (Šćiban and Klašnja, 2004). As the pH increased, the adsorption surface become less positive and therefore electrostatic attraction between the metal ions and OPLP surface is likely to be increased. However, at higher pH values of 6 to 8 the metal adsorption decreased due to the formation of soluble hydroxyl complexes. The maximum sorption efficiency is detected around pH 6. A similar phenomenon was observed for the adsorption of copper (II) ions from aqueous solution by modified bagasse (Jiang et al., 2009). Therefore, pH 6 was selected to be the optimum pH for further studies.

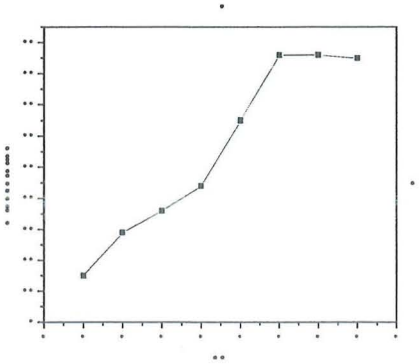

Figure 2 Effect of pH on biosorption

Effect of dosage of biosorbent

Adsorbent dosage is an important parameter because it determines the capacity of an adsorbent for a given concentration of the adsorbate. The adsorption studies of copper (II) ions on OPLP were done at 30 °C temperature with particle size of 500 μm – 250 μm. Several dosages of biosorbent were used in a range of 0.1 g to 3.0 g while keeping the volume of the metal solutions constant at pH 6. When the adsorbent dosage was increased from 0.1 to 3.0 g/L, the percentage adsorption generally increases, but the amount adsorbed per unit mass of adsorbent decreases considerably as shown in Fig. 3. The increase in the adsorption percentage or decrease in unit adsorption with increase in the dose of adsorbent is due to the increase in active sites on the adsorbent and thus making easier penetration of the metal ions to the adsorption sites (Aydin et al., 2008).

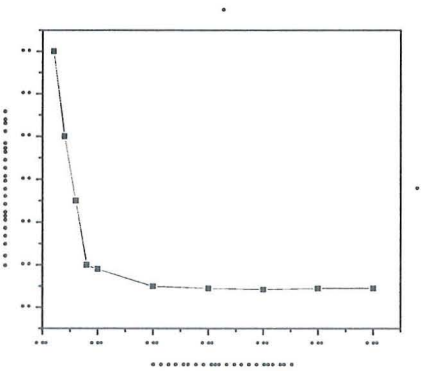

Figure 3 Effect of dosage of adsorbent

Effect of size of oil palm leaf particles

Size of biosorbent particles greatly influences the biosorption rate. Decreasing particle size will increase the surface area which contributes to increases of the biosorption opportunity at the outer surface of the sawdust materials. Intraparticle diffusion from the outer surface into the pores of the material is also possible factor increasing the biosorption rate of biosorbent (Shukla et al., 2002). Fig. 4 clearly showed us that increasing the particle size of oil palm leaf particles decreases the biosorption percentage.

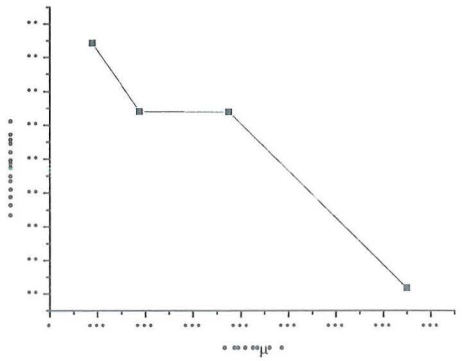

Figure 4 Effect of particle size

Biosorption behaviour of oil palm leaf particles (isotherm models)

Langmuir model

Langmuir model assumes biosorption occurred on homogenous surface of biosorbent at specific localized site where each site accommodates one and only one adsorbed entity (Bansal and Goyal, 2005). The correlation coefficient (R^2) values were used to judge the applicability of Langmuir model on the biosorption. Fig. 5 showed Ce/A_m is plotted against Ce, with a slope ($1/K_L$) and an intercept at ($1/bK_L$). According to this model;

$$Ce/Am = (1/k)\,(1/b) + (1/b)\,Ce \qquad (2)$$

Where Ce stands for the equilibrium concentration (mg/L), Am is the amount adsorbed per specified amount of biosorbent (mg/g), k is the equilibrium constant and *b* is the amount of adsorbate required to form monolayer. A graph of Ce/Am versus Ce was plotted to obtain values of k and b as reported in Table 1. The correlation coefficient (R^2) values of 0.981 to 0.991 indicated that the adsorption data of copper (II) ions onto oil palm leaf particles was well fitted to the Langmuir isotherm.

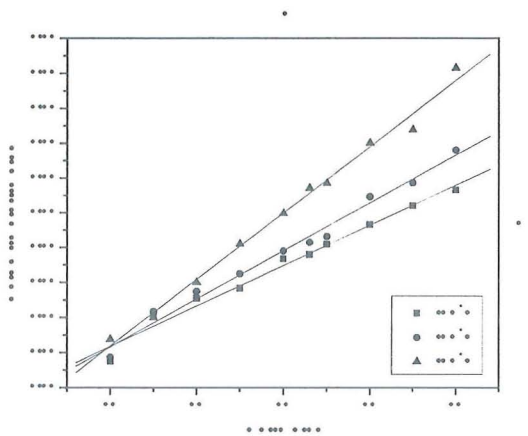

Figure 5 Langmuir adsorption isotherm of oil palm leaf particles

Freundlich model

Freundlich model assumes adsorbate has a heterogeneous surface. Biosorption sites have different biosorption energies which are not always available (Walker and Weatherley, 2001). This model deals with the multilayer sorption of the substance on the biosorbent. According to Freundlich model;

$$A_m = (K)(Ce)^{1/n}$$

$$\ln A_m = \ln k + (1/n) \ln Ce$$

Where all terms same like stated before with n stands for an empirical constant. A straight line was obtained by plotting $\ln A_m$ versus ln Ce graph with a slope of 1/n and intercept of ln k. A plot of $\ln A_m$ vs ln Ce was done resulting a straight line with a slope 1/n and an intercept of ln K as shown in Fig. 6. The related parameters were calculated and reported in Table 1.

Temkin model

Temkin isotherm model considered adsorbate - adsorbate interaction on biosorption isotherm (Odaloja et al., 2008);

$$A_m = (RT/b)\,(K_T Ce)$$
$$A_m = B \ln K_T + B \ln Ce$$

Where B is heat of biosorption (RT/b) and K_T as Temkin equilibrium binding constant (L/mg) corresponding to the maximum binding energy. A_m versus ln Ce was plotted to get a straight line graph as shown in Fig. 7 for determination of B and K_T values as reported in Table 1.

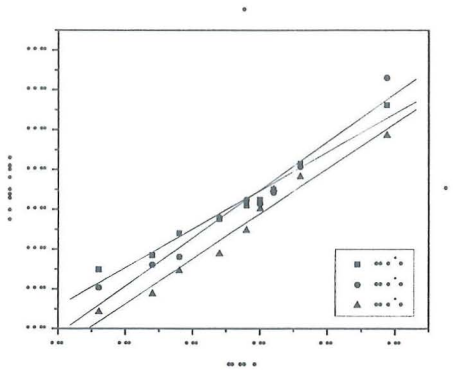

Figure 6 Freundlich adsorption isotherm of oil palm leaf particles

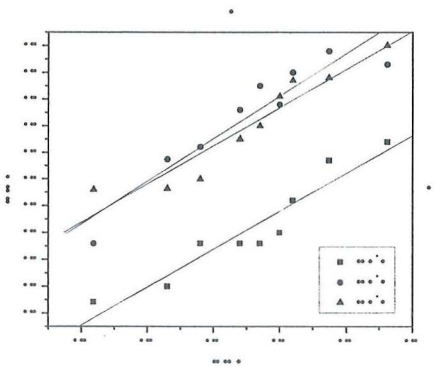

Figure 7 Temkin adsorption isotherm of oil palm leaf particles

Table 1 Adsorption isotherm constants and correlation coefficients for the adsorption of copper (II) ions on OPLP at different temperatures

Adsorption isotherms and its constants	Temperatures (°C)		
	0	**5**	**0**
Langmuir adsorption isotherm constants			
b (mg/g)	34.78	70.37	63.15
K_L (L/mg)	.109	.170	.644
R^2	.981	.985	.991
Freundlich adsorption isotherm constants			
K_F (mg/g)(L/mg)$^{1/n}$	.996	.707	.909
n	.537	.137	.498

R^2			
	.904	.883	.903
Temkin adsorption isotherm constants			
K_T (L/mg)			
	.386	.482	.452
B			
	.240	.742	.080
R^2			
	.969	.959	.970

From Table 1, the Langmuir adsorption isotherm model yielded best fit as indicated by the highest R^2 values at all temperatures compared to the Freundlich and Temkin adsorption isotherm models. Table 2 lists a comparison of maximum monolayer adsorption capacity of copper (II) ions on various agricultural waste adsorbents. Oil palm leaf particle is found to have a relatively large adsorption capacity of 434.78 mg/g and this indicates that it could be considered a promising material for the removal of copper (II) ions from aqueous solutions.

Table 2 Comparison of maximum adsorption capacities of different adsorbents for copper (II) ions

Adsorbents	Maximum monolayer adsorption capacity (mg/g)	References
Oil palm leaf powder	434.78	This work
Orange peel	289.00	Feng et al., 2009
Soybean hulls	154.90	Ucun et al., 2009
Pecan nutshell	91.20	Vaghetti et al., 2009
Meranti sawdust	32.051	Rafatullah et al., 2009
Soybean straw	28.60	Zhu et al., 2008

Thermodynamic study of biosorption

To evaluate the thermodynamic parameters for the biosorption of copper (II) ions from aqueous solution, the biosorption studies were carried out at different temperatures 303K, 318K and 333K. Since Langmuir biosorption isotherm is the best fit so value of b was used in place of K in the calculations of all thermodynamic parameters. The spontaneity of a process can be predicted using standard free energy change ($\Delta G°$):

$$\Delta G° = - RT \ln K$$

Where, R is the universal gas constant (8.314 $Jmol^{-1}K^{-1}$) and T is the absolute temperature (K) and *K* (L/mg) is the Langmuir isotherm constant. Similarly, the standard enthalpy change $\Delta H°$ from 303.15K to 333.15K was computed from the following equation,

$$\ln K = \Delta S°/R - \Delta H°/RT$$

A plot of ln K versus 1/T gives a straight line as shown in Fig. 8$\Delta H°$ and $\Delta S°$ values were obtained from the slope ($\Delta H°/R$) and intercept of this plot ($\Delta S°/R$) respectively. The standard free energy change ($\Delta G°$), standard enthalpy change ($\Delta H°$), and standard entropy change ($\Delta S°$) were calculated from equation 7 and 8 and its values associated with the biosorption of copper (II) ions on oil palm leaf particles are listed in Table 3. Negative values of $\Delta G°$ indicate the possibility of the process and spontaneous nature of the biosorption with a high performance of copper (II) for oil palm leaf particles. Negative values of $\Delta G°$ indicate the feasibility of the process and spontaneous nature of the adsorption. Positive value of $\Delta H°$ indicates the endothermic nature of the process, while positive value of $\Delta S°$ reflects the affinity of the adsorbents for the copper (II) ions (Panday et al., 1985; Aydin et al., 2008).

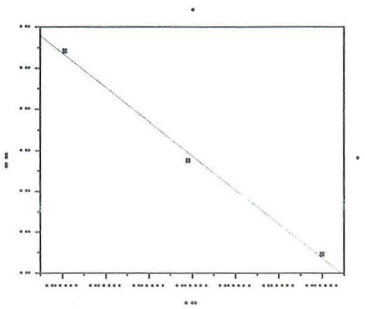

Figure 8 Plot of K versus 1/T

Table 3 Values of thermodynamic parameters for adsorption of copper (II) ions on OPLP

Temp. (K)	ΔG^0 (kJmol^{-1})	ΔH^0 (kJmol^{-1})	ΔS^0 (kJmol^{-1}K^{-1})	R^2
303	-4.887	69.304	0.238	.995
313	-6.289			
323	-10.274			

CONCLUSION

This study showed that utilisation of oil palm leaf as biosorbent for removal of copper (II) ions from aqueous solution. The percent biosorption of copper (II) was found to increase with increase in contact time, pH and biosorbent dosage until its equilibrium point. Equilibrium data fitted very well in the Langmuir biosorption isotherm with a monolayer sorption capacity of 434.78 mg/g mg/g at 30°C. The thermodynamic calculations prove biosorption process was spontaneous and endothermic in nature. Considering all the results above, oil palm leaf particles could be an alternative biosorbent for copper (II) ions uptakes from aqueous solution which is indeed possible to be used in industrial waste water treatment, replacing those costly activated carbons.

ACKNOWLEDGEMENT

The authors acknowledge the research grant provided by the Universiti Sains Malaysia under the Short Term Research Grant Scheme (304/PTEKIND/639062) and the Postdoctoral Fellowship to M. Rafatullah.

REFERENCES

Ahmad A., Rafatullah M., Danish M., 2007. Sorption studies of Zn(II)- and Cd(II)ions from aqueous solution on treated sawdust of sissoowood. Holz Roh Werkst 65, 429–436

Aydin H., Bulut Y., Yerlikaya C., 2008. Removal of copper (II) from aqueous solution by adsorption onto low-cost adsorbents. Journal of Environmental Management 87 (1), 37-45.

Bansal R. C., Goyal M., 2005. Activated Carbon Adsorption. USA, Taylor & Francis Group, LLC.

Feng, N., Guo, X., Liang. S., 2009. Adsorption study of copper (II) by chemically modified orange peel. Journal of Hazardous Materials 164 (2-3), 1286–1292

Gaetke L. M., Chow C. K., 2003. Copper toxicity, oxidative stress, and antioxidant nutrients. Toxicology (189) 147 - 163

Hameed B.H., 2009. Spent tea leaves: A new non-conventional and low-cost adsorbent for removal of basic dye from aqueous solutions. Journal of Hazardous Materials 161, 753–759

Jiang Y., Pang H., Liao B., 2009. Removal of copper (II) ions from aqueous solution by modified bagasse. Journal of Hazardous Materials 164 (1), 1–9

Ngah W.S. W., Hanafiah M.A.K.M., 2008. Adsorption of copper on rubber (Hevea brasiliensis) leaf powder: Kinetic, equilibrium and thermodynamic studies. Biochemical Engineering Journal 39, 521–530

Oladoja N. A., Aboluwoye C. O., Oladimeji Y. B., 2008. Kinetics and Isotherm Studies on Methylene Blue Adsorption onto Ground Palm Kernel Coat. Turkish Journal of Engineering and Environmental Sciences 32, 303 – 312

Panday K. K., Prasad G., Singh V. N., 1985. Cu (II) removal from aqueous solutions by fly ash. Water Research 19 (7), 869–873

Rafatullah M., Sulaiman O., Hashim R., Ahmad A., 2009. Adsorption of copper (II), chromium (III), nickel (II) and lead (II) ions from aqueous solutions by meranti sawdust. Journal of Hazardous Materials 170, 969 - 977

Šćiban M., Klašnja M., 2004. Wood sawdust and wood originate materials as adsorbents for heavy metal ions. Holz Roh Werkst 62, 69–73

Shukla A., Zhang Y., Dubey P., Margrave J.L., Shukla S. S., 2002. The role of sawdust in the removal of unwanted materials from water. Journal of Hazardous Materials B95, 137–152

Sud D., Mahajan G., Kaur M.P., 2008. Agricultural waste material as potential adsorbent for sequestering heavy metal ions from aqueous solutions – A review. Bioresource Technology 99 (2008) 6017–6027

Ucun H., Aksakal O., Yildiz E., 2009. Copper(II) and zinc(II) biosorption on Pinus sylvestris L. Journal of Hazardous Materials 161 (2-3), 1040-1045.

Vaghetti J. C. P., Lima E. C., Royer B., da Cunha B. M., Cardoso N. F., Brasil J. L., Dias S. L. P., 2009. Pecan nutshell as biosorbent to remove Cu (II), Mn (II) and Pb (II) from aqueous solutions. Journal of Hazardous Materials 162 (1), 270–280

Walker G.M., Weatherley L.R., 2001. Adsorption of dyes from aqueous solution - the effect of adsorbent pore size distribution and dye aggregation. Chemical Engineering Journal 83, 201–206

Yu L. J., Shukla S. S., Dorris K. L., Shukla A., Margrave J. L., 2003. Adsorption of chromium from aqueous solutions by maple sawdust. Journal of Hazardous Materials B100, 53–63

Zhu B., Fan T., Zhang D., 2008. Adsorption of copper ions from aqueous solution by citric acid modified soybean straw. Journal of Hazardous Materials 153 (1-2), 300–308.

USM
UNIVERSITI SAINS MALAYSIA

2nd ICERT 2010

2 - 4th June 2010 | Penang, Malaysia

International Conference on Environmental Research and Technology

ICERT 2010
School of Industrial Technology
Universiti Sains Malaysia
11800 Penang, Malaysia.
Phone : +604-653 2824/5208/2110
Fax : 604 657 3678
E-mail : icert@usm.my
URL : http://www.ppti.usm.my/ICERT

ISBN 978 - 967 - 5417 - 79 - 5

Purchase Requisition | Purchase Order | Suppliers | Maintenance | Financials | Coda Info | Reports | Admin

UserCode: MNIZAM / USMPGLIVE / PTEKIND **Program Code: Votebook9100** **Current Program : Votebook (Header)**

Current Date : 26/09/2013 3:25:25 PM **Version: 15.03, Last Updated at 03/12/2012** **DB: 13.02, 9/27/2010 VB: 13.01, 3/14/2011** **Switch Language : English / Malay**

Wildcard : eg. Like 100%, Like 10%1, Like %1

Element 1: 304 Element 2: % Element 4: PTEKIND

Element 5: 639062 Year: 2013 Search Export to Excel

Detail	Excel	Budget Rule	Budget Control	Account Description	Budget Account Code	Roll over	Budget	Cash Received	Advanced	Commit	Actual	Available	Percentage
Detail	Excel	374	T	Projek Jangka Pendek Penang	304.111.0.PTEKIND.639062	3,627.60	0.00	0.00	0.00	0.00	0.00	3,627.60	0.00%
Detail	Excel	374	T	Projek Jangka Pendek Penang	304.114.0.PTEKIND.639062	1,000.00	0.00	0.00	0.00	0.00	0.00	1,000.00	0.00%
		374	T	SubTotal		4,627.60	0.00	0.00	0.00	0.00	0.00	4,627.60	0.00%
Detail	Excel	375	T	Projek Jangka Pendek Penang	304.221.0.PTEKIND.639062	4,019.90	0.00	0.00	0.00	0.00	0.00	4,019.90	0.00%
Detail	Excel	375	T	Projek Jangka Pendek Penang	304.222.0.PTEKIND.639062	400.00	0.00	0.00	0.00	0.00	0.00	400.00	0.00%
Detail	Excel	375	T	Projek Jangka Pendek Penang	304.223.0.PTEKIND.639062	1,000.00	0.00	0.00	0.00	0.00	0.00	1,000.00	0.00%
Detail	Excel	375	T	Projek Jangka Pendek Penang	304.227.0.PTEKIND.639062	-5,840.72	0.00	0.00	0.00	0.00	0.00	-5,840.72	0.00%
Detail	Excel	375	T	Projek Jangka Pendek Penang	304.228.0.PTEKIND.639062	1,000.00	0.00	0.00	0.00	0.00	0.00	1,000.00	0.00%
Detail	Excel	375	T	Projek Jangka Pendek Penang	304.229.0.PTEKIND.639062	-5,541.06	0.00	0.00	0.00	0.00	0.00	-5,541.06	0.00%
		375	T	SubTotal		-4,961.88	0.00	0.00	0.00	0.00	0.00	-4,961.88	0.00%
Detail	Excel	376	T	Projek Jangka Pendek Penang	304.335.0.PTEKIND.639062	3,000.00	0.00	0.00	0.00	0.00	0.00	3,000.00	0.00%
		376	T	SubTotal		3,000.00	0.00	0.00	0.00	0.00	0.00	3,000.00	0.00%
Detail	Excel	378	T	Projek Jangka Pendek Penang	304.552.0.PTEKIND.639062	-61.21	0.00	0.00	0.00	0.00	0.00	-61.21	0.00%
		378	T	SubTotal		-61.21	0.00	0.00	0.00	0.00	0.00	-61.21	0.00%
		9999		GrandTotal		2,604.51	0.00	0.00	0.00	0.00	0.00	2,604.51	0.00%